p68 RNA helicase:

a novel mediator of nitric oxide and mitogen functions in keratinocytes

DISSERTATION

zur Erlangung des Doktorgrades

der Naturwissenschaften

vorgelegt beim Fachbereich

Chemisch und Pharmazeutische Wissenschaften

der Johann Wolfgang Goethe-Universität

in Frankfurt am Main

von

Kornelija Kahlina

aus Gross-Umstadt

Frankfurt am Main 2004

Vom Fachbereich
Chemische und Pharmazeutische Wissenschaften
der Johann Wolfgang Goethe-Universität
als Dissertation angenommen.

Dekan:	Prof. Dr. Harald Schwalbe
Gutachter:	PD Dr. Stefan Frank Prof. Dr. Bernd Ludwig
Datum der Disputation:	09. November 2004

The work outlined in this thesis is based on experimental studies published in the following article:

Kahlina K, Goren I, Pfeilschifter J, Frank S

p68 DEAD box RNA helicase expression in keratinocytes: regulation, nuclear localization, and functional connection to proliferation and VEGF gene expression.

J Biol Chem 279: 44872-44882, 2004

Contents

1

Introduction

1.1 The skin

The skin represents the body´s largest organ system and is the principle site of interaction with the environment. The skin serves as a barrier which mediates protection against harmful environmental conditions, such as mechanical damage, noxious agents, invading pathogens and ultraviolet light. Moreover, the skin limits water loss and participates in the maintenance of body temperature. Special receptors enable the skin organ system to sense heat, cold, pain and pressure (Thews *et al*., 1999; Freinkel and Woodley, 2001).

The skin consists of the outer epidermal, the underlying dermal and the subcutaneous layers. Comparable to other epidermal structures in the body, the epidermis represents a stratified, self-renewing tissue compartment of multiple cell types. Keratinocytes represent the major epidermal cell type and are responsible for cutaneous barrier function. To a lesser extent, melanocytes (melanin synthesis), Langerhans cells (antigen-presenting), and Merkel cells (sensory functions) are found in the epidermal layer. Keratinocytes are organized into four different layers that correspond to the progressive stages of differentiation: *stratum basale, stratum spinosum, stratum granulosum, and stratum corneum*. While passaging through these layers, keratinocytes show an increase in size and cell flattening, they loose organelles, change their keratin (intermediate filament protein) expression and are no longer able to proliferate (Haake *et al*., 2001). The *stratum basale* is separated by a basement membrane from the underlying dermis. It consists primarily of mitotically active keratinocytes, namely keratinocyte stem cells, and transient amplifying cells (Bickenbach, 1981; Lavker and Sun, 1982; Bickenbach and Mackenzie, 1984). The stem cells are self-renewing and able to produce daughter transient amplifying (TA) cells that undergo a finite number of cell divisions before they differentiate and leave the proliferative basal compartment (Lajtha, 1979; Potten, 1997). The *stratum spinosum* is characterized by polyhedral keratinocytes, connected by desmosomes (intercellular adhesion complexes). The keratinocytes of the granular layer (*stratum*

granulosum) contain keratinohyaline granules (Holbrooke, 1989). Within these granules the filaggrin precursor is present which promotes aggregation of keratin filaments (Fukuyama *et al*., 1980; Dale, 1990). In the *stratum corneum* itself, the keratinization process ends with terminally differentiated cells, the corneocytes. Corneocytes are lacking nuclei and cytoplasmic organelles and form a resistant keratinous skeleton.

The dermis is the connective tissue component of the skin. The structural components of the dermis include collagen and elastic fibres as well as glycoproteins, proteoglycans and glycosaminoglycans (Uitto *et al*., 1999; Sakai *et al*., 1986; Yanagishita, 1994). Epidermal appendages, neurovascular networks, sensory receptors and dermal cells are embedded within. The dermis can be divided into the upper papillary dermis and the lower reticular dermis. The papillary dermis supplies the epidermis with nutrients and oxygen. It is characterized by a high cellularity, since fibroblasts and resident immune cells (lymphocytes, monocytes, macrophages, and mast cells) are located here. The lower reticular dermis is rich in collagen and elastic fibers and thereby provides elasticity and tensile strength. The innermost subcutaneous layer is predominantly consisting of adipocytes which are organized into lobules defined by septa of fibrous connective tissue. Nerves, vessels and lymphatics are located within the septa and richly supply the region. The hypodermis has the ability to protect the body from cold, to absorb trauma, and finally, it serves as an additional energy storage. Actively growing hair follicles extend into the subcutaneous fat and the apocrine and eccrine sweat glands are normally confined to this depth of the skin (Haake *et al*., 2001).

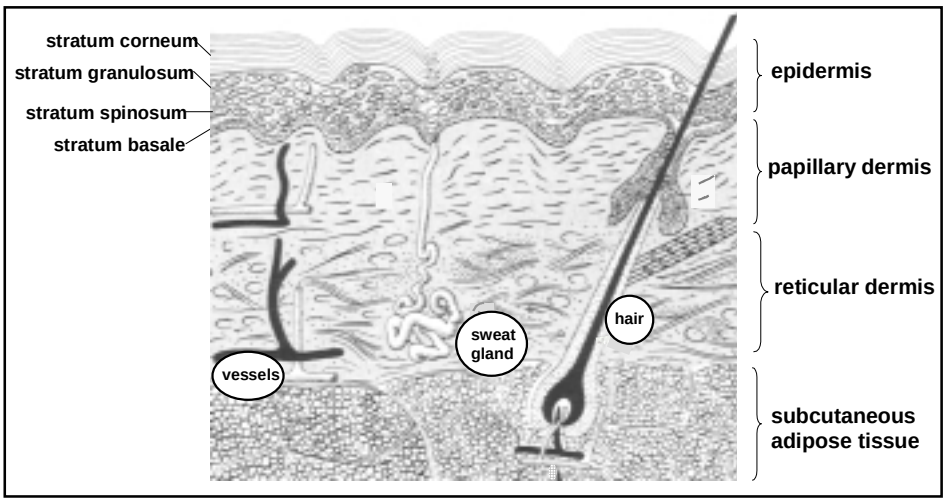

Figure 1 Overview of human skin architecture

1.2. Phases of cutaneous wound repair

The wound healing process which is initiated immediately upon injury is subdivided into different temporally and spatially overlapping phases, namely hemorrhage, inflammation, reepithelialization, granulation tissue formation and, the late phase of repair (Singer and Clark, 1999).

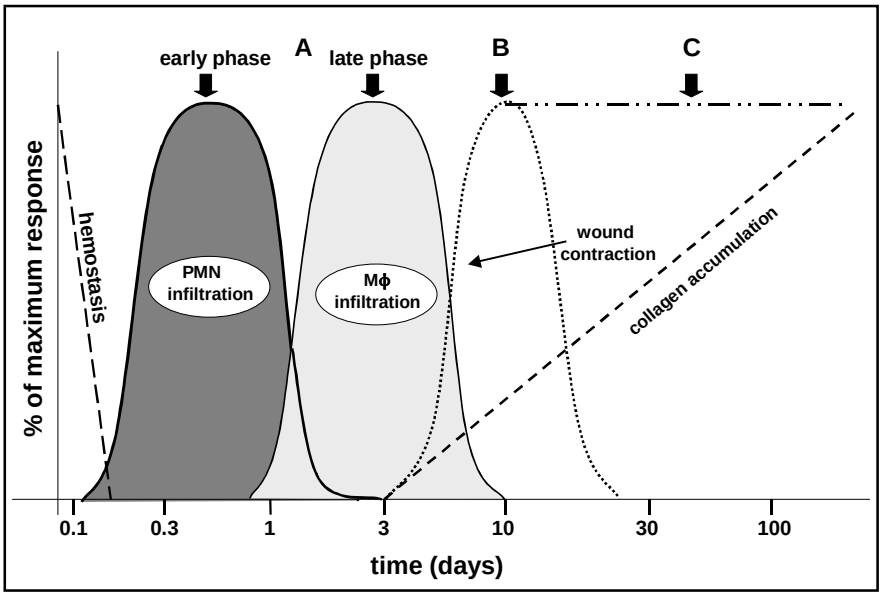

Figure 2 Phases of cutaneous wound repair.

Healing of a wound comprises different phases: (A) inflammation (early and late), (B) reepithelialization, angiogenesis and granulation tissue formation, and (C) matrix formation and remodeling. These wound repair processes are plottet along the abscissa as a logarithmic function of time. The phases of wound repair overlap in a temporal manner. Inflammation is divided into early and late phases denoting neutrophil-rich and monocytic-rich infiltrates, respectively. Begin of wound contraction is indicated by an arrow. Collagen accumulation begins shortly after the onset of granulation tissue formation (Clark, 1996: modified)

1.2.1. Hemorrhage

Wounding disrupts blood vessels and causes hemorrhage. Platelet aggregation and blood coagulation occurs, and a fibrin clot is formed. The clot is mainly composed of cross-linked fibers derived by thrombin-mediated cleavage of fibrinogen. Small amounts of plasma fibronectin, vitronectin and thrombospondin are also found (Clark, 1996; Martin, 1997). Activated platelets release a variety of different factors: fibrinogen, fibronectin and thrombospondin act as ligands for platelet aggregation (Clark, 1996), while von Willebrand factor enables platelet adhesion to fibrillar

collagens (Ruggeri, 1993). Furthermore, the fibrin clot serves as a matrix scaffold for the recruitment of circulating inflammatory cells to the wound site. The recruitment is ensured by different chemotactic and/or mitogenic factors released from degranulating platelets. These factors include the platelet-derived growth factor (PDGF), epidermal growth factor (EGF), transforming growth factor-α and -β (TGF-α, TGF-β) and insulin-like growth factor-1 (IGF-1) (Ross and Raines, 1990; Derynck, 1988; Sporn and Roberts, 1992; Naney and King, 1996; Rappolee *et al*., 1988).
Taken together, the blood clot reestablishes hemostasis, it represents a matrix for invading cells and it serves as a reservoir of growth factors, required during the later stages of tissue regeneration.

1.2.2 Inflammation

The inflammatory phase starts as polymorphonuclear neutrophils (PMN) enter the wound bed. PMN, which are potently attracted by the CXC- (α-) chemokines including interleukin-8 (IL-8) (Luster, 1998; Baggiolini, 1998), arrive in great numbers within minutes after wounding. Additionally, PMN are attracted by more general leukocyte chemoattractants, such as fibrinopeptides (cleaved from fibrinogen by thrombin), fibrin degradation products (produced by plasmin degradation of fibrin), C5a (generated after the activation of the complement cascade), leukotriene B_4 (released by activated neutrophils), platelet activating factor (PAF, released from endothelial cells or activated neutrophils) (Clark, 1996). They immediately start to attack bacteria in the wound area via phagocytosis, enzymatic mechanisms and production of highly reactive oxygen species (ROS) (Tonnesen *et al*., 1988; Elsbach and Weiss, 1992; Klebanoff, 1992). Notably, PMN have been shown to produce IL-1α, -1β and TNF-α which are early activators of growth factor expression in macrophages, keratinocytes, and fibroblasts (Hübner *et al*., 1996). Recently, Dovi *et al.* (2003) investigated the role of neutrophils in wound healing by neutrophil depletion. Neutropenia, induced by injection of a rabbit anti-mouse neutrophil serum, accelerated the rate of wound epithelial closure without altering the overall quality of the dermal healing process. During undisturbed healing, neutrophil cell number rapidly declines after a few days. Neutrophils become entrapped within the wound clot or die by apoptosis. The cells are subsequently phagocytosed by macrophages (Newman *et al*., 1982). While neutrophil cell numbers decline, macrophages (Mϕ)

continue to accumulate, thus becoming the predominant leukocyte cell type. Monocytes are preferentially attracted through CC- (β-) chemokines such as macrophage inflammatory protein-1α (MIP-1α) and monocyte chemoattractant protein-1 (MCP-1) (DiPietro *et al*., 1995, 1998). Factors that trigger the process of Mϕ activation are tissue debris, bacterial factors, cell-derived mediators and microenvironmental conditions (e.g. hypoxia). Activated Mϕ release a variety of growth factors and cytokines (DiPietro *et al*., 1995; Moulin, 1995), mediating angiogenic (basic fibroblast growth factor [bFGF], TGF-α, TGF-β, TNF-α) or fibrotic (PDGF,TGF-β) properties. Mϕ facilitate extracellular matrix degradation by expression of matrix degrading proteases and by regulation of fibroblast metalloprotease secretion (Riches, 1996). Leibovich and Ross (1975) demonstrated the central role of the tissue Mϕ for wound repair, since depletion of Mϕ led to a severe impairment of wound healing. The authors observed a severe retardation of tissue debris and a delay in fibroblast proliferation and fibrosis.

Close to the end of the inflammatory phase, T-lymphocytes come into play, peaking at day 7 of repair (Fishel *et al*., 1987). Their major function is assumed to be the downregulation of fibrous tissue growth. T-helper cells ($CD4^+$) drive the process of tissue regeneration while cytotoxic T-cells ($CD8^+$) are more likely to interfere with the repair process (Barbul and Regan, 1990). γδT-cells are found to stimulate keratinocyte proliferation by producing keratinocyte growth factor (KGF) (Boismenu and Havran, 1994). Furthermore, T-cells release angiogenic mediators such as heparin-binding EGF (HB-EGF) and bFGF (Blotnick *et al*., 1994). T-cells and Mϕ are detectable beyond the acute inflammatory phase of repair suggesting a function which is not restricted to the inflammatory response during tissue regeneration.

1.2.3 Reepithelialization

The process of reepithelialization starts within hours upon injury as keratinocytes of the cut edge begin to migrate. Notably, hair follicle remnants behave like normal cut epidermal wound edges and spread out from the follicle stump (Martin, 1997; Gambardella and Barrandon, 2003). Keratinocyte migration is characterized by several morphological changes. The basal keratinocytes lose polarity which is maintained as long as the cells remain in contact to the basement membrane (Odland and Ross, 1968). Cells become flat and elongated, and form peripheral

cytoplasmic actin filaments (lamellipodia) (Gabbiani *et al*., 1978). Remarkably, those keratinocytes display a more basal-like phenotype as they do not differentiate. However, they differ from cells of the basal layer as they contain involucrin, a cellular marker for keratinocyte differentiation (Mansbridge and Knapp, 1987). In order to crawl through the wound bed, the migrating cells must be able to sense extracellular matrix proteins. This active contact guidance is achieved by the expression of integrins that recognize the extracellular matrix components fibronectin, vitronectin and collagen (Clark, 1990; Clark *et al*., 1996). Furthermore, migrating keratinocytes have to lyse the provisional matrix of the wound bed. To this end, keratinocytes upregulate a fibrinolytic machinery that consists of enzymes such as tissue-type plasminogen activator and urokinase-type plasminogen activator (Grondahl-Hansen *et al*., 1988; Romer *et al*., 1991, 1994), and different members of the matrix metalloprotease (MMP) family such as gelatinase B (MMP-9) (Salo *et al*., 1994), interstitial collagenase (MMP-1) (Pilcher *et al*., 1997), and stromelysin-2 (MMP-10) (Saarialho *et al*., 1994). To overcome the loss of cells during wounding, epithelial cells start to proliferate at the wound margin. Different growth factors and growth factor receptors are discussed to initiate this proliferation (Singer and Clark, 1999). Members of the EGF and FGF family are considered to be key players (Nanney *et al*., 1990; Werner *et al*., 1994; Nanney and King, 1996; Abraham and Klagsbrun, 1996; Werner and Grose, 2003). The EGF family of mitogens comprises several members, including EGF, TGF-α, and HB-EGF which exert their function via binding to the EGF-receptor (EGF-R). Binding to the EGF-R initiates a cascade of signal transduction events that induce migration and proliferation of keratinocytes (Barrandon and Green; 1987; Chen *et al*., 1994; Danilenko *et al*., 1995; Cha *et al*., 1996;). Furthermore, EGF and TGF-α were reported to enhance reepithelialization when exogenously applied to burn wounds (Brown *et al*., 1986; Schultz *et al*., 1987). FGF7 (keratinocyte growth factor, KGF-1) is a specific and potent growth factor for epithelial cells, at least in the adult organism (Werner, 1998). It has been shown that FGF7 is upregulated in both, mouse and human wounds (Werner *et al*., 1992; Marchese *et al*., 1995). FGF7 acts in a paracrine manner, since FGF7 mRNA is predominantly detected in dermal fibroblasts adjacent to the wound and in fibroblasts of the granulation tissue, but its specific receptor FGFR2IIIb (splice variant of FGF receptor 2 (FGFR2) (Ornitz *et al*., 1996)) is expressed in keratinocytes of the normal and wounded epidermis as well as in hair follicles of murine, porcrine, and human

wounds (Danilenko *et al*., 1995; Marchese *et al.*, 1995). It has been demonstrated by Werner *et al.* (1994) that wounds of transgenic mice which express a dominant-negative FGFR2IIIb mutant in the epidermis displayed a severe delay in reepithelialization. Another factor that participates in the process of reepithelialization is nitric oxide (NO). NO has been convincingly shown to be a mitogenic mediator for keratinocytes *in vitro* (Krischel *et al*., 1998; Frank *et al*., 2000a) and *in vivo* (Frank *et al*., 2002; Stallmeyer *et al*., 1999; Yamasaki *et al*., 1998; Frank *et al*., 1998a). Additionally, the cytokine leptin contributes to cutaneous reepithelialization processes (Frank *et al*., 2000b; Stallmeyer *et al*., 2001).

TGF-β1 has been suggested as a negative regulator of keratinocyte proliferation *in vitro* and *in vivo* (Coffey *et al*., 1988; Sarret *et al*., 1992; Sellheyer *et al*., 1993).

1.2.4 Granulation tissue formation

Formation of the granulation tissue starts approximately 4 days after injury. Mϕ, fibroblasts, and blood vessels move into the wound bed at the same time (Hunt, 1980). Mϕ provide a continuous source of growth factors which stimulate fibrotic and angiogenic processes. Fibroblasts synthesize new extracellular matrix to support fibroblast and endothelial cell ingrowth. Newly formed blood vessels supply oxygen and nutrients to sustain cell metabolism. Fibroblasts located within the developing granulation tissue are characterized by three main capacities: proliferation, migration and production of extracellular matrix. Due to cytokines and extracellular-matrix molecules present at the wound site, resident fibroblasts adjacent to the injured tissue start to proliferate and move into the wounded area (Nathan and Sporn, 1991; Gray *et al*., 1993; Xu and Clark, 1996). Moreover, fibroblasts are activated to secrete important mediators such as KGF and connective tissue growth factor (CTGF) (Werner *et al*., 1992; Igarashi *et al*., 1993). The actual migration of fibroblasts predominantly occurs via fibronectin bundles (Hsieh and Chen, 1983), which are the main component of the provisional blood clot. Binding to the substratum is mediated via integrin receptors on the surface of invading fibroblasts (Ruoslahti, 1991; Hynes, 1992). The upregulation of integrins is induced by PDGF and TGF-β1 (Heino *et al*., 1989; Ahlen and Rubin, 1994; Gailit *et al.,* 1996). In order to make their way through the provisional matrix fibroblasts also synthesize proteolytic enzymes, such as matrix metalloproteinases MMP-1 (collagenase), -2 (gelatinase) and -3 (stromelysin)

(Mignatti, 1996; Vaalamo *et al.,* 1997). After invading and activation, wound fibroblasts switch on extracellular matrix protein synthesis. The provisional extracellular matrix is gradually replaced by collagens (Welch *et al*., 1990). This collagen production is believed to be stimulated by TGF-β1 (Ignotz and Massague, 1986; Roberts *et al*., 1986) which is found in high amounts during the granulation phase of repair (Frank *et al*., 1996). Some fibroblasts differentiate into myofibroblasts, harboring smooth muscle actin and thus, provide the motive force for wound contraction (Desmouliere and Gabbiani, 1996). The contraction is likely to require stimulation by TGF-β1, β2 (Montesano and Orci, 1988) and PDGF (Clark *et al*., 1989), attachment of fibroblasts to the collagen matrix through integrin receptors (Schiro *et al*., 1991), and cross-links between individual bundles of collagen (Woodley *et al*., 1991). Interestingly, wound contraction is only present in adult skin wounds, as fetal wounds heal without contraction (Ferguson *et al*., 1996; Martin, 1996). The endpoint of granulation tissue formation is reached as fibroblasts undergo apoptosis and fibroblasts-rich granulation tissue is converted into a relative acellular scar (Desmouliere *et al*., 1995).

1.2.5 Neovascularisation

New blood vessels are formed in the granulation tissue in order to supply the newly formed tissue with oxygen and nutrients. Invading endothelial cells derive from the microvasculature (Madri *et al*., 1991, 1992a,b). Capillary buds sprout from blood vessels adjacent to the wound and extend into the wound space. On the sprouting tip of ingrowing capillaries $\alpha_V\beta_3$ integrins are present, allowing binding to fibrin, fibronectin and vitronectin of the provisional matrix (Brooks *et al*., 1994). Additionally, movement into granulation tissue through digestion of the basement membrane is promoted via plasmin and collagenase. Both proteases are activated by the action of plasminogen activator which is released from endothelial cells upon stimulation with bFGF (Clark, 1996; Pintucci *et al*., 1996). A major regulator of angiogenesis is vascular endothelial growth factor (VEGF), which is one of the most potent stimulators for endothelial cell proliferation *in vitro* (Keck *et al.,* 1989). The VEGF family currently includes VEGF-A, -B, C, D, E and placenta growth factor (PLGF). In fact, VEGF-A is strongly upregulated upon wounding and keratinocytes, together with Mϕ, are the major producers (Brown *et al*., 1992; Frank *et al*., 1995). Reduced VEGF-

A expression or its accelerated degradation are associated with impaired wound healing (Frank *et al*., 1995; Swift *et al*., 1999; Lauer *et al*., 2000; Kämpfer *et al.,* 2001). It has been demonstrated that proinflammatory cytokines can induce expression of VEGF in keratinocytes and Mϕ (Frank *et al*., 1995; Perez-Ruiz *et al*., 1999). Additionally, several growth factors, including FGF7, EGF, TGF-α and hepatocyte growth factor (HGF) have been shown to stimulate the production of VEGF by cultured keratinocytes (Detmar *et al*., 1995; Frank *et al.,* 1995; Gille *et al*., 1998). Recently, PLGF has been identified as a regulator of wound angiogenesis, since PLGF knock-out mice were characterized by impaired wound healing as a result of a defect in angiogenesis (Carmeliet *et al*., 2001). There are several other molecules and conditions that mediate angiogenic properties, including IL-8, PDGF, biogenic amines and lactic acid as well as low oxygen tension (Folkman and Shing, 1992; Koch *et al*., 1992; Battegay *et al*., 1994; Lane *et al*., 1994). Resolution of the angiogenic process (termination and stabilization of new vessels) is most likely regulated via a well-defined homeostasis of pro- and anti-angiogenic mediators (Iruela-Arispe and Dvorak, 1997). Factors that are associated with the phase of resolution include thrombospondins 1 and 2, angiostatin, endostatin and angiopoietin 2 (Guo *et al*., 1997; Folkman, 1997; Holash *et al*., 1999; Kämpfer *et al*., 2001).

1.2.6 Remodeling

The remodeling of the extracellular matrix and maturation of the neoepidermis, fibroplasia, and neovasculature begin at the wound margin while granulation tissue is still invading the wound space (Kurkinen *et al*., 1980). Initially, the extracellular matrix is rich in fibronectin but as soon as fibroblasts start their synthesizing activity (see *1.2.4*), collagen becomes the predominant constituent. Subsequently, this randomly distributed collagen fibers become cross-linked and aggregate into fibrillar bundles. Due to this process the healing tissue gains tensile strength. The matrix alteration is due to a well coordinated process of collagen synthesis and collagen degradation which is controlled by extracellular collagenases, i.e. matrix metalloproteinases (Mignatti, 1996). However, the collagen bundles of scar tissue are organized in parallel but not in a basket-weave meshwork as it is typical for unwounded skin. Thus, the breaking strength of injured tissue is lower (≤70%) compared to intact skin

(Levenson *et al*., 1965). Furthermore, lost epidermal appendages do not regenerate, nor do nerves or melanocytes (Martin, 1997).

1.3 Nitric oxide and skin

Nitric oxide (NO) is a free radical gas, which has been recognized as a versatile player involved in a variety of different physiological and pathophysiological processes (Beck *et al.,* 1999; Moncada *et al*., 1991). The synthesis of NO is catalyzed by NO synthases (NOS) which exist in three distinct isoforms: endothelial (eNOS), neuronal (nNOS) and inducible NOS (iNOS) (Nathan and Xie, 1994). eNOS is mainly expressed in endothelial cells, while nNOS is predominantly present in neurons. However, both enzymes have been found in many other cells and tissues (Nakane *et al*., 1993; Gath *et al*., 1996; Shimizu *et al*., 1997; Stallmeyer *et al*., 2002). nNOS and eNOS, which are regulated by Ca^{2+} fluxes and subsequent binding to calmodulin, have been considered to be constitutively expressed proteins (MacMicking *et al*., 1997). However, it turned out that these two isoforms are also subject to expressional regulation (Förstermann *et al*.,1998). By contrast, the inducible isoform (iNOS) is expressed upon stimulation by inflammatory cytokines or endotoxin in a variety of different cell types (Moncada *et al.*, 1991; Nathan and Xie, 1994). All three NOS isoenzymes are homodimeric proteins which catalyze the oxidation of the amino acid L-arginine to give rise to citrulline and NO. The activity of the NO synthases depends on nicotinamide adenine dinucleotide phosphate (NADPH), reduced flavins, heme-bound iron, and 6 (R) 5,6,7,8-tetrahydrobiopterin (BH_4) as essential cofactors (Baeck *et al.,* 1993; Klatt *et al*., 1993).

All three NOS isoforms are present in the skin, with respect to different distributions. nNOS is reported to be expressed in keratinocytes and melanocytes (Baudouin and Tachon, 1996; Romero-Graillet *et al*., 1996; Boissel *et al*., in press) while eNOS could be detected in keratinocytes of the basal layer, dermal fibroblasts, endothelial capillaries, and ecrine glands (Wang *et al*., 1996; Shimizu *et al*., 1997). Skin keratinocytes, fibroblasts, Langerhans and endothelial cells express iNOS (Wang *et al*., 1996; Bruch-Gerharz *et al*., 1996; Sirsjo *et al*., 1996; Qureshi *et al*., 1996, Kuhn *et al*., 1998). The NOS give rise to NO which is involved in the modulation of the microvascular tone and permeability in the skin, the regulation of melanogenesis and as a protecting agent against invading pathogens (Bruch-Gerharz *et al*., 1998). Moreover, the presence of iNOS has been described for inflammatory skin diseases

such as psoriasis (Bruch-Gerharz *et al*., 1996; Frank *et al*., 2000a), lupus erythematosus (Kuhn *et al*., 1998), inflammatory dermatoses (Rowe *et al*., 1997), and hypersensitivity reactions (Bruch-Gerharz *et al*., 1998). In fact, NO plays an important role throughout the process of wound healing. Yamasaki *et al.* (1998) convincingly showed a functional evidence for iNOS-derived NO during repair. The authors demonstrated that a delayed wound closure present in iNOS deficient mice could be reversed by adenoviral-mediated expression of human iNOS cDNA. Upon wounding, iNOS expression is dramatically induced and persists during inflammation, granulation tissue formation and reepithelialization (Frank *et al*., 1998a). Remarkably, iNOS expression is not restricted to PMN and Mϕ, as proliferating keratinocytes of the wound margins, and to a smaller extent also wound fibroblasts express iNOS (Frank *et al*., 1998a; Reichner *et al*., 1999). The observation that proliferating keratinocytes of the wound margins strongly express iNOS (Frank *et al*., 1998a) and that this proliferation is decreased by the iNOS inhibitor L-NIL (Stallmeyer *et al*., 1999), pointed towards a role of NO to serve as a keratinocyte mitogen. Keratinocytes tend to respond to NO in a biphasic manner: increased proliferation is mediated by low NO concentrations, while keratinocytes differentiate in the presence of high NO concentrations (Krischel *et al.,* 1998). Additionally, NO is linked to keratinocyte gene expression, since the important angiogenic factor VEGF (Frank *et al*., 1999) and chemokines (Frank *et al*., 2000c; Wetzler *et al*., 2000) have been shown to be dependent on the availability of iNOS-derived NO at the wound site. The deposition of wound matrix by fibroblasts is likely to be regulated by NO, also, since Schaffer *et al.* (1996) demonstrated that the inhibition of wound NO synthesis is paralleled by a decreased wound collagen synthesis. Moreover, an increase in collagen accumulation could convincingly be linked to iNOS-derived NO production *in vivo* (Thornton *et al*., 1998).

It has been demonstrated that eNOS is also participating in cutaneous healing, since eNOS deficient mice are characterized by a delayed excisional wound closure and reduced wound breaking strength (Lee *et al.,* 1999). The observed data indicate an important role for eNOS-derived NO in extracellular matrix production. Furthermore, the authors suggest defects in angiogenesis during repair. Stallmeyer *et al.* (2002) observed a reduced proliferative activity in wound keratinocytes in eNOS deficient mice.

1.4 RNA helicases

RNA helicases are highly conserved and found in all organisms from bacteria to humans and in many viruses. The main function of RNA helicases is likely to be the unwinding of dsRNA (de la Cruz *et al*., 1999; Tanner and Linder, 2001) or RNA-protein complexes (Staley and Guthrie, 1998; Jankowsky *et al*., 2001; Linder *et al*., 2001; Schwer *et al*., 2001). Biochemical studies revealed that the unwinding occurs in an energy-dependent fashion through hydrolysis of nucleoside triphosphate (generally ATP) (Lüking *et al*., 1998). Most RNA helicases belong to superfamily II which is subdivided in DEAD (Asp-Glu-Ala-Asp) (Fig. 3) and DExH (Asp-Glu-x-His) box families according to consensus sequences in their conserved motifs (Wassermann and Steitz, 1991). It is now well established that RNA helicases are involved in various aspects of RNA metabolism such as nuclear transcription, pre-mRNA splicing, ribosome biogenesis, nucleocytoplasmic transport, translation, RNA decay, organellar gene expression, and virus propagation (de la Cruz *et al*., 1999; Kadare and Haenni, 1997). For example, the prototypic member of the DEAD-box family, the eukaryotic translation initiation factor eIF4A, promotes ribosome binding by unwinding the secondary structure in the 5` untranslated region of eukaryotic mRNAs (Pause and Sonenberg, 1992, 1993; Pause *et al*., 1993). In contrast to DNA helicases that unwind their substrate in a processive manner (West, 1997), RNA helicases are believed to modulate only short duplex regions, generally below 10 bp. In general, RNA helicases show very little substrate specificity when analyzed *in vitro* (Kim *et al*., 1998), a circumstance which seems to be also true for DNA helicases (Caruthers *et al*., 2000; Lin and Kim, 1999).

1.4.1 p68 RNA helicase

p68 was initially discovered by a cross-reaction with an antibody against simian virus (SV) 40 large T protein (Lane and Hoeffler, 1980). p68 RNA helicase, which is encoded by a single gene locus on chromosome 17 in humans, is a prototypical member of the DEAD-box family (Ford *et al*., 1988, Hirling *et al*., 1989) (Fig. 3).

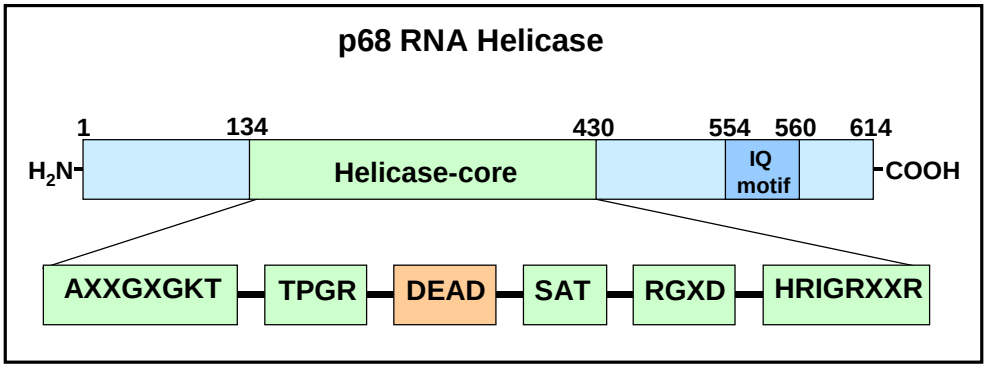

Figure 3 Schematic illustration of domain structure of p68 RNA helicase.

The lower panel represents the helicase-core region of DEAD-box proteins: motifs **AXXGXGKT**, **TPGR** and **DEAD** comprise the NTP-binding and hydrolysis domains; **SAT** motif links NTP hydrolysis with unwinding activity; **RGXD** represents the substrate-binding motif; **HRIGRXXR** motif binds RNA. The IQ domain in the upper panel contains CaM binding and PKC phosphorylation sites (Yang *et al*., 2003; modified)

Sequence analysis of p68 cDNA revealed a striking homology to eIF-4A (Ford *et al.*, 1988) leading to the definition of DEAD box family of proteins (Linder *et al.,* 1989). p68 helicase shows ATP-dependent RNA helicase and RNA-dependent ATPase activities *in vitro* (Iggo and Lane, 1989) and is, besides eIF-4A, the second example of a DEAD-box RNA helicase that is able to unwind RNA duplexes in a bi-directional manner (Pause *et al.,* 1992; Huang and Liu, 2002). p68 RNA helicase is highly conserved throughout evolution. Human and murine p68 proteins are 98% identical (Lemaire and Heinlein, 1993), and even the *Saccharomyces cerevisiae* p68 homologue shares 55% sequence identity with the human protein (Iggo *et al*., 1991). Moreover, protein function appears to be even more conserved, as the growth defect in *S. cerevisiae* DBP2 null cells could be reversed by human p68 (Bond *et al*., 2001). p68 RNA helicase was shown to be nearly absent in quiescent cells, but dramatically induced upon serum treatment implying a functional link between expression and proliferation (Stevenson *et al*., 1998). However, expression levels of p68 protein do not always correlate to the proliferation status in adult tissue, although there is evidence that p68 expression correlates with organ differentiation and maturation of the fetus (Stevenson *et al*., 1998). Additionally, p68 has been demonstrated to be overexpressed in nuclei of epithelial cells under hyperproliferative conditions of colorectal adenocarcinoma (Causevic *et al*., 2001). Immunocytochemical studies revealed a granular nuclear staining which is excluded from the nucleoli during interphase (Lane and Hoeffler, 1980; Iggo *et al*., 1989). During late telophase,

however, p68 was found to co-localize with the nucleolar protein fibrillarin in nascent nucleoli (Nicol *et al*., 2000). Moreover, p68 has been identified as a member of the IQ domain-containing family (Buelt *et al*., 1994). The IQ domain is a 19 amino acid sequence, containing a calmodulin (CaM) binding and a protein kinase C (PKC) phosphorylation site. Studies with recombinant p68 showed that both Ca^{+}-dependent CaM binding and PKC phosporylation inhibited p68 ATPase function, suggesting a possible way of p68 RNA helicase regulation (Buelt *et al*., 1994).

1.5 Aim of the thesis

Nitric oxide (NO) is an important messenger molecule in normal skin biology and also diseased skin (Weller, 1999; Bruch-Gerharz *et al*., 1998). Studies on skin tissue have also demonstrated a key function of NO in the process of cutaneous wound healing (Frank *et al*., 2002). Moreover, NO is known to function as a potent mitogenic mediator for keratinocytes *in vitro* (Krischel *et al*., 1998; Frank *et al*., 2000a) and during the process of reepithelialization *in vivo* (Frank *et al*., 1998a, Stallmeyer *et al*., 1999). However, it is particularly not much known about how NO exerts its unique actions on keratinocytic cells. To gain further insight into these mechanisms, we established and subsequently screened a subtractive keratinocyte cDNA library, which was enriched for NO-regulated genes. In fact, we were aiming for new players, which could provide the “missing link” between NO and the resulting mitogenic response in keratinocytes. We identified p68 DEAD box RNA helicase as a novel NO-induced gene in keratinocytes. Published data suggest p68 to play a role in cell growth and division (Lane and Hoeffler, 1980; Stevenson *et al*., 1998; Tanner and Linder, 2001). Additionally, p68 is discussed to be involved in transcription (Endoh *et al*., 1999; Watanabe *et al*., 2001; Rossow and Janknecht, 2003). Due to these observations p68 might at least partially contribute to or, moreover, mediate some of the well-established actions of NO in keratinocyte biology, such as regulation of gene expression and keratinocyte proliferation.

2

Materials and Methods

2.1 Materials

2.1.1 Chemicals

[α-^{32}P]UTP	Amersham Pharmacia, Braunschweig
5-Bromo-4-chloro-3-indolyl-β-D-galactoside	Roth, Karlsruhe
8-Hydroxyquinoline	Sigma Aldrich Fine Chemicals, Deisenhofen
Acrylamide/bisacrylamide-solutions	Roth, Karlsruhe
Actinomycin D	Sigma Aldrich Fine Chemicals, Deisenhofen
Agar	Gibco Life Technologies, Karlsruhe
Agarose	Biozym, Oldendorf
Ammoniumpersulfate	Sigma Aldrich Fine Chemicals, Deisenhofen
Ampicillin	Sigma Aldrich Fine Chemicals, Deisenhofen
Aprotinin	Roche Biochemicals, Mannheim
Aquatex mounting media	Merck, Darmstadt
Bovine serum albumin	Sigma Aldrich Fine Chemicals, Deisenhofen
Cell culture media	Gibco Life Technologies, Karlsruhe
Cycloheximide	Sigma Aldrich Fine Chemicals, Deisenhofen
DETA NONOate	Calbiochem, Schwalbach
Diamidino phenylindole	Sigma Aldrich Fine Chemicals, Deisenhofen
Diethylpyrocarbonate	Sigma Aldrich Fine Chemicals, Deisenhofen
Dithiothreitol	Sigma Aldrich Fine Chemicals, Deisenhofen
EDTA	Sigma Aldrich Fine Chemicals, Deisenhofen
EGTA	Sigma Aldrich Fine Chemicals, Deisenhofen
Ethidium bromide	Sigma Aldrich Fine Chemicals, Deisenhofen
Fetal calf serum	Gibco Life Technologies, Karlsruhe
G418	Gibco Life Technologies, Karlsruhe
Glutathione	Sigma Aldrich Fine Chemicals, Deisenhofen
Guanidinium thiocyanate	Sigma Aldrich Fine Chemicals, Deisenhofen
Hematoxylin solution	Sigma Aldrich Fine Chemicals, Deisenhofen
Hydroxylammoniumchloride	Merck, Darmstadt
Isopropylthiogalactoside	Roth, Karlsruhe
JNK Inhibitor I	Calbiochem, Schwalbach
Ketamin (-hydrochloride)	Amersham Pharmacia, Braunschweig
Leupeptin	Roche Biochemicals, Mannheim
Lipofectamine	Gibco Life Technologies, Eggenstein
Lipopolysaccharide	Sigma Aldrich Fine Chemicals, Deisenhofen
L-N^6-(1-iminoethyl)lysine	Alexis, Grünberg

Molecular weight markers (DNA)	MBI Fermentas, St. Leon-Rot
Molecular weight markers (protein)	Amersham Pharmacia, Braunschweig
N^G-monomethyl-L-arginine	Alexis, Grünberg
N-naphtylethylendiamine dihydrochloride	Sigma Aldrich Fine Chemicals, Deisenhofen
NS 2028	Alexis, Grünberg
Nucleotide triphosphates	*PE* Biosystems, Weiterstadt
ODQ	Alexis, Grünberg
Oligonucleotides	MWG Biotech, Ebersberg
Pepstatin A	Roche Biochemicals, Mannheim
Peptone	Gibco Life Technologies, Eggenstein
Phenol	Roth, Karlsruhe
Phenylmethylsulfonyl fluoride	Roche Biochemicals, Mannheim
Phytohaemagglutinin	Roche Biochemicals, Mannheim
Ponasterone A	InVitrogen, Groningen, Netherlands
Ponceau S	Serva, Heidelberg
RNasin	Promega, Mannheim
SB 202190	Calbiochem, Schwalbach
Skim milk (non fat)	Fluka, Deisenhofen
Sn-Protoporphyrin IX	Alexis, Grünberg
Sodium nitroprusside	Sigma Aldrich Fine Chemicals, Deisenhofen
Sodiumlaurylsarcosyl	Serva, Heidelberg
Spermine-NONOate	Calbiochem, Schwalbach
Sulfanilamide	Sigma Aldrich Fine Chemicals, Deisenhofen
Tetramethylethylendiamine	Sigma Aldrich Fine Chemicals, Deisenhofen
Tissue freezing media	Leica Instruments, Nussloch
Triton X-100	Sigma Aldrich Fine Chemicals, Deisenhofen
tRNA, RNase free	Roche Biochemicals, Mannheim
Trypan blue	Gibco Life Technologies, Eggenstein
Tween 20	Sigma Aldrich Fine Chemicals, Deisenhofen
U0126	Calbiochem, Schwalbach
Xylazin (-hydrochloride)	Bayer, Leverkusen
YC-1	Alexis, Grünberg
Yeast extract	Gibco Life Technologies, Eggenstein
[^{35}S]methionine- and [^{35}S]cystein pro mix	Amersham Pharmacia
α-^{32}P[CTP]	Amersham Pharmacia, Braunschweig
β-Mercaptoethanol	Sigma Aldrich Fine Chemicals, Deisenhofen

Acetone, acids, chloroform, ethanol, ether, methanol and isopropanol were from the supply store of the Universitätsklinikum Frankfurt. All other, not listed chemicals were purchased from Merck (Darmstadt), Roth (Karlsruhe) or Sigma Biochemicals (Deisenhofen).

2.1.2 Other materials and kits

ECL detection system	Amersham Pharmacia, Braunschweig
Human VEGF ELISA	R & D Systems, Wiesbaden
Nanoquant	Roth, Karlsruhe
NucleoSpin Extrakt 2 in 1	Machery & Nagel, Düren
PCR-Select^{TM} cDNA Substraction Kit	Clontech, Heidelberg
Plasmid Purification kit (Qiagen-tip 100)	Qiagen, Hilden
siRNA	Qiagen-Xeragon, Germantown, USA
TNT^{R} Coupled Reticulocyte Lysate System	Promega, Mannheim
AdvanTAge PCR Cloning Kit	Clontech, Heidelberg
NucleotrapR mRNA Kit	Machery & Nagel, Düren

2.1.3 Laboratory equipment

ABI-Prism 310 Genetic Analyser	Applied Biosytems Applera, Weiterstadt
Circular shaker	Unitron Infors AG, Bottmingen, Switzerland
Gel dryer 583	Bio-Rad, München
Gene Quant II	Amersham Pharmacia, Braunschweig
GeneAmp 2400/9600 Thermocycler	Applied Biosytems Applera, Weiterstadt
GS Gene Linker	Bio-Rad, München
Herasafe clean bench	Heraeus, Hanau
Incubator Heraeus BBD 6220	Heraeus, Hanau
Microplate reader Benchmark	Bio-Rad, München
Phosphoimager BAS 1500	Raytest, Straubenhardt
Trans-Blot SD	Bio-Rad, München
TRI-CARB 2100 TR β-counter	Canberra-Packard, Dreieich
UltraTurrax	IKA, Staufen
Zeiss LSN 510 META	Zeiss, Jena

2.1.4 Enzymes

Alkaline phosphatase	Roche Biochemicals, Mannheim
Pfu-DNA polymerase	Stratagene, Heidelberg
Proteinase K	Roche Biochemicals, Mannheim
Restriction enzymes	MBI-Fermentas, St. Leon-Rot Roche Biochemicals, Mannheim; Stratagene, Heidelberg;
Reverse transcriptase	Gibco Life Technologies, Eggenstein
RNA polymerase T3 and T7	Roche Biochemicals, Mannheim
RNase A and T1	Roche Biochemicals, Mannheim
T4-DNA ligase	Roche Biochemicals, Mannheim
Taq-DNA polymerase	Roche Biochemicals, Mannheim

2.1.4.1 Pretreatment of enzymes

Proteinase K

The lyophilized enzyme was dissolved in $Aqua_{dest}$ (10 mg/ml), incubated for 30 min at 37°C and aliquoted. The aliquots were stored at –20°C until use.

RNase A

RNase A was dissolved to a final concentration of 10 mg/ml in RNase-buffer [Tris/HCl (10 mM, pH 7.5), NaCl (15 mM)]. The enzyme solution was incubated for 30 min at 95°C and cooled to room temperature over night. Aliquots were stored at –20°C until use.

2.1.5 Antibodies and antisera

anti-human *C23/ Nucleolin* (mouse, monoclonal)	Santa Cruz Biotechnologies, Heidelberg
anti-*green fluorescent protein* (mouse, monoclonal)	Roche Biochemicals, Mannheim
anti-murine *Ki-67* (rabbit, polyclonal)	Dianova, Hamburg
anti-human *PCNA* (rabbit, polyclonal)	Santa Cruz Biotechnologies, Heidelberg
anti-human *p68* (rabbit, polyclonal)	Eurogentec, Belgium
anti-mouse IgG (FluoroLink^{TM}Cy^{TM}3 labelled)	Amersham Pharmacia, Freiburg
anti-mouse IgG (horseradish-peroxidase coupled)	Pierce, Rockford, USA
anti-rabbit IgG (horseradish-peroxidase coupled)	Dianova, Hamburg

2.1.6 Recombinant and purified proteins

EGF	Roche Biochemicals, Mannheim
IFN-γ (human)	PeproTech, Frankfurt
IFN-γ (human)	Roche Biochemicals, Mannheim
IL-1β	Roche Biochemicals, Mannheim
KGF	Roche Biochemicals, Mannheim
TGF-α	Roche Biochemicals, Mannheim
TGF-β	Roche Biochemicals, Mannheim
TNF-α	Roche Biochemicals, Mannheim

2.1.7 Plasmids

2.1.7.1 Vectors

pBluescript II KS (+)	Stratagene, Heidelberg
pcDNA3.1 (+)	InVitrogen, Groningen, Netherlands
pEGFP-N1	Clontech Laboratories, Heidelberg

2.1.7.2 Recombinant plasmids

pBKS(+)*p68* (human, nucleotides 1891-2161)	Hloch *et al.* 1990; Acc.No.NM_004396
pBKS(+)*p68* (murine, nucleotides 551-785)	Lemaire and Heinlein, 1993
pBKS(+)*GAPDH* (human, nucleotides 148-302)	Tokunaga *et al.* 1987
pBKS(+)*GAPDH* (murine, nucleotides 128-282)	Sabath *et al.* 1990
pBKS(+)*VEGF* (human, nucleotides 339-498)	Weindel *et al.* 1992
pcDNA3.1 (+)*p68* (human, nucleotides 169-2018)	Hloch *et al.* 1990; Acc.No.NM_004396
pEGFP-N1*p68* (human, nucleotides 169-2012)	Hloch *et al.* 1990; Acc.No.NM_004396
pBKS(+)*PFK* (human, nucleotides 487-742)	Simpson and Fothergill-Gilmore, 1991

2.1.8 Bacterial strains

E. coli XL-1 blue	Stratagene, Heidelberg

2.1.9 Eukaryotic cell lines

HaCaT	Human adult keratinocytes [Boukamp *et al*. 1988]
HEK 293	kindly provided by H. Radeke, Frankfurt
PAM 212	Epidermal keratinocytes
pcDNA3.1p68	p68 RNA Helicase overexpressing HaCaT cells
RAW 264.7	Mouse macrophages (American Type Tissue Collection, Rockville, USA)

2.1.10 Buffers

PBS-buffer 10fold	1,5 M NaCl, 30 mM KCl, 15 mM KH_2PO_4, 60 mM Na_2HPO_4
TAE-buffer 10fold	400 mM Tris acetate, 10 mM EDTA
TBE-buffer 10fold	900 mm Tris borate, 20 mM EDTA
SSC-buffer 20fold	3 M NaCl, 300 mM Na_2Citrat

All buffers were prepared with highly purified water from a Milli-Q-system (Millipore).

2.1.11 S-nitroso-glutathione

Glutathione was dissolved in 0.625 N HCl at 0°C to a final concentration of 625 mM. $NaNO_2$ was added in an equimolar amount and the mixture was stirred at 0°C for 40 min. After the addition of 2.5 volumes of acetone stirring went on for additional 20 min, followed by filtration of the precipitate. GSNO was washed once with 80% acetone, two times with 100% acetone, and finally three times with diethylether and dried under vacuum. The powder was aliquoted in Eppendorf tubes and stored at –20°C until use.

2.1.12 Computer Software

DNA/protein homology search	BLAST search (National Center of Biotechnology, USA; URL: *http://www.ncbi.nlm.nih.gov*)
Graphic processing	Corel Draw 8.0 and 10.0
Presentations	PowerPoint 2000
Statistical analysis	Sigma Plot 4.0
Text processing	Microsoft Word 2000

Programs belonging to special devices are mentioned separately in the appropriate sections.

2.2 Bacterial culture

The *E. coli* strain XL1-blue (Stratagene) was used for amplification of plasmid DNA. Bacteria were grown in liquid LB (Lauria-Bertani) medium (1% bacto-tryptone w/v, 0,5% bacto-yeast-extract w/v and 1% NaCl w/v). For selection, the media contained ampicillin or kanamycin (50 µg/ml). Agar-plates were generated with LB-ampicillin or -kanamycin medium supplemented with agar (15 g/l). For long-term preservation of transformed bacteria (*2.2.2*), cells were mixed with sterile glycerol [30% (v/v)] and stored at –20°C.

2.2.1 Competent bacteria for transformation

To yield high transformation efficiencies from plasmid DNA in bacteria, cells have to be pretreated chemically. To this end, 100 ml LB-Medium were inoculated with 200 µl

of an overnight bacterial culture and grown at 37°C until the suspension reaches an optical density of 0.5 (OD_{600}). Bacterial cells were concentrated by centrifugation (15 min, 4000 rpm, 4°C; Heraeus Megafuge 1.0, rotor 7570F). The cellular pellet was subsequently resuspended in 33 ml solution A, mixed and incubated on ice for 45 min. The bacterial suspension was centrifuged again (15 min, 4000 rpm, 4°C), the pellet was gently resuspended in 9 ml of solution B and incubated on ice for additional 15 min. Aliquots of competent bacteria were snap frozen in liquid nitrogen and stored at –80°C.

Solution components	**Solution A** (sterile filtrated)	**Solution B** (sterile filtrated)
RbCl	100 mM	10 mM
$MnCl_2$	50 mM	---
$CaCl_2$	10 mM	75 mM
KOAc	30 mM	---
Glycerol	15% (v/v)	15% (v/v)
MOPS	---	10 mM

Transformation

100 µl of a competent bacteria suspension (*2.2.1*) were thawed on ice and 10 µl of the ligation reaction (*2.3.6.2*) was added. The bacteria/DNA mixture remained on ice for additional 30 min followed by an incubation at 42°C for 3 min. The bacteria were chilled on ice again for 2 min, before 300 µl of LB-medium were added. For initial expression of the plasmid encoded ampicillin resistance, bacteria were incubated for 45 min at 37°C on a circular shaker. Subsequently, 100 µl of this transformation solution were plated on ampicillin containing agar plates. To enable a blue/white screening for recombinant clones, the agar plate was supplemented with 100 µl X-Gal (2% w/v in DMF) and 40 µl IPTG (0.1 M in $Aqua_{dest}$). The plates were incubated overnight at 37°C.

2.3 Nucleic acid techniques

2.3.1 Preparation of plasmid DNA

Plasmids have been routinely isolated from bacterial cultures using a modified protocol originally described by Birnboim and Doly [1979]. 3 ml of medium containing the appropriate antibiotic(s) were inoculated with a single bacterial colony from a

selective agar plate and incubated overnight by vigorous shaking at 37°C. 1.5 ml of the cell-suspension was centrifuged for 2 min at 7000 x g, and the medium was removed carefully by aspiration. The bacterial pellet was resuspended in 100 µl of solution I. Subsequently, 200 µl of freshly prepared solution II were added to the dispersed bacteria, mixed five times by inverting the tubes and stored on ice for exactly five minutes. This step lyses the bacterial cells and denatures the DNA. The lysate was neutralized by 150 µl acidic potassium buffer (solution III), which was gently mixed after addition and stored on ice for additional 10 minutes. The high salt concentration causes SDS to precipitate, and the denatured proteins, cellular debris and chromosomal DNA become trapped by salt-detergent complexes. Plasmid DNA, being smaller and covalently closed, renatures correctly and remains in solution. The tube was centrifuged for 10 min at 15,000 x g and the supernatant containing the plasmids transferred to a new Eppendorf tube. A subsequent cleaning step using phenol/chloroform was performed optionally, as trace amount of phenol could disturb subsequent enzymatic reactions processing the plasmid-DNA. Plasmid-DNA was precipitated using 2 volumes of ethanol at room temperature and a centrifugation step for 10 min at 15,000 x g. The pellet was air dried for 10-15 min and the DNA was finally dissolved in 15 µl of $Aqua_{dest}$.
High amounts of pure plasmid DNA (up to 100 µg) were prepared using the QIAGEN Plasmid Midi Kit as described by the manufacturer.

Solution components	Solution I	Solution II	Solution III
Glucose	50 mM	---	---
Tris/HCl (pH 8.0)	25 mM	---	---
EDTA (pH 8.0)	10 mM	---	---
NaOH	---	200 mM	---
SDS	---	1%	---
KOAc (pH 5.5, adjusted with glacial acetic acid)	---	---	3 M

2.3.2 RNA isolation

2.3.2.1 Isolation from cultured cells

RNA isolation was performed according to a protocol from Chomczynski and Sacchi (1987). Cells were grown and stimulated as described in *2.5.1*. Cells were washed twice with PBS and last traces of PBS were removed by a pipette tip attached to a

vacuum line. Subsequently, cells were lysed with 400 µl of GSCN-solution per 10 cm-plate, scraped with a rubber policeman and the lysate was transferred into an Eppendorf tube. After addition of 40 µl 2 M NaOAc (pH 4.0), 400 µl acidic phenol (H_2O-saturated) and 120 µl chloroform, the samples were vortexed vigorously for 20 sec. The vortexed tubes were stored 15 minutes on ice, centrifuged (15,000 g, 10 min) and the aqueous upper phase was transferred into a fresh tube. RNA was precipitated using 1 ml of EtOH, and isolated by a single centrifugation step (15,000 x g, 10 min). The RNA pellet was dissolved in DEPC-treated water, followed by an additional phenol/chloroform (pH 9.5, 1M Tris/HCl saturated) extraction. After centrifugation (15,000 x g, 10 min), the RNA was finally precipitated form the aqueous phase by addition of 40 µl 3 M NaOAc (pH 5.2) and 1 ml ethanol. The samples were centrifuged (15,000 x g, 10 min) and the final RNA pellet was resuspended in 200 µl DEPC-treated water. Following a 10 min incubation at 65°C, the amount of isolated RNA was quantified photometrically (*2.3.3*). 2 µg of the isolated RNA was controlled for integrity by agarose gel electrophoresis (1.5%, 1 x TAE buffer). Finally, RNA was aliquoted and stored in ethanol at -20°C until use.

Solution components	**GSCN-solution**
Guanidinium thiocyanate	50% (w/v)
Sodiumlaurylsarcosyl	0.5% (w/v)
Sodiumcitrate, pH 7.0	15 mM
β-Mercaptoethanol	0.7% (v/v)

2.3.2.2 Isolation from tissue

Skin samples (murine wounds) were homogenized in Falcon tubes using an UltraTurrax (IKA Labortechnik) in 4 ml of GSCN-solution. Homogenates were cleared by a centrifugation step (4000 rpm, 10 min; Heraeus Megafuge 1.0, rotor 7570F). Subsequently, RNA was isolated from the supernatants as described in section *2.3.2.1*.

2.3.3 Quantification of nucleic acid concentrations

Concentrations of nucleic acids were determined photometrically using a wavelength of 260 nm (Gene Quant II, Amersham Pharmacia). An optical density (OD) of 1

corresponds to approximately 50 µg/ml double-stranded DNA or 40 µg/ml for single stranded DNA and RNA (Sambrook *et al*. 1989). The ratio between the readings at 260 nm and 280 nm (OD_{260}/OD_{280}) provides an estimation of the purity of the nucleic acid preparation. Highly pure DNA or RNA are characterized by ratios between 1.8 and 2.0. Low amounts of DNA were estimated by agarose gel electrophoresis (*2.3.4*) in comparison with a known standard concentration.

2.3.4 Agarose gel electrophoresis of nucleic acids

Nucleic acids were separated by gel electrophoresis using agarose gels. The agarose concentration was dependent on the molecular weight of the analyzed nucleic acids. For separation of DNA molecules from 0.5 to 2 kbp usually 1% agarose gels (w/v) were used. Smaller DNA fragments (100-500 bp) were separated in high density gels (1.5-2% agarose gels) (Sambrook *et al*., 1998). Agarose (Biozym) was dissolved in 1x TAE gel electrophoresis buffer. Ethidium bromide was added to a final concentration of 500 ng/µl. Ethidium bromide binds to DNA or RNA by intercalation between the bases and, thus enables an ultraviolet fluorescence illumination of nucleic acids. The DNA/RNA probes were diluted with loading buffer [6x loading buffer: 30% glycerol (v/v), 0.25% bromophenol blue (w/v), 0.25% xylenecyanole (w/v), 60% 10x TAE buffer (v/v)] and transferred into the appropriate gel wells. Electrophoresis was performed in 1x TAE buffer with a voltage of 5-10 V/cm gel. DNA fragment sizes were estimated using molecular weight markers (MBI Fermentas).

2.3.4.1 DNA isolation from agarose gels

The use of the NucleoSpin Extract 2 in 1 Kit (Macherey & Nagel) enables a pure extraction of DNA fragments directly from agarose gels. The system is based on a silica matrix, which binds single and double stranded DNA. The DNA fragments of interest were cut from the gel with a razor blade and further processed to the instructions of the manufacturer.

2.3.5 Reverse transcriptase polymerase chain reaction

2.3.5.1 Reverse transcription

The enzyme reverse transcriptase, originally discovered in RNA tumor viruses, synthesizes a complementary DNA strand using RNA as a template. This enzymatic activity provides access to the generation of cDNA. In general, eukaryotic mRNAs are characterized by a series of adenine nucleotides at the 3´-end, the so called poly-(A) tail. Through hybridization with oligo-(dT) primers, these poly-(A) sites are ideal start points for the reverse transcriptase enzyme. Additionally, random hexamers (50 ng/µl) were used as internal enzyme start sites.

Reverse transcriptase reaction:	7 µl	RNA (0.5 µg/µl)
	1 µl	oligo-(dT) primer (0.5 µg/µl)
	4 µl	5x reverse transcriptase buffer
	2 µl	DTT (0.1 M)
	1 µl	RNasin (Promega)
	4 µl	dNTP-mix (dATP, dCTP, dGTP, dTTP; 10mM)
	1 µl	superscript II enzyme (200 units/µl, Gibco Life Technologies)

7 µl of total RNA (0.5 µg/µl) were mixed with 1 µl oligo-(dT) primer (0.5 µg/µl) and incubated for 10 min at 70°C. The tube was chilled on ice and the reagents were added as listed in the table. The reaction was performed for 1 h at 37°C. The mix was terminated by incubation for 5 min at 95°C, and aliquots of the cDNAs were stored at –20°C.

2.3.5.2 Polymerase chain reaction (PCR)

This methods enables the *in vitro* amplification of DNA fragments without time consuming cloning and identification steps (Mullis & Foloona, 1987). The method is based on the availability of heat-stable DNA polymerases which allow multiple denaturing of template DNA, annealing of driver sequences (primer) and synthesis of DNA by amplification steps within one tube.

Polymerase chain reaction:	3 µl	cDNA (*2.6.5.1*) or
	X µl	Plasmid-DNA (5-10 ng)
	5 µl	10x *taq*-buffer (containing Mg^{2+})

	4 µl	dNTP-mix (dATP, dCTP, dGTP, dTTP; 5 mM)
	5 µl	forward/reverse primer-mix (10 µM)
	1 µl	*taq*-polymerase (1 unit)
ad	50µl	H_2O

The reaction was performed in a thermocycler (GeneAmp 2400 or 9600, *PE* Biosystems) with 25-30 cycles of the following steps: 1 min 94°C, 1 min 52°C and 1 min 72°C. The amplification was completed by a final 10 min incubation step at 72°C. Depending on special conditions of the template or the primers the protocol was adapted individually. The samples were stored at 4°C and analyzed by gel electrophoresis.

For amplification of the p68 RNA helicase open reading frame, the *Pfu* polymerase (Stratagene) was chosen. In contrast to T*aq* polymerase (Roche Biochemicals), this enzyme exhibits 3`- to 5`-exonuclease proofreading activity. The reaction was performed in a thermocycler (GeneAmp 2400 or 9600, *PE* Biosystems) with 28 cycles of the following steps: 1 min 94°C, 1 min 59°C and 4 min 72°C. A final extension at 72°C for 10 minutes completed the reaction.

2.3.5.3 Cloning of PCR products

After amplification, PCR products were separated by gel electrophoresis. The band of the appropriate size was cut out and subsequently re-amplified by *Pfu*-polymerase (Stratagene). Once again PCR product was purified by gel electrophoresis and isolated from the agarose gel using a column gel extracting kit (Macherey & Nagel). Finally, DNA of interest was ligated into pBluescript II (+) KS vector (Statagene) at the *Eco*RV restriction site as described in *2.3.6.2*.

2.3.6 Manipulation of DNA

2.3.6.1 Restriction

Type II endonucleases isolated from bacteria specifically bind palindromic sequences with a subsequent cleavage of the DNA molecule at their recognition site. This process generates either blunt-end fragments or overhanging cohesive ends, which allow the generation of recombinant DNA by enzymatic ligation. The standard

approach for DNA digestion is subsequently listed. After incubation at the appropriate temperature, DNA cleavage was checked by agarose gel electrophoresis (*2.3.4*).

DNA restriction:	10.0 µl	DNA (500 ng)
	2.0 µl	10 x buffer
	0.2 µl	restriction enzyme (3 units)
	ad 20 µl	H_2O

2.3.6.2 Ligation

Generation of covalent phosphodiester bonds between the 5´-phosphate and the 3´-OH of DNA fragments is catalyzed by T4-DNA ligase. The ligation reaction was performed with restricted or PCR amplified DNA. The DNA was separated in a agarose gel. Subsequently the DNA of interest was isolated using a column gel extracting kit by (Macherey & Nagel). The gel extracted fragment was added to the ligation reaction. The mixture was incubated for at least 5 h at room temperature. Afterwards, an aliquot of this reaction was transformed into competent bacteria as described in section *2.2.2*.

DNA ligation:	4 µl	10 x ligase buffer
	1 µl	vector DNA (500 ng)
	10 µl	Gel-extracted DNA fragment (5 µg)
	1 µl	T4-DNA ligase (1 unit)
	ad 40 µl	H_2O

2.3.6.3 Dephosphorylation

If the vector DNA carried identical cohesive termini after enzymatic restriction, the plasmid was treated additionally with alkaline phosphatase (Roche Biochemicals) prior to ligation. Phosphatases remove the 5´-phosphates from DNA strands. This technique prevents a re-ligation of restricted plasmids without incorporation of insert DNA. To this end, the restricted DNA was incubated with alkaline phosphatase (0.1 unit/µg DNA) for 30 min at 37°C. Afterwards, the phosphatase was heat-inactivated for 10 min at 70°C and the denatured protein extracted with phenol/chloroform. The ligation of the DNA fragments was performed as described in *2.3.6.2*.

2.3.6.4 Cloning pcDNA-p68

The human p68 RNA helicase cDNA (Acc.No. NM_004396) was cloned from HaCaT keratinocytes using 5´-CCA TGT CGG GTT ATT CGA GTG ACC-3´ as a 5´-primer and 5´-GTC TTA TTG GGA ATA TCC-3´ as a 3´-primer. The *Pfu*-amplified PCR product corresponded to nucleotides 169 to 2018, including 2 nucleotides upstream the ATG start codon and 3 nucleotides downstream the TAA stop codon. The blunt-end 1849 bp p68 RNA helicase cDNA was cloned into the *Eco*RV restriction site of the pBluescript II KS (+) vector (Stratagene). To verify the correct sequence, both strands were sequenced. Subsequently, the p68 RNA helicase cDNA was subcloned into the pcDNA3.1(+) expression vector by *BamHI/HindIII* sites.

2.3.6.5 Cloning pEGFP-N1-p68

The human p68 RNA helicase cDNA (Acc.No. NM_004396) was cloned from HaCaT keratinocytes using 5´-CCA TGT CGG GTT ATT CGA GTG ACC-3´ as a 5´-primer and 5´-TTG GGA ATA TCC TGT TGG-3´ as a 3´-primer. The *Pfu*-amplified PCR product corresponded to nucleotides 169 to 2012, starting 2 nucleotides upstream the ATG start codon, ending 3 nucleotides upstream the TAA, thus missing the stop codon. The blunt-end 1846 bp p68 RNA helicase cDNA was cloned into the *Eco*RV restriction site of the pBluescript II KS (+) vector (Stratagene). To verify the correct sequence, both strands were sequenced. Subsequently, the p68 RNA helicase cDNA w/o stop was subcloned in frame into the pEGFP-N1 expression vector using compatible *HindIII/XbaI* sites and *HindIII/NheI* sites.

2.3.7 DNA sequencing

DNA sequencing was performed using the ABI-Prism 310 Genetic Analyser (*PE* Biosystems) based on the dideoxynucleotide chain termination method [Sanger *et al.* 1977]. In the termination labeling mix, the four dideoxy terminators (ddNTPs) were tagged with different fluorescent dyes. This technique allows the simultaneous sequencing of all four reactions (A, C, G, T) in one reaction tube. The probes were separated electrophoretically using a micro capillary. As each dye terminator emits light at a different wavelength when excited by laser light, all four colors corresponding to the four nucleotides can be detected and distinguished within a

single run. Raw data were evaluated by the Abi Prism sequencing analysis software on a Power G3 Macintosh computer. The sequencing reaction, as listed in the table, was performed in a thermocycler (GeneAmp 2400, *PE* Biosystems) with 25 cycles of the following temperature steps: 96°C for 10 sec, 55°C for 5 sec, 60°C for 2 min. For the detection process, probes were prepared as described by the manufacturer.

DNA sequencing:	1 µl	DNA (250 ng plasmid DNA or 50 ng PCR derived DNA)
	2 µl	sequencing premix
	1 µl	primer (5 pmol)
	6 µl	H_2O

2.3.8 RNase protection assay

This method was used to quantify the amounts of specific RNA transcripts from total cellular RNA. Compared to Northern blot analysis, this technique possesses an increased sensitivity and specificity. The assay is based on the principle that double stranded RNA hybrids are protected from cleavage by RNases A and T1.

2.3.8.1 Preparation of a radiolabeled antisense probe

The desired probes (150-450 nt in length) were cloned into the transcription vector pBluescript II KS (+) as described in section *2.6.6*. The recombinant plasmids (see *2.1.5.2*) were linearized with restriction enzymes, phenol/chloroform extracted, precipitated and dissolved in $Aqua_{dest}$ to a final concentration of 1 µg/µl. A pure single stranded, [α-^{32}P]UTP radiolabeled antisense transcript was synthesized using T3 or T7 RNA polymerase. The reaction mix was prepared as listed in the table and incubated for 1 h at 37°C.

In vitro transcription:	1.1 µl	H_2O, DEPC-treated
	1.0 µl	nucleotides (ATP, CTP, GTP; each 5 mM)
	2.0 µl	transcription buffer (5 x)
	0.4 µl	RNasin (40 U/µl)
	1.0 µl	T3 or T7 RNA polymerase, depending on the vector
	2.5 µl	[α-^{32}P]UTP (800 Ci/mM)
	1.0 µl	linearized template (1 µg/µl)

Subsequently 90 µl DEPC-H_2O were added. The reaction was extracted with an equal volume of phenol/chloroform and centrifuged (15,000 x g, 2 min). The radiolabeled RNA was precipitated form the aqueous phase using 40 µl of 7.5 M ammoniumacetate, 1.5 µl of tRNA (10 µg/µl) and 350 µl of ethanol for 15 min at –20°C. Following a 15 min centrifugation step at 4°C, the radiolabeled pellet was dissolved in 20 µl FLB 80 and purified using an acrylamide/urea gel (5% acrylamide/bisacrylamide, 29:1; 8 M urea; 1x TBE). Electrophoresis (1x TBE buffer, 300 V) was terminated after 90 min. The radiolabeled probe was located by autoradiography, cut out and eluated into 300 µl elution buffer (0.1x TBE, 0.2% SDS). The incorporated activity of the freshly prepared radiolabeled probe was determined using a β-counting device (TRI-CARB 2100 TR, Canberra-Packard).

Buffer components	**FLB 80 buffer**	**FAB buffer**	**RNase buffer**
Formamide (deionized)	80% (v/v)	80% (v/v)	---
EDTA (pH 8.0)	1 mM	1 mM	5 mM
PIPES (pH 6.4)	---	40 mM	---
NaCl	---	400 mM	---
NaOAc (pH 7.0)	---	---	300 mM
Tris/HCl (pH 7.5)	---	---	10 mM
TBE (1 x)	0.01% (w/v)	---	---
Bromophenol blue	0.05% (w/v)	---	---
Xylenecyanole	0.05% (w/v)	---	---

2.3.8.2 Hybridization and cleavage

10-30 µg of total RNA from cell culture or animal experiments (see *2.6.2*) were used for the experiments. Total RNA and 100,000 cpm of the radiolabeled probe were co-precipitated using a 2.5-fold excess of ethanol/0.1 M NaOAc. The samples were incubated at –20°C for 15 min and subsequently centrifuged (15,000 x g, 10 min). The supernatants were removed and the RNA/antisense probe pellet was resuspended carefully in 30 µl FAB hybridization buffer. Samples were subsequently denatured for 10 min at 85°C and hybridized overnight (42°C in a water bath). Following hybridization, samples were treated with 300 µl RNase T1/A-mix (RNase buffer supplemented with 10 µg of RNase A and 200 units of RNase T1) for 1 h at 30°C [Melton *et al*. 1984]. Under these conditions, every single mismatch was recognized by the RNases. RNases were inactivated by an addition of 6.6 µl SDS

(10%) and 4.4 µl proteinase K (10 µg/ml) for 15 min at 42°C. The samples were extracted with phenol/chloroform and centrifuged (15,000 x g, 2 min). Protected double-stranded RNA hybrids were precipitated using 880 µl of ethanol and 1.5 µl of tRNA (10 µg/µl). After centrifugation, (15,000 x g, 15 min), the pellet was resuspended in 25 µl FLB 80 buffer, heated for 5 min at 95°C and loaded on the gel.

2.3.8.3 Analytical gel electrophoresis and signal detection

The protected RNA fragments were separated on acrylamide/urea gels (5% acrylamide/bisacrylamide, 29:1; 8 M urea; 1x TBE). 1000 cpm of the radiolabeled antisense probe served as a size marker. Electrophoresis (300 V, 1x TBE buffer) was stopped after 60 min. The gel was fixed on Whatman 3MM paper and subsequently dried on a gel drying system (Bio Rad). The radiolabeled gel was exposed to a phosphoimager plate (BAS-MP 2040S, Fuji) and analyzed using a Fuji Phosphoimager BAS-1500. To permit appropriate statistical analysis, all protection assays were carried out with at least three different sets of RNA from independent cell culture or animal experiments.

2.3.9 Differential screening of a subtractive library

Subtractive hybridization represents a technique by which two different populations of mRNA can be compared. We have chosen this approach to discover genes that are differentially expressed in HaCaT keratinocytes by nitric oxide treatment. The PCR-Select cDNA Subtraction Kit and the AdvanTAge PCR Cloning Kit (Clontech) were used.

2.3.9.1 PCR-Select cDNA subtraction

HaCaT cells were stimulated with 500 µM GSNO for 5 hours. RNA was isolated, enriched for mRNA (Nucleotrap^{R} mRNA Kit, Macherey & Nagel) and subsequently used as starting material for PCR-Select cDNA subtraction. Subtraction was performed according to the instructions of the manufacturer (Clontech). Briefly, cDNA was synthesized from 2 µg of mRNA from the GSNO [500 µM] stimulated and unstimulated HaCaT cells. The resulting cDNAs were subdivided into two fractions, and ligated to different cDNA adaptors, respectively. The adaptor molecules differ in

their PCR primer annealing sequence. In the next step, an excess of cDNA from control HaCaT cells was added. Both fractions were denatured and subsequently hybridized. Finally, the ends were filled by DNA polymerase and differentially expressed sequences were amplified by PCR. Only the cDNAs with two different annealing sites were amplified exponentially. These molecules represent the differentially expressed sequences. To reduce background PCR products and to further enrich differentially expressed sequences, a secondary PCR amplification was performed using nested primers.

2.3.9.2 Subtracted cDNA Library Construction

3 µl of the secondary PCR product were cloned using the AdvanTAge PCR Cloning Kit, a T/A-based cloning system from Clontech. Thermostable polymerases (2.3.9.1) synthesize PCR products, that contain a single unencoded deoxyadenosine at their 3`ends. Those products can be easily ligated to pT-Adv vectors, possessing 3`T-overhangs. The ligation products were subsequently transformed into competent *E. coli.*

2.3.9.3 Colony Array

96 bacterial colonies were picked randomly and grown in 100 µl LB-amp medium in a 96-well plate at 37°C with shaking over night. Nylon membranes were placed onto LB/agar plates containing ampicillin. From each bacterial culture 2 x 1 µl were transferred onto membranes using a multi-channel pipettor. The membranes were generated in duplicates. After incubation at 37°C overnight, the colonies were prepared for filter screening. For this purpose, membranes were placed onto Whatman 3MM paper saturated with denaturing solution (0,5 M NaOH, 1,5 M NaCl). After 4 minutes membranes were neutralized (0,5 M Tris-HCl [pH 7.4], 1,5 M NaCl). Finally, membranes were allowed to air dry and DNA was fixed by incubation at 80°C for 1-2 hours.

2.3.9.4 Preparation of [α-^{32}P]dCTP labeled probe

4 µl of mRNA (0.5 µg/µl) were mixed with 1 µl oligo-(dT) primer (0.5 µg/µl) and incubated at 70°C for 10 minutes. The tubes were chilled on ice and reagents were added as listed in the table. Reverse transcription was performed at 37°C for one hour and terminated by an incubation at 95°C for 5 minutes. Samples were treated with 80 µl RNase T1/A-mix (RNase buffer supplemented with 3 µg of RNase A and 80 units of RNase T1) at 30°C for one hour [Melton *et al*. 1984]. Probes were extracted with 100 µl phenol/chloroform and centrifuged (15,000 x g, 2 min). To purify probes from unincorporated dNTPs, 40 µl of 7.5 M ammoniumacetate, 2 µl of tRNA (10 µg/µl) and 350 µl of ethanol were added. Samples were stored at -20°C for 15 minutes and subsequently centrifuged (15,000 x g, 4°C, 15 min). The radiolabeled pellet was dissolved in 200 µl of $Aqua_{dest}$ and activity of each probe was determined using a β-counting device (TRI-CARB 2100 TR, Canberra-Packard).

Reverse transcriptase reaction:	4 µl	Poly A^+ RNA (0.5 µg/µl)
	1 µl	oligo-(dT) primer (0.5 µg/µl)
	4 µl	5x reverse transcriptase buffer
	2 µl	DTT (0.1 M)
	1 µl	Rnasin (Promega)
	1 µl	dATP
	1 µl	dGTP
	1 µl	dTTP
	2,5 µl	[α-^{32}P]dCTP (3000 Ci/mM)
	1 µl	superscript II enzyme (200 units/µl Gibco Life Technologies)
ad	20 µl	H_2O

2.3.9.5 Hybridization

[^{32}P]-labeled probes were hybridized to the subtracted clones on nylon membranes. Each membrane was pre-hybridized in 30 ml pre-hybridization solution (7% SDS w/v, 1% BSA w/v, 0.5 M Na-phosphate buffer, pH 7.2, 1mM EDTA) at 68°C for 2 hours. Membranes were transferred into 5 ml of hybridization solution (prehybridization solution containing 1x 10^5 cpm probe per milliliter). Hybridization was performed at 68°C overnight. Membranes were washed with low stringency (2x SSC, 0,5% SDS) and high stringency (0,2x SSC, 0,5% SDS). Finally, membranes were exposed to a phosphoimager plate (BAS-MP 2040S, Fuji) overnight, and subsequently analyzed.

2.4 Protein techniques

2.4.1 Preparation of lysates

2.4.1.1 Cell lysates

Cells were grown and stimulated as described above (*2.5.1*). For harvesting, cells were washed twice with ice-cold PBS. Last traces of PBS were removed by a pipette tip attached to a vacuum line. Cells were scraped off from the culture dishes using a rubber policeman and triton/homogenization buffer (500 µl/10 cm dish). Subsequently, cells were sonicated (3 x 10 sec, Banson Sonifier 450) and the homogenate was stored on ice for additional 60 min. To remove cellular debris, probes were centrifuged (15,000 x g, 10 min, 4°C) and the supernatants were stored at –80°C until use. Protein concentrations were determined using the Roth Nanoquant Protein Assay (*2.4.3*)

Buffer components	**Homogenization buffer (1x)**
137 mM	NaCl
20 mM	Tris/HCl, pH 8.0
5 mM	EDTA, pH 8.0
10% (v/v)	Glycerol
1 mM	PMSF (freshly added!)
1 µg/ml	Leupeptin
1 % (v/v)	Triton X-100 (must not be included for isolation of cytoplasmic fractions)

2.4.1.2 Preparation of fractionated cell lysates

A 10 cm dish of confluent cells was washed twice with ice-cold PBS. Cells were scraped into 2 ml ice-cold PBS and concentrated (13,000 rpm, 5 min, 4°C). Cells were resuspended in 300 µl buffer C and incubated for 15 minutes by vigorous shaking at 4°C. 20 µl of 10% NP-40 were added to the homogenate, the sample was vortexed and centrifuged (15,000 x g, 5 min, 4°C). The supernatant containing the cytosolic fraction was stored at -80°C.

The pellet was resuspended in 100 µl buffer N and incubated for 20 minutes by vigorous shaking at 4°C. Finally, the lysate was centrifuged (15,000 x g, 5 min, 4°C). The supernatant, carrying the nuclear fraction, was collected and stored at -80°C.

Protein concentrations were determined using the Roth Nanoquant Protein Assay (*2.4.3*).

buffer components	buffer C (1x)	buffer N (1x)
Hepes pH 7.9	10 mM	20 mM
KCl	10 mM	-
NaCl	-	400mM
EDTA	0,1 mM	0,1 mM
EGTA	0,1 mM	0,1 mM
NaF (freshly added)	50 mM	50 mM
DTT (freshly added)	1 mM	1 mM
PMSF (freshly added)	1 mM	1 mM
Leupeptin (freshly added)	1 ng/ml	1 ng/ml
Aprotinin (freshly added)	1 ng/ml	1 ng/ml
Na_3VO_4 (freshly added)	2 mM	2 mM

2.4.1.3 Tissue lysates

Skin samples (murine wounds) were homogenized (UltraTurrax, IKA Labortechnik) in 4 ml of 2x triton/homogenization buffer. The tissue extract was cleared by centrifugation (4,000 rpm, 30 min, 4°C; Heraeus Megafuge 1.0, rotor 7570F). The supernatant was diluted using an equal volume of water. Protein concentrations were determined using the Roth Nanoquant Protein Assay (*2.4.3*). Aliquoted samples were stored at –80°C until use.

2.4.2 Trichloroacetic acid (TCA) precipitation

This method was used to concentrate proteins from a defined volume of cell culture supernatants for Western blot analysis. Cell culture supernatants were cleared from cellular contaminations using a single centrifugation step (1000 rpm, 5 min, 4°C; Heraeus Megafuge 1.0, rotor 7570F). Subsequently, 10% (v/v) of 70% trichloroacetic acid (TCA) was added to 1 ml of conditioned cell culture supernatant, mixed and incubated for 30 min on ice. TCA-precipitated proteins were concentrated by centrifugation (15,000 x g, 30 min, 4°C). The protein pellet was washed in 200 µl of ice-cold acetone, centrifuged for 5 min at 15,000 x g and finally resuspended in 20 µl of 2x Laemmli buffer. After neutralization (1 µl of 1 M Tris/HCl, pH 8.5), the samples were ready to use for Western blot analysis (*2.4.4*).

2.4.3 Determination of protein concentration

The amount of protein in cellular and tissue lysates was determined using Roth Nanoquant Protein Assay (Bradford method). 5 µl of the samples diluted in 795 µl of distilled water were combined with 200 µl Nanoquant 5x dye solution, vortexed and pipetted in duplicate into appropriate wells of a 96-well ELISA plate. Different BSA concentrations (2.5-50 µg/ml) were used to generate a standard curve. After 10 min of incubation, the optical density was measured at a wavelength of 595 nm using a microplate reader (Bio Rad). The absorption values were calculated using the Microplate Manager 4.0 software (Bio Rad).

2.4.4 Western blot analysis

The Western blot technique represents a sensitive method to detect specific polypeptides within a complex mixture of proteins. Proteins are separated electrophoretically and transferred to a membrane, which is subsequently incubated with antibodies specific for the protein of interest. Finally, the bound antibody is recognized by a second anti-immunoglobulin that is coupled to horseradish peroxidase or alkaline phosphatase. The detection limit of this method ranges between 1-5 ng of an average-sized protein.

Buffer components	**Laemmli buffer (4x)**	**Electrophoresis buffer (1x)**	**Transfer buffer (1x)**	**TBST buffer (10x)**
Tris/HCl	125 mM (pH 6.8)	25 mM	25 mM	100 mM (pH 8.0)
SDS	10% (w/v)	0.1% (w/v)	---	---
Glycine	---	250 mM	192 mM	---
Dithiothreitol	50 mM	---	---	---
Bromophenol blue	0.01% (w/v)	---	---	---
Glycerol	30% (v/v)	---	---	---
Methanol	---	---	20% (v/v)	---
Tween 20	---	---	---	5% (v/v)
NaCl	---	---	---	1.5 M

2.4.4.1 SDS gel electrophoresis

Electrophoretic separation of proteins was carried out in the discontinuous buffer system for SDS polyacrylamide gels as originally described by Laemmli (1970).
50 µg of total protein were dissolved in 2x Laemmli buffer. Diluted protein samples were concentrated by acetone precipitation: the desired amount of protein-containing solution was mixed with 3 volumes ice-cold acetone and chilled at –20°C for 2 h. Protein was concentrated by centrifugation (15,000 x g, 15 min, 4°C). The protein-containing pellet was suspended in 2x Laemmli buffer. After heating for 5 min at 95°C, samples were loaded on the gel. Subsequently, the gel was run at a current of 30 mA for a period of 1-3 hours.

Resolving gel

Solution components	Component volumes (ml) per 20 ml gel		
	6% (> 120 kDa)	10% (60-120 kDa)	12% (< 60 kDa)
H_2O	10.6	7.9	6.6
Acrylamide mix (30%)	4.0	6.7	8.0
Tris/HCl (1.5 M, pH 8.8)	5.0	5.0	5.0
SDS (10%)	0.2	0.2	0.2
Ammonium persulfate (10%)	0.2	0.2	0.2
TEMED	0.016	0.008	0.008

Stacking gel

Solution components	Component volumes (ml) per gel volume of		
	2 ml	5 ml	10 ml
H_2O	1.4	3.4	6.8
Acrylamide mix (30%)	0.33	0.83	1.7
Tris/HCl (1.5 M, pH 6.8)	0.25	0.63	1.25
SDS (10%)	0.02	0.05	0.1
Ammonium persulfate (10%)	0.02	0.05	0.1
TEMED	0.002	0.005	0.01

2.4.4.2 Transfer to PVDF membrane

After gel electrophoresis, proteins were transferred to a polyvinylidene fluoride (PVDF) membrane by electroblotting (Trans-Blot SD, Bio Rad). Prior to use, the PVDF membrane was activated in isopropanol for 3 min and subsequently rinsed in deionized water. Six pieces of Whatman 3MM paper were soaked in transfer buffer and positioned on the anode side of the transfer apparatus. The PVDF membrane was placed directly on the stack of 3MM paper. The SDS gel containing the

separated proteins was taken off the glasplates, rinsed shortly in transfer buffer, and placed on the top of the PVDF membrane. Finally, the gel was covered with four additional, transfer buffer-soaked Whatman 3MM papers. Air bubbles were squeezed out by a roller apparatus. The upper electrode (cathode) was positioned on the top of the stack and a current of 0.8 mA/cm^2 was applied. Transfer of proteins was carried out at room temperature and terminated after 75 min. After blotting, the membrane was checked by Ponceau S staining for correct electrophoretic transfer and equal loading.

2.4.4.3 Immunodetection

The air-dried PVDF membrane was reactivated in isopropanol and rinsed in 1x TBST buffer. Non-specific binding sites were blocked by shaking the membrane in a 1x TBST-buffered non-fat skim milk solution (5-10%) for 1 h at room temperature or overnight at 4°C. The membrane was subsequently exposed to antibodies (diluted 1:500–1:2000 in 1x TBST buffer) specific for the protein of interest. The incubation time varied between 1 h at room temperature, or 15 h at 4°C depending on the antiserum. The blot was washed three times for 15 min in 1x TBST. The primary antibody was detected by incubation of the membrane with a specific secondary antibody coupled to horseradish peroxidase (diluted 1:5000–1:20,000 in 1x TBST) for 45 min at room temperature. For detection of the corresponding bands, we used the enhanced chemiluminescence (ECL) detection kit (Amersham Pharmacia) according to the instructions of the manufacturer. The membrane was exposed to a film (Hyperfilm, Amersham Pharmacia) and developed (Hyperprocessor, Amersham Pharmacia). Developed films were scanned (GS 700 Imaging Densitometer, Bio Rad) and analyzed using the Molecular Analyst software from Bio Rad.

2.4.5 Generation of a p68 RNA helicase antibody

A synthetic peptide (H_2N-FNTFRDRENYDRGY-COOH) based on the C-terminal sequence of the human p68 RNA helicase (GenBankTM/EBI Data Bank accession number NM_004396) was synthesized, coupled to keyhole limpet hemocyanin, and used to immunize rabbits. Notably, the peptide sequence allows immunodetection of both human and murine p68 RNA helicase.

2.4.6 Enzyme-linked immunosorbent assay (ELISA)

The enzyme-linked immunosorbent assay (ELISA) technique is the most sensitive method to specifically determine protein concentrations from different sources. Sensitivity is approximately 100-fold increased compared to the Western blot technique (*2.4.4*). The ELISA was performed according to the instructions of the manufacturer (R&D Systems, PharMingen). Briefly, microtiter plates were pre-coated with a monoclonal antibody specific for VEGF. Equal volumes of cell culture supernatant samples were pipetted into the wells of the microtiter plate and incubated for 2 h. Subsequently, wells were washed. An enzyme-linked polyclonal antibody specific for VEGF was added for 2 hours, and wells were subsequently washed for three times. Wells were then incubated with substrate solution. The color reaction develops in direct proportion to the amount of bound antigen. The optical densities were calculated using the Microplate Manager 4.0 software from Bio Rad.

2.4.7 Immunohistochemistry

2.4.7.1 Preparation of frozen tissue sections

Wounds were excised as described in section *2.7.1*. They were fixed on a membrane, bisected and frozen in tissue freezing medium (Leica Instruments) at -80°C. 6 µm frozen sections were generated on a cryostat (CM 3050S, Leica Instruments) and adhered to glass slides (Roth). The sections were fixed in acetone for 1 min, air-dried and stored at –80°C.

2.4.7.2 Immunoperoxidase staining

Immunodetection of proteins in frozen tissue sections was performed using the ABC staining systems from Santa Cruz. After thawing the slides to room temperature, tissue sections were treated as indicated in the flow chart. Blocking reaction and antibody incubation were performed in a humidified chamber.

tissue section
▼
acetone
(10 min)
▼

PBS
(3 x 5 min)
▼
hydrogen peroxide
(1% in PBS, 10 min)
▼
PBS
(2 x 5 min)
▼
blocking serum
(1.5% in PBS, 60 min)
▼
1. antibody
(0.1-20 µg/ml in blocking serum, 1-20 h)
▼
PBS
(3 x 5 min)
▼
2. antibody
(45 min)
▼
PBS
(3 x 5 min)
▼
avidin/biotin complex
(30 min)
▼
PBS
(3 x 5 min)
▼
peroxidase substrate

2.4.7.3 Hematoxylin staining

To visualize nuclei in tissue specimens, the sections were counterstained with hematoxylin solution as shown in the flow chart:

tissue section
▼
hematoxylin solution
(1-10 min)
▼
$Aqua_{dest}$
(3 x 30 sec)
▼
Scott water
(30 sec)
▼
$Aqua_{dest}$
▼
slides mounted

2.5 Cell culture

All cell lines were cultured at 37°C in a humidified atmosphere containing 5% CO_2 (Heraeus BBD 6220 incubator). For subcultivation, cells were washed once in phosphate buffered saline (PBS), subsequently trypsinized (Trypsin, EDTA) and diluted in a appropriate ratio (1:12 for HaCaT cells, 1:10 for HEK 293 cells). For long-term storage, the cells were treated as follows: after trypsinization, cells were pelleted (5 min at 1100 rpm, Heraeus Megafuge 1.0, rotor 75750F), diluted in freezing medium (growth medium with 20% FCS supplemented with 10% DMSO) and stored in cryotubes (Nunc). The cryotubes were cooled down slowly and finally stored in liquid nitrogen.

2.5.1 Culture and stimulation of HaCaT cells

The human keratinocyte cell line HaCaT (Boukamp *et al*. 1988) was grown in DMEM supplemented with 10% FCS and the antibiotics penicillin (100 U/ml)/streptomycin (100 µg/ml). Under these culture conditions the cells remain undifferentiated. For the induction experiments, cells were grown to confluence without changing the medium and rendered quiescent by 24 h incubation in serum-free DMEM. Cells were then incubated for varying periods on fresh DMEM containing the factors or reagents of interest.

2.5.2 Culture of HEK 293 cells

Human embryonic kidney cells (HEK) were grown in DMEM supplemented with 10% FCS and the antibiotics penicillin (100 U/ml) and streptomycin (100 µg/ml).

2.5.3 Transfection

For transfection experiments $2x10^5$ cells/6 cm dish were plated and grown for 24 h to reach 50-80% confluence. The DNA of interest (5 µg) and lipofectamine (10 µl) were diluted into 250 µl of unsupplemented DMEM, combined and mixed gently. The solutions were allowed to form DNA-liposome complexes for 15 min at room temperature. Full medium covering the target cells was replaced with 1,5 ml serum-

and antibiotic-free DMEM. The diluted DNA-liposome complex was added and cells were incubated for 3 hours. Subsequently, 2ml medium containing 20% serum was added. 24 hours after transfection, medium was replaced for full medium. For stable transfection 1000 µg/ml geneticin (Gibco Life Technologies) was added two days after transfection. The transfected cells were selected for a period of 6 weeks in the presence of geneticin. Surviving clones were isolated, subcultured and tested for p68 RNA helicase expression by western blotting.

2.6 *In vitro* transcription/translation

We performed an *in vitro* transcription/translation experiment to control the specificity of the p68 antibody. The TNT^{R}Coupled Reticulocyte System was used as described by the manufacturer. The following reaction components were added into a 1,5 ml microcentrifuge tube:

component	radioactive reaction	non-radioactive reaction
TNT^{R}Rabbit Reticulocyte Lysate	12,5 µl	12,5 µl
TNT^{R}Reaction buffer	1,0 µl	1,0 µl
T3 RNA polymerase	1,0 µl	1,0 µl
Amino acid mixture, minus Leucine, 1mM	-	0,5 µl
Amino acid mixture, minus Methionine, 1mM	0,5 µl	0,5 µl
[^{35}S]methionine	1,0 µl	-
RNasin	0,5 µl	0,5 µl
Template (pcDNA-p68) [1µg/µl]	1 µl	1 µl
H_2O	7 µl	7 µl

After an incubation for 90 minutes at 30°C, 2,5 µl and 5 µl aliquots from each reaction were removed and SDS-PAGE was performed. The gel carrying the non radioactive in vitro translation products was analyzed by Western blot using p68 specific antibody. The gel carrying the [^{35}S]methionine labeled samples was fixed in 25% isopropyl alcohol v/v, 10% acidic acid v/v, dried and exposed on a Phosphoimager plate for analysis.

2.7 Proliferation

0.5 x 10^5 cells (HaCaT keratinocytes or cell lines) per well were seeded into 24-well plates. After reaching 50-80% confluence cells were transfected with siRNA specific for p68. Transfected cells or cell lines were starved for 24 hours with serum-free DMEM. Proliferation of cells was assessed using 1 µCi/ml of [^{3}H]-methyl-thymidine in the presence or absence of serum for 24 hours. After 24 h, cells were washed twice with PBS, incubated in 5% trichloroacetic acid (TCA) at 4°C for 30 min, and the DNA was solubilized in 0.5 M NaOH for 30 min at 37°C. Finally, [^{3}H]-thymidine incorporation was determined.

2.8 Confocal microscopy

Confocal microscopy was performed using the Zeiss LSM 510 META microscope (Carl Zeiss, München, Germany) equipped with a 405nm laser for DAPI/ blue (emission at 458nm), a 488nm laser for GFP/ green (emission at 520nm) and a 543nm laser for CY3/ red (emission at 633nm). To assess expression of p68-GFP fusion protein, transfected cells were fixed (0.2% (w/v) EDTA in methanol) at -20 °C for at least 1 h. For indirect immunofluorescence, cells were incubated with bovine serum albumin (1 mg/ml in PBS) for 1 h to block nonspecific binding sites. Incubation with the nucleolin-specific antibody (1:100 in PBS/BSA) was done at 4°C overnight. After a final wash with PBS/BSA, the FluoroLink™ Cy™3 labelled goat anti-mouse IgG (1:2000) (Amersham Pharmacia, Freiburg, Germany) was added for 1 h and DNA was stained with 4,6-diamino-2-phenylinole (1:1000, 5 min) (Sigma Aldrich Fine Chemicals, Deisenhofen, Germany). Preparations were mounted with ProLong Antifade kit (Molecular Probes, Germany).

2.9 Silencing p68 RNA helicase gene expression by siRNA

Short interfering RNA species (siRNAs) can be used to silence gene expression in a sequence-specific manner (Fire *et al*., 1998). Synthetic siRNAs are characterized by

5`phosphorylated ends, a 19-nucleotide (nt) duplexed region and 2-nt unpaired and unphosphorylated 3`ends. After siRNAs have entered the cell via transfection, they are incorporated into a multiprotein RNA-induced silencing complex (RISC). The siRNA-protein complex targets endogenous mRNA whose sequence matches that of the siRNA. Finally, the target mRNA is cleaved at a single site by the RISC endonuclease activity (Elbashir *et al*, 2001).

p68-specific siRNA was generated by Qiagen-Xeragon (Hilden, Germany) using AA**CCGCAACCATTGACGCCAT** (nt 152-172; Acc.No. NM_004396) as the cDNA target sequence. The delivered siRNA duplex sequence was formed by the sense 5`-CCGCAACCAUUGACGCCAUdTdT-3` and antisense 5`-AUGGCGUCAAUGGUUG CGGdTdT-3` oligonucleotides. As a control, a non-silencing siRNA duplex with symmetric 2-nt 3`overhangs of the cDNA target sequence 5`-AATTCTCCGAACGTGTCACGT-3` was used. This sequence only matched with a sequence derived from *Thermotoga maritime*. The sense oligonucleotide was coupled to Rhodamine to assess transfection efficiencies. Transfection of cells (HaCaT, HEK) was performed as described above (*2.5.3*).

2.10 Wound healing studies

Female C57BLKS mice were obtained from Charles River (Sulzfeld, Germany). Female C57BLKS-*iNOS*$^{-/-}$ mice were a generous gift of G. Geisslinger, Frankfurt. Mice were maintained under a 12h light/12h dark cycle at 22°C until they were 8 weeks of age. At this time they were caged individually, monitored for body weight and wounded as described below.

2.10.1 Wounding of mice

Mice were anesthetized with a single i.p. injection of ketamine (80 mg/kg body weight)/xylazine (10 mg/kg body weight). The hair on the back of each mouse was cut, and the back was subsequently wiped with 70% ethanol. Six full-thickness wounds (5 mm in diameter, 3-4 mm apart) were made on the back of each mouse by excising the skin and the underlying *panniculus carnosus*. The wounds were allowed to form a scab. Skin biopsy specimens were obtained from the animals 1, 3, 5, 7 and 13 days after injury. At each time point, an area which included the scab and the

complete epithelial margin was excised from each individual wound. As a control, a similar amount of skin was taken from the backs of nonwounded mice. For each experimental time point, tissue from four wounds each from four animals (n=16 wounds, RNA analysis) and from two wounds each from four animals (n=8 wounds, protein analysis) were combined and used for RNA and protein preparation. Non-wounded back skin from four animals served as a control. All animal experiments were carried out according to the guidelines and with the permission from the local government of Hessen (Germany).

3

Results

3.1 Identification of p68 as a novel NO-regulated gene in keratinocytes

3.1.1 Identification of novel NO-regulated genes by a differential cDNA library from GSNO-stimulated HaCaT keratinocytes

It is now well established that the short-lived radical NO pivotally drives epithelial movements and gene expression during skin repair (Frank *et al*., 2002). To gain a deeper insight into NO actions on keratinocyte behavior, a differential cDNA library from NO-stimulated HaCaT keratinocytes was established. For this purpose, HaCaT cells were grown to confluence, starved and subsequently stimulated with 500 µM GSNO. RNA was isolated and used as starting material for the synthesis of

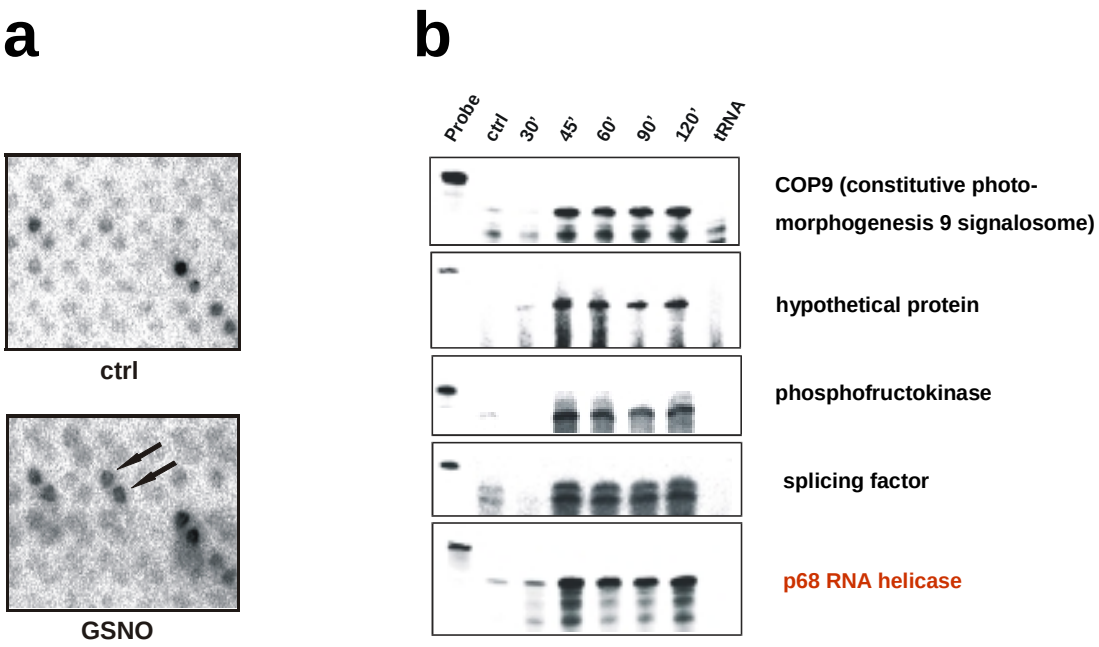

Figure 3.1 Identification of novel NO-regulated genes by a differential cDNA library from GSNO-stimulated HaCaT keratinocytes. *a*, bacterial colonies from a NO-induced differential HaCaT keratinocyte cDNA library were spotted in duplicate onto nylon membranes and screened for regulated sequences by hybridization using [α-^{32}P]-radiolabeled cDNAs from non-stimulated control (*ctrl*) and GSNO-treated HaCaT cells (*GSNO*) as indicated. The initially identified p68 cDNA clone is indicated by *arrows*. *b,* keratinocytes were rendered quiescent and subsequently stimulated with 500 µM GSNO for the indicated time periods. Induction of mRNA expression in the cells was assessed by RNase protection assay. 1000 counts of the hybridization probes as used as a size marker. tRNA was used as a negative control. Representative experiments are shown.

subtractive complementary DNA (cDNA). Screening of duplicate filters with radioactive-labeled cDNAs from GSNO- and non-treated HaCaT cells identified different bacterial clones which carried cDNA-fragments from potentially NO-inducible transcripts. Among these clones a 270 bp cDNA fragment with a 100% nucleotide homology to human p68 DEAD box RNA helicase (p68, Gen Bank Accesion Number NM_004396) was found (**Figure 3.1a**). After propagation of the identified clones, the plasmids were isolated and subsequently analyzed by sequence analysis. To confirm the NO-inducibility of the identified clones, RNase protection assays were performed using RNA from GSNO-stimulated HaCaT keratinocytes (**Figure 3.1b,** see also **3.1.2**).

3.1.2 NO induces p68 mRNA expression

As a next step, we had to confirm the potency of NO to induce p68 mRNA expression in keratinocytes *in vitro*. To this end, we stimulated quiescent HaCaT keratinocytes using GSNO as NO-donating substance. Indeed, we could detect a marked and dose-dependent induction of p68 mRNA expression in the cells (**Figure 3.2a, b**)

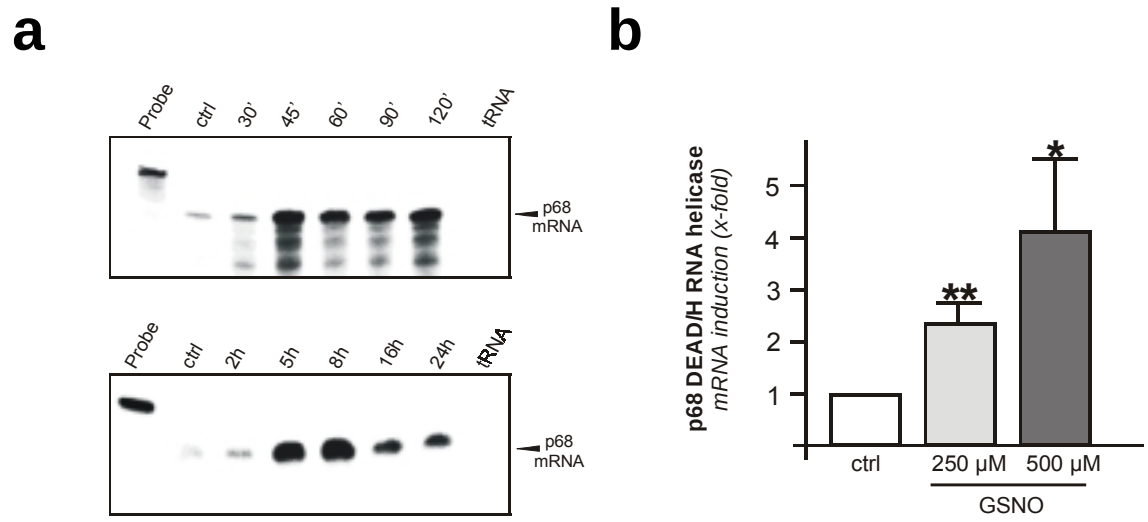

Figure 3.2 NO induces p68 mRNA expression. *a*, keratinocytes were rendered quiescent and subsequently stimulated with 500 µM GSNO for the indicated time periods. Induction of p68 mRNA expression in the cells was assessed by RNase protection assay. 1000 counts of the hybridization probe was used as a size marker. tRNA was used as a negative control. One representative experiment is shown. *b*, quantification of GSNO-induced p68 mRNA (x-fold induction, 5 h after stimulation). **, $P < 0.01$; *, $P < 0.05$ (Student's *t* test) as compared to control. Bars indicate the mean ±SD obtained from four (n=4) independent cell culture experiments.

3.1.3 NO regulates p68 expression at the transcriptional level

Next, we determined whether NO might act by transcriptional activation of the p68 gene. Additionally gene activation might be dependent from *de novo* protein synthesis. Thus, we added 2 µg/ml actinomycin D (inhibitor of transcription) or 25 µg/ml cycloheximide (inhibitor of protein synthesis) to quiescent HaCaT keratinocytes 45 min prior to GSNO treatment (**Figure 3.3).** We determined a GSNO-mediated increase in p68 mRNA levels, that could be blocked in the presence of actinomycin D (**Figure 3.3**, *as indicated*) while cycloheximide did not suppress GSNO-induced p68 mRNA expression (**Figure 3.3**, *as indicated*). These findings suggest that GSNO-triggered p68 gene activation is independent from *de novo* protein synthesis, but resembles characteristics common to activation primary of response genes.

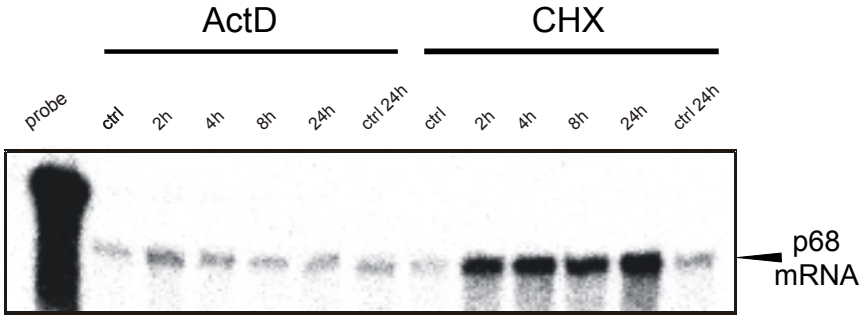

Figure 3.3 NO regulates p68 expression at the transcriptional level. RNase protection assay demonstrating the inducion of p68 mRNA expression by the NO-donating agent GSNO. Cells were rendered quiescent by serum starvation and stimulated with 500 µM GSNO in the presence or absence of 2 µg/ml actinomycin D (ActD) or 25 µg/ml cycloheximide (CHX) for the indicated time periods. 20 µg of total cellular RNA were analysed p68 mRNA expression. 1000 cpm of the hybridization probe were used as a size marker. tRNA was used as a negative control. One representative experiment is shown The GSNO-induced increase in p68 mRNA levels was assessed by PhosphoImager (Fuji).

3.1.4 NO regulates p68 protein expression

To date, we had to face the situation that no anti p68 specific antibody was commercially available. In order to investigate p68 protein expression, we decided to generate a p68 specific antibody. For this purpose, rabbits were immunized with a synthetic peptide (H_2N-FNTFRDRENYDRGY-COOH) based on the C-terminal sequence of the human p68 RNA helicase (GenBankTM/EBI Data Bank accession number NM_004396).

3.1.4.1 Characterization of the p68 specific antibody

As a crucial step, we had to confirm specificity of our anti-p68 antiserum, which had been raised in rabbits as described above. For this reason, we cloned the cDNA of the p68 open reading frame (ORF) into the eukaryotic expression vector pcDNA3.1(+) (**Figure 3.4a**). First, we performed an *in vitro* transcription/translation assay in the presence of [^{35}S]-methionine. Exposure of the corresponding radiolabeled gel revealed the presence of two major bands, from which one clearly represented the expected 68 kDa protein. Moreover, as we transferred the transcription/translation reaction to a PVDF membrane for immunoassay, we could clearly demonstrate the specificity of the p68 antibody which detects a 68 kDa protein

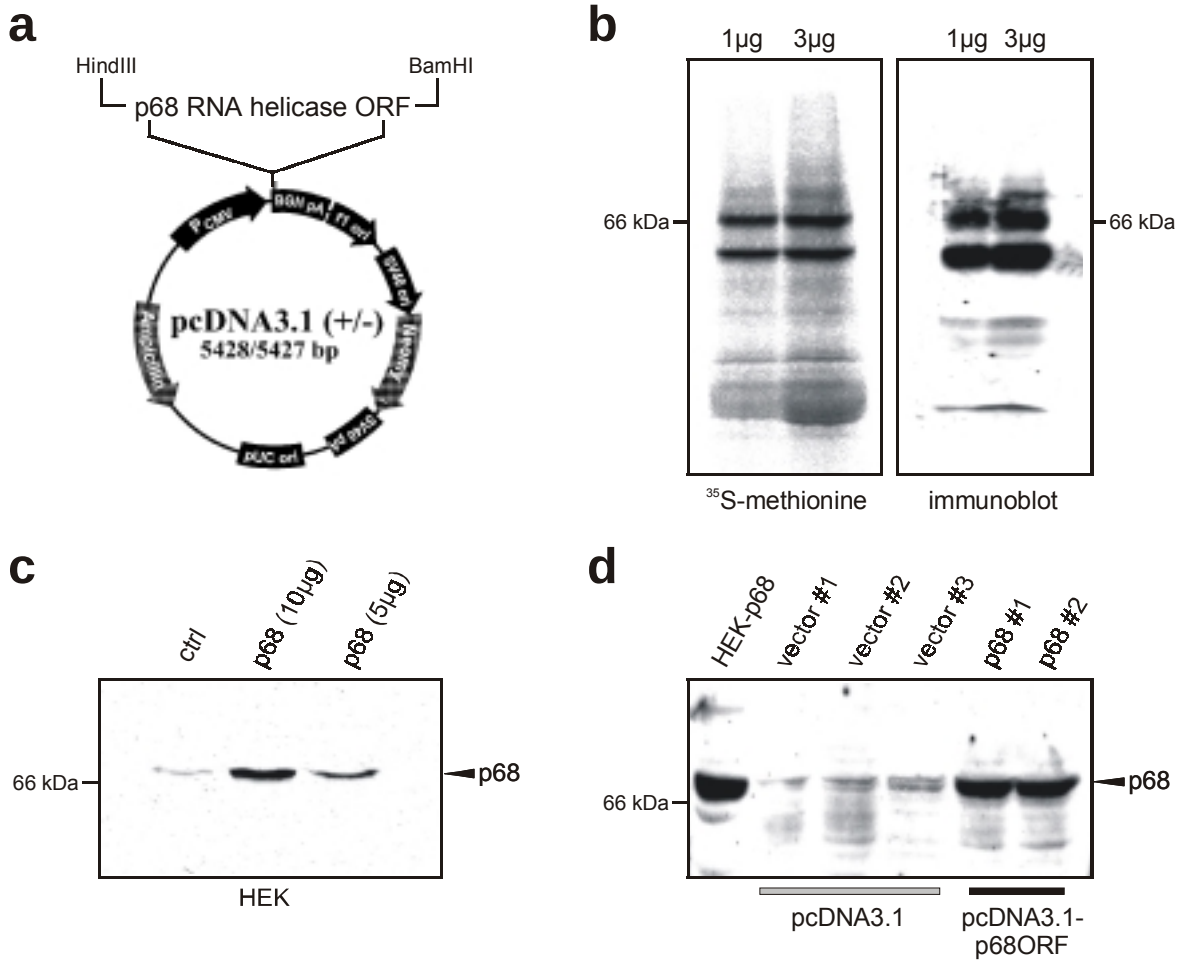

Figure 3.4 Specificity of the anti-p68 antiserum. A polyclonal antiserum against p68 protein was raised in rabbits. *a*, to verify the specificity of the antiserum, the full-length p68 cDNA was cloned into pcDNA3.1(+). *b*, SDS-gel electrophoresis of the *in vitro*-transcription/translation reaction of p68 cDNA using the pcDNA3.1(+) construct and [^{35}S]-methionine (*left panel*). The immunoblot of the *in vitro* transcription/translation reaction is shown in the *right panel*. *c*, immunoblot for the presence of p68 protein in pcDNA3.1(+)- (*ctrl*) and pcDNA3.1(+)-p68- (*p68*) transfected HEK cells. *d*, immunoblot for the presence of p68 in stably transfected HaCaT control (*vector #1-3*) and stable p68-overexpressing (*p68 #1-2*) cell lines. Transiently transfected HEK cells (*HEK-p68*) were used as a control.

and also the second band, which is most likely to represent an incomplete translation product (**Figure 3.4b**). Additionally, we detected strongly increased levels of p68 in pcDNA3.1-p68-ORF transiently transfected human embryonal kidney (HEK) cells (**Figure 3.4c**) and stably transfected HaCaT keratinocyte cell lines (**Figure 3.4d**).

3.1.4.2 NO induces p68 protein expression

As a next step, we had to confirm the potency of NO to induce p68 protein expression in keratinocytes. For this purpose, we stimulated quiescent HaCaT keratinocytes using different NO-donating substances. p68 protein induction was determined using the verified p68 specific antibody.

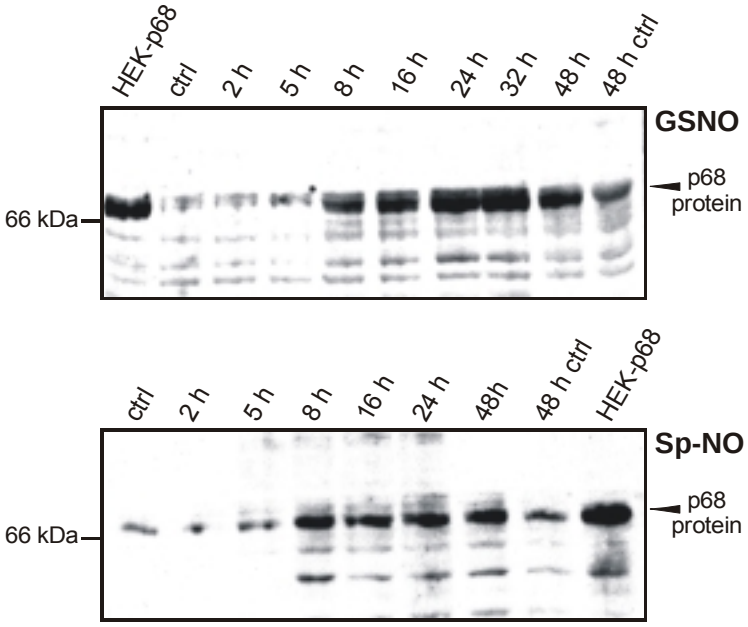

Figure 3.5 NO induces p68 protein expression. Immunoblots demonstrating the stimulation of p68 protein expression in quiescent HaCaT cells by the NO-donors GSNO (*upper panel*) and Sp-NO (*lower panel*). p68-transfected HEK cells (*HEK-p68*) were used to control the specificity of the anti-p68 antiserum.

As shown in **Figure 3.5**, low basal levels of p68 protein expression were detected in quiescent keratinocytes (*ctrl*) whereas a strong increase in p68 protein expression was observed upon NO treatment. More important, induction of p68 expression was not restricted to GSNO alone, as additional the NO-donating agent Sp-NO (**Figure 3.5**, *lower panel*) mediated comparable effects on p68 expression.

3.1.5 Potential involvement of cGMP or MAPK pathways in p68 induction

To gain more insight into the signaling pathway by which NO induces the observed p68 mRNA and protein up-regulation, we investigated possible signaling pathways which might be involved.

3.1.5.1 NO mediated p68 expression is not dependent on activation of soluble guanylyl cyclase

NO is able to activate the soluble guanylyl cyclase (sGC) (Garthwaite *et al*., 1988; Schmidt and Walter, 1994) and thereby leads to an increase in the intracellular levels of cGMP which is the second messenger for most of the physiological actions of NO. To examine whether the NO-induced p68 expression is secondary to activation of soluble guanylyl cyclase and hence cGMP, we treated HaCaT keratinocytes with the membrane-permeable cGMP analogue 8-bromo-cGMP (500 µM). As shown in **Figure 3.6a**, the cGMP treatment did not alter p68 protein expression levels.

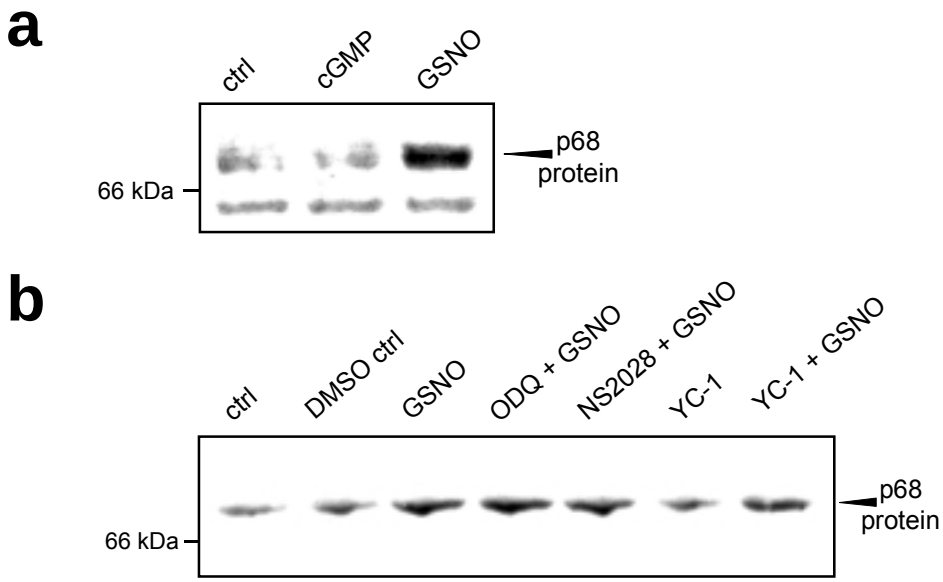

Figure 3.6 NO-induced p68 protein expression is not mediated by activation of soluble ganylyl cyclase. Serum-starved HaCaT keratinocytes were stimulated with (*a*) 500 µM cGMP or 500 µM GSNO for 16 hours. *b*, starved cells were stimulated with activator and inhibitors of sGC 30 min before 500 µM GSNO were added. After 16 hours lysates (50 µg) were analyzed by immunoblot.

Furthermore, we tested the two guanylate cyclase inhibitors NS 2028 (100nM) and ODQ (200µM), which were added to the cells 30 min prior to GSNO treatment. Additionally, the sGC stimulator YC-1 (10µM) was tested in the presence or absence

of GSNO. **Figure 3.6b** shows that neither the inhibitors nor the stimulator of sGS activity had any influence on NO-mediated p68 expression. These results indicate that NO-mediated induction of p68 expression is most likely independent of the intracellular formation of cGMP.

3.1.5.2 MAPK cascade is not involved in NO-induced p68 expression

It was shown that NO is able to activate mitogen-activated protein kinase (MAPK) cascades in different cell types (Lander *et al*., 1996; Pfeilschifter and Huwiler, 1996; Callsen *et al*., 1998). Therefore, we decided to investigate the potential involvement of MAPK cascades in NO-induced p68 protein expression. To this end, starved HaCaT keratinocytes were treated with different cell-permeable MAPK cascade inhibitors prior to the addition of GSNO. Neither the JNK inhibitor II which is a selective and reversible inhibitor of c-Jun N-terminal kinase (JNK) nor U0126 which is a specific inhibitor of MEK1 and MEK2, nor the highly specific inhibitor of p38 kinase were able to alter p68 protein expression.

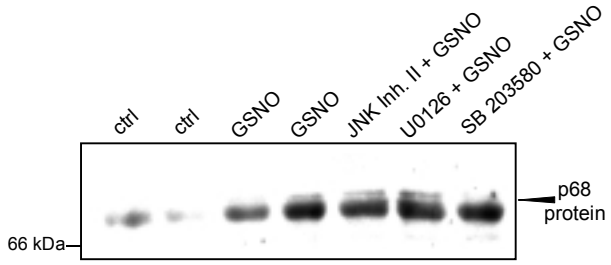

Figure 3.7 MAPK cascade is not involved in NO-induced p68 expression. Starved HaCaT keratinocytes were stimulated with GSNO (500 µM) in the presence or absence of JNK Inhibitor II (1 µM), U0126 (1 µM) or SB 203580 (10 µM). Lysates (50 µg) were analyzed by immonoblot for the presence of p68 protein.

3.2 Growth factors, serum and cytokines induce p68 expression

3.2.1 Growth factors and serum stimulate p68 expression

As we are especially interested in keratinocyte movements in the context of skin repair, we now investigated the potency of those mediators to regulate p68 expression that are well established to drive keratinocyte actions during healing *in vivo* (Martin, 1997; Werner and Grose, 2003). Notably, the potent keratinocyte

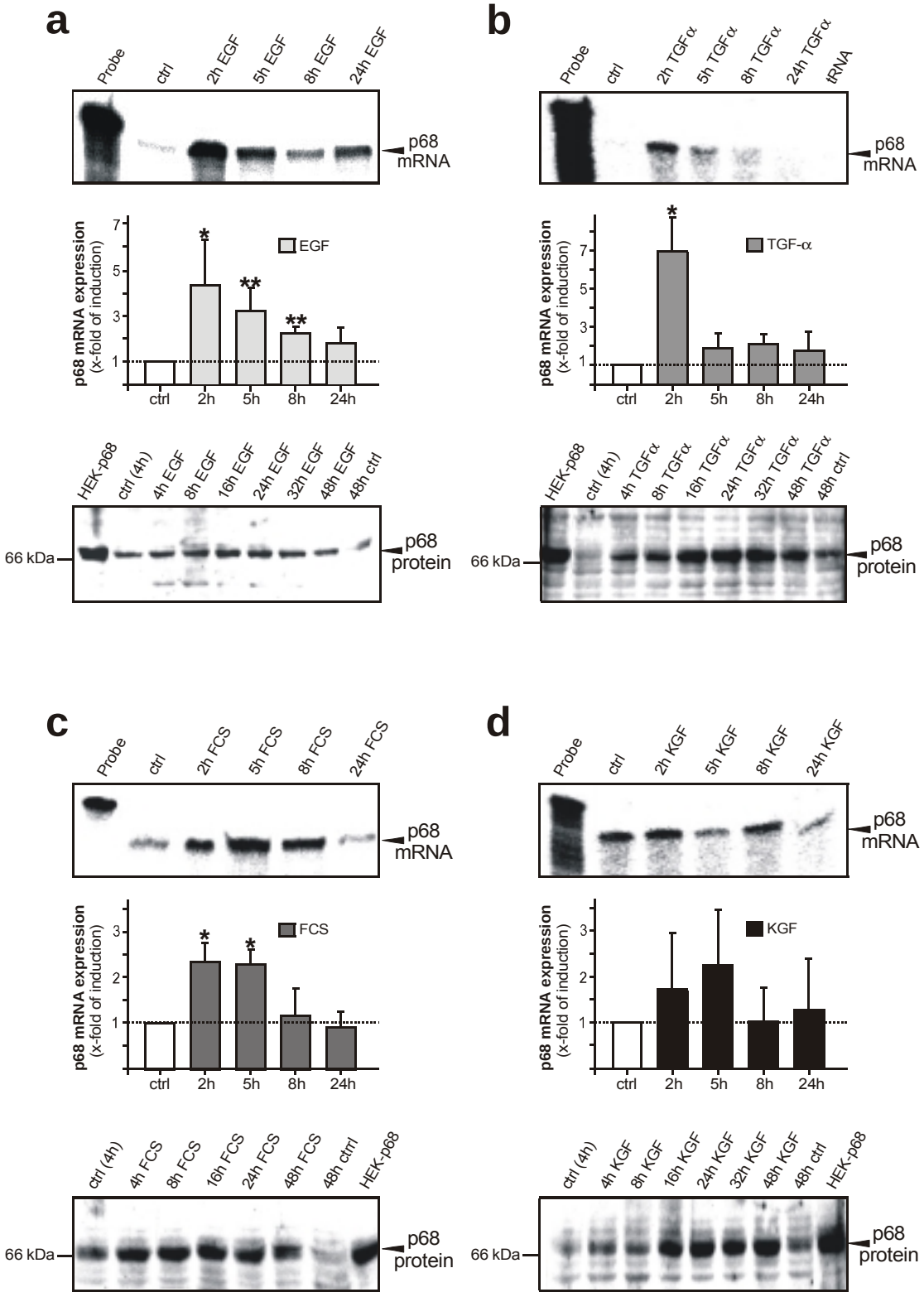

Figure 3.8 Growth factors and serum stimulate p68 expression in keratinocytes. HaCaT keratinocytes were starved for 24 and subsequently stimulated with 10 ng/ml EGF (*a*), 10 ng/ml TGF-α(*b*), 10% FCS (*c*), or 10 ng/ml KGF (*d*) for the indicated time periods. Induction of p68 mRNA expression in the cells was assessed by RNase protection assay. 1000 counts of the hybridization probe was used as a size marker (*upper panels*). A quantification of p68 mRNA (x-fold induction) is shown in the *middle panels*. **, $P < 0.01$; *, $P < 0.05$ (ANOVA, Dunnett's method) as compared to control. Bars indicate the mean ±SD obtained from four (n=4) independent cell culture experiments. Immunoblots demonstrating growth factor and serum stimulation of p68 protein expression in HaCaT cells are shown in the *lower panels*. p68-transfected HEK cells (*HEK-p68*) were used to control the specificity of the anti-p68 antiserum.

mitogens EGF (**Figure 3.8a**), TGF-α (**Figure 3.8b**), serum (**Figure 3.8c**) and also KGF (**Figure 3.8d**) were potent inducers of p68 expression in cultured HaCaT cells. Interestingly, the increase in p68 protein expression was long-lasting for all growth factors tested, as we found still elevated p68 levels after 48h of stimulation (**Figures 3.8a-d**).

3.2.2 Pro-inflammatory cytokines induce p68 expression

Inflammation, reepithelialisation, and granulation tissue formation are driven in part by a complex mixture of growth factors and cytokines, which are released into the area of injury (Clark, 1996). Especially, pro-inflammatory cytokines are important mediators of cellular actions during tissue regeneration.

We could show that also a mixture of pro-inflammatory cytokines clearly induced p68 expression in HaCaT keratinocytes (Figure 3.9), although p68 protein levels declined earlier when compared to growth factor-stimulated cells.

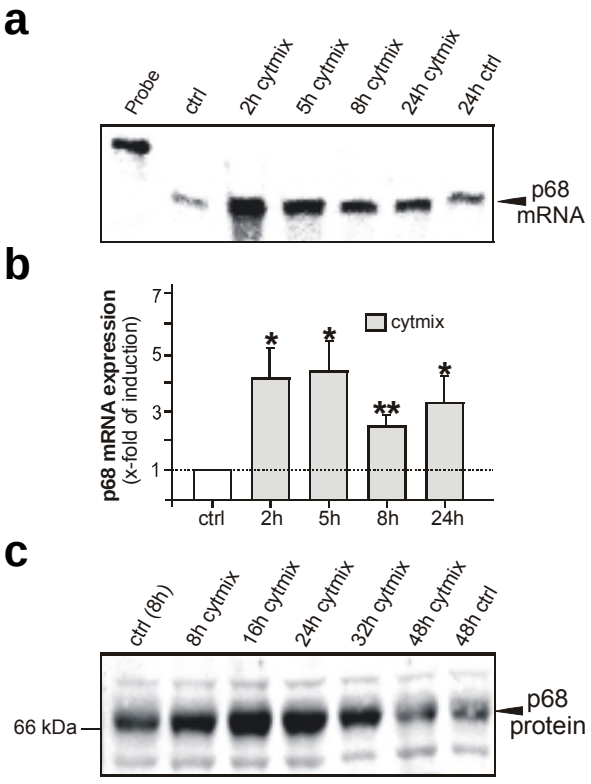

Figure 3.9 Pro-inflammatory cytokines induce p68 expession in keratinocytes. Starved HaCaT keratinocytes were stimulated with a combination of IL-1β (2 nM), TNF–α (2 nM) and IFN-γ (100U/ml) for the indicated time periods. *a*, induction of p68 mRNA expression in the cells was assessed by RNase protection assay. 1000 counts of the hybridization probe was used as a size marker. *b*, a quantification of p68 mRNA (x-fold induction). **, $P < 0.01$; *, $P < 0.05$ (ANOVA, Dunnett's method) as compared to control. Bars indicate the mean ±SD obtained from four (n=4) independent cell culture experiments. *c*, an immunoblot demonstrating cytokine stimulation of p68 protein expression in HaCaT cells.

It is known that a mixture of cytokines also induces iNOS expression in keratinocytes (Frank *et al*., 1998, 2000). To determine a possible role of endogenously produced NO in p68 expression, we treated cells with cytokines (IL-1β, TNF-α, IFN-γ) in the presence or absence of the NOS inhibitor N^G-monomethyl-L-arginine (L-NMMA). However, and most probably due to the delayed appearance of iNOS in the cells after 12 h (Frank *et al*., 1998, 2000), we could not detect an influence of endogenous NO on p68 expression (**Figure 3.10**).

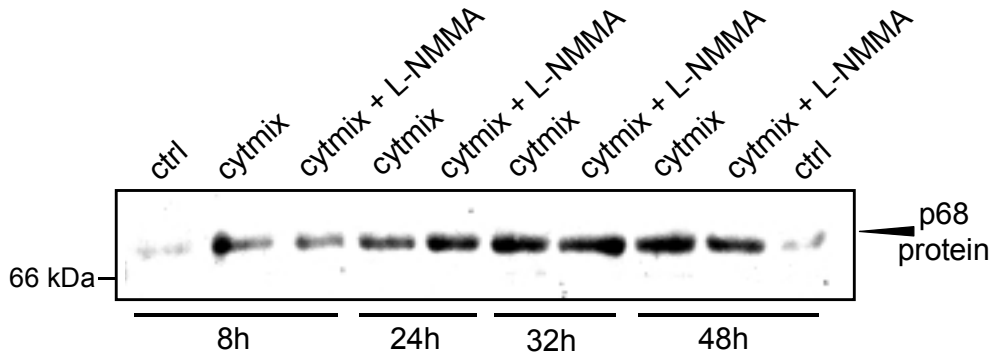

Figure 3.10 p68 expression is not induced by endogenously produced NO. HaCaT keratinocytes were rendered quiescent by serum starvation and subsequently treated with a combination of inflammatory cytokines (2 nM of IL-1β, 2 nM TNF–α, 100 U/ml IFN-γ) in the presence or absence of 2 mM L-NMMA for the indicated time periods. Induction of p68 protein expression in the cells was assessed by immonoblot.

In summary, we could determine a series of wound healing associated mediators, in addition to exogenous NO, as potent inducers of p68 expression in keratinocytes.

3.3 p68 is localized in the nucleus

3.3.1 p68 is localized in nuclei of human and murine keratinocytes *in vitro*

p68 has been described to localize in the nuclei of interphase cells *in vitro* (Lamm *et al*., 1996; Nicol *et al*., 2000). To determine if this is also true for keratinocytes, we separated lysates of human HaCaT and murine PAM 212 keratinocytes into cytosolic and nuclear fractions. As shown in **Figure 3.11** p68 protein was predominantly localized in the nuclear compartment in human and murine keratinocytes.

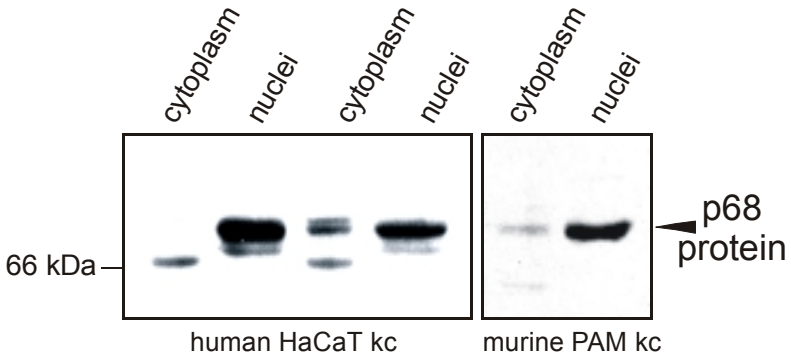

Figure 3.11 p68 is localized in nuclei of human and murine keratinocytes *in vitro.* Lysates of exponentially growing human HaCaT and murine PAM 212 keratinocytes were separated into cytosolic and nuclear fractions and subsequently analyzed by immunoblot for the presence of p68 protein as indicated

3.3.2 Construction of a p68/ GFP fusion protein

As a next step, we intended to further characterize the subcellular localization of p68, as we had found the protein predominantly localized in the nuclei of keratinocytes. To this end, we first constructed a p68/GFP fusion protein by cloning the human p68 ORF without stop codon into the pEGFP-N1 vector (**Figure 3.12**).

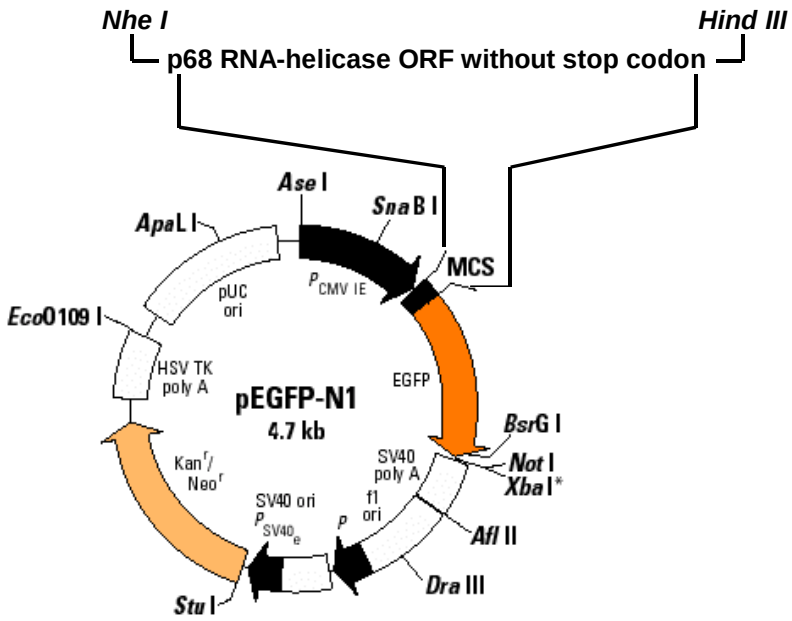

Figure 3.12 Map of the pEGFP-N1-p68 construct

The pEGFP-N1-p68 construct was transiently transfected into HaCaT keratinocytes. Again, we could confirm the presence of the transfected p68/GFP fusion protein in nuclear preparations of the cells using a GFP-specific antibody (**Figure 3.13a**). Furthermore, fluorescent microscopy revealed the nuclear staining of the p68/GFP

fusion protein. Interestingly, the nuclear staining showed dense nuclear accumulations (**Figure 3.13b**).

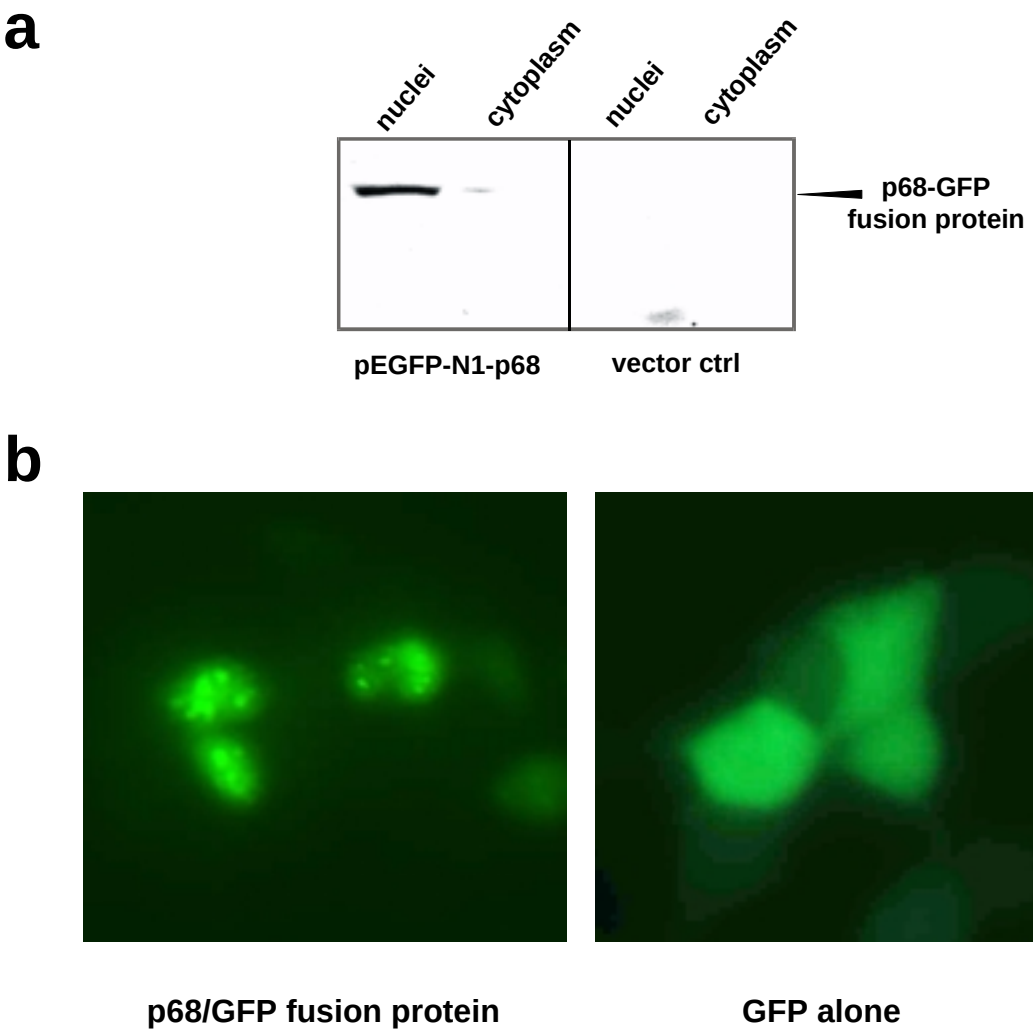

Figure 3.13 p68 localizes in keratinocyte nuclei. Localization of the p68/GFP fusion protein in nuclei of transiently transfected HaCaT cells. *a*, lysates of pEGFP-N1-p68-transfected or vector-transfected keratinocytes were separated into cytosolic and nuclear fractions and subsequently analyzed by immunoblot for the presence of p68/GFP fusion protein (*anti-GFP-antibody*). *b*, localization of p68/GFP fusion protein (left panel) or GFP alone (right panel) as assessed by fluorescent microscopy.

3.3.3 p68 localizes in nucleoli of keratinocytes

It is known from the literature that during late telophase p68 was found to co-localize with the nucleolar protein fibrillarin in nascent nucleoli (Nicol *et al*., 2000). Therefore, we speculated whether nuclear accumulations of p68/GFP fusion protein of transfected keratinocytes (**Figure 3.13b**) are localized into nucleoli. To address this question, we transiently transfected HaCaT keratinocytes with the pEGFP-N1-p68 construct. Nucleolin was chosen to specifically identify nucleoli. Nucleolin represents

a nonhistone nucleolar protein of eucaryotic cells that is present in abundance at the dense fibrillar and granular regions of the nucleolus (Bugler *et al*., 1982; Shaw and Jordan, 1995). Confocal microscopy revealed a strong co-localization of p68/GFP

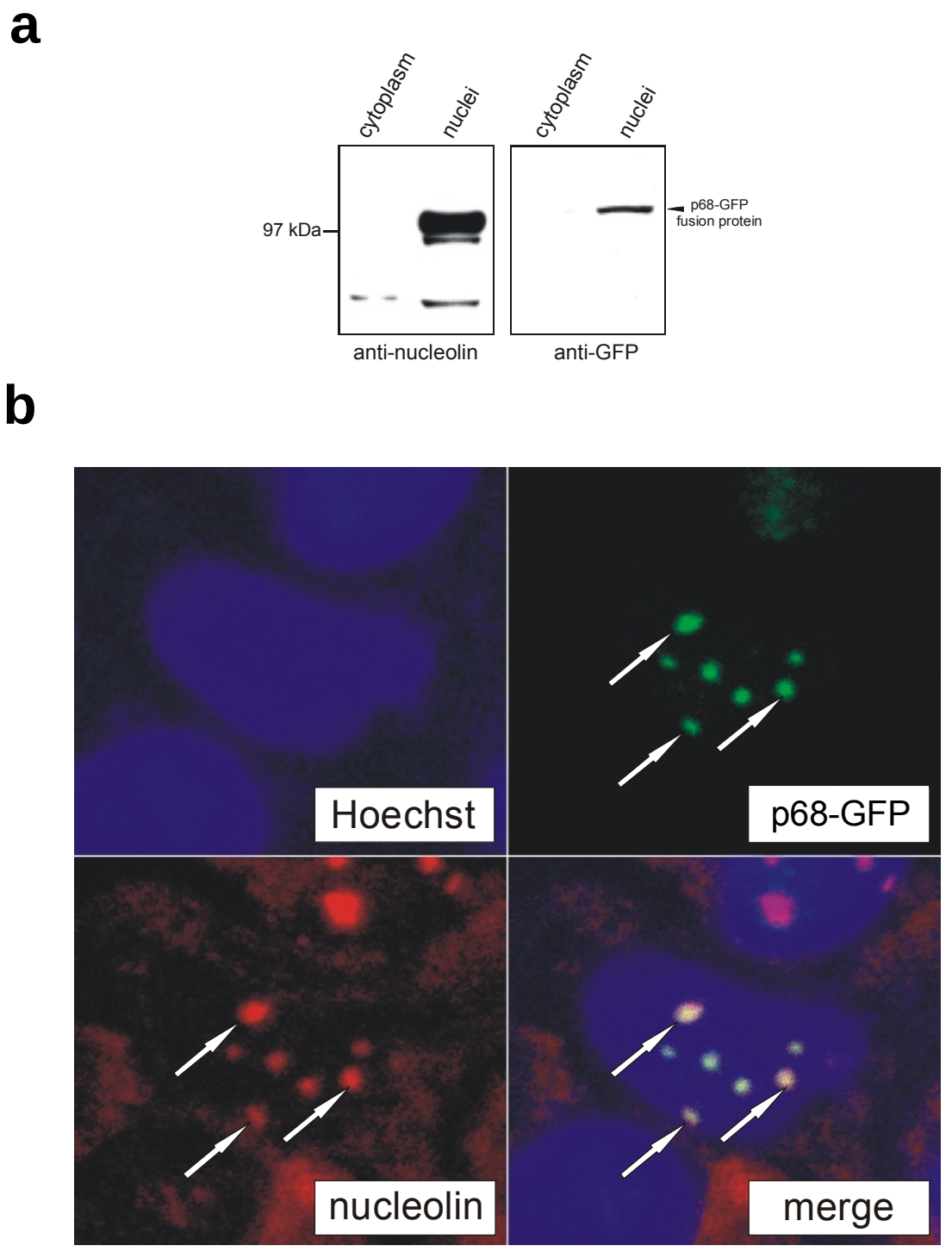

Figure 3.14 p68 localizes to nucleoli in keratinocytes. *a*, co-localization of nucleolin and the p68/GFP fusion protein in nuclei of transiently transfected HaCaT cells. Lysates of p68-transfected keratinocytes were separated into cytosolic and nuclear fractions and subsequently analyzed by immunoblot for the presence of nucleolin (*anti-nucleolin*) and p68-GFP fusion protein (*anti-GFP*) as indicated. *b*, co-localization of p68/GFP fusion protein and nucleolin as assessed by confocal microscopy.

with nucleolin in transfected keratinocytes, and both proteins matched completely in their spatial expression pattern (**Figure 3.13b**). The observed localization strongly suggested the presence of p68 within the nucleoli of the cells, as nucleolin is established to be present in the fibrillar and granular regions this distinct nuclear sub-compartment (Bugler *et al*., 1982; Shaw and Jordan, 1995; Srivastava and Pollard, 1999).

3.4 p68 and skin repair

3.4.1. p68 protein expression is transiently decreased in wounded skin

Next, we investigated the presence of p68 mRNA and protein expression in normal and wounded murine skin. Moreover, as we had isolated p68 as a NO-inducible gene in keratinocytes, we also analyzed iNOS-deficient ($iNOS^{-/-}$) mice for p68 expression. We found a constitutive expression of p68 in non-wounded skin in both wild-type and iNOS-deficient animals (**Figure 3.15a, b;** *ctrl skin*). However, wounding led to an unexpected expression pattern of p68 in wild-type and iNOS knock-out animals. Whereas p68 mRNA levels were not significantly altered in healthy animals, we detected a doubling of p68 mRNA expression in wounds from NO-deficient mice which turned out to be significant (**Figure 3.15b**). However, in both experimental setups, p68 protein expression diminished rapidly after wounding in the presence of p68 mRNA (**Figure 3.15c**). Interestingly, p68 protein reappeared at the end of the inflammatory phase of repair in control mice (**Figure 3.15c**, *upper panel*). Unexpectedly, as we had described p68 to be under a positive regulatory control of exogenously added NO in keratinocytes *in vitro*, we found a marked re-increase of p68 after injury in NO-deficient mice that paralleled the increase in p68 mRNA in these animals. Notably, p68 was clearly detectable after 3 and 5 days of repair in iNOS knock-out mice, at time points when p68 was not yet present in those amounts that could be detected by immunoblotting (**Figure 3.15c**).

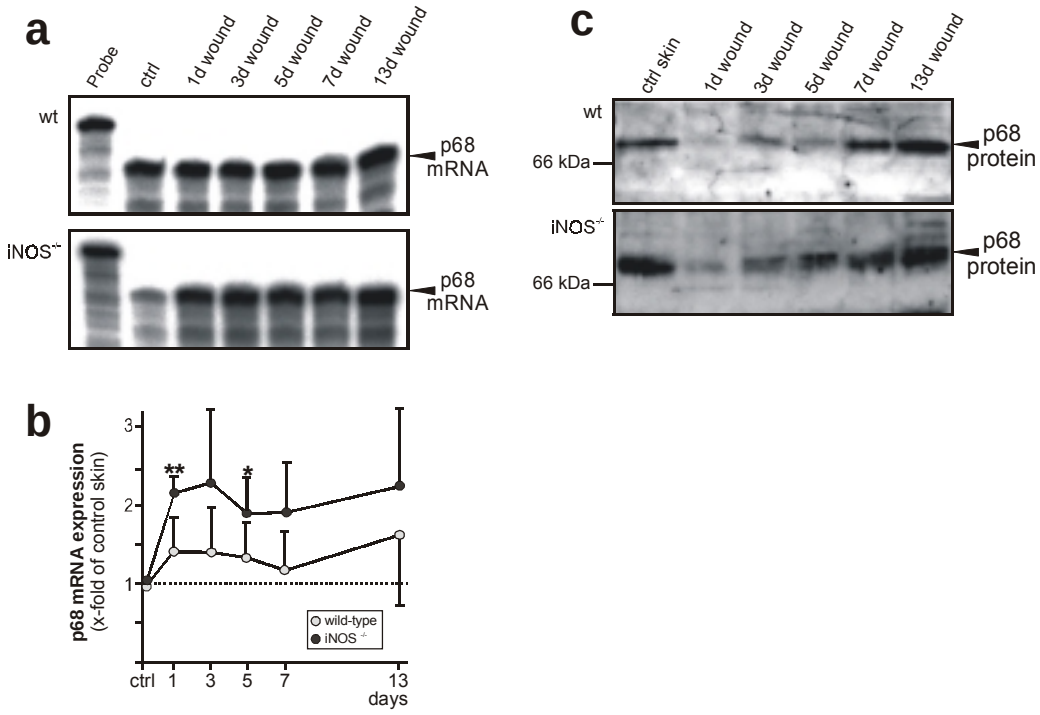

Figure 3.15 Expression of p68 upon skin wounding. *a*, regulation of p68 mRNA expression in C57BLKS (wild-type) and C57BLKS-iNOS$^{-/-}$ (iNOS$^{-/-}$) mice was assessed by RNase protection assay. 1000 counts of the hybridization probe was used as a size marker. *b*, a quantification of p68 mRNA (x-fold induction) is shown. **, $P < 0.01$; *, $P < 0.05$ (ANOVA, Dunnett's method) as compared to control skin. Bars indicate the mean ±SD obtained from wounds (n=48) isolated from animals (n=12) from three independent animal experiments. *c*, total protein (100 µg) from lysates of non-wounded and wounded back skin (day 1, 3, 5, 7, and 13 after injury as indicated) isolated from C57BLKS (wt) and C57BLKS-iNOS$^{-/-}$ (iNOS$^{-/-}$) mice as indicated were analyzed by immunoblot for the presence of p68 protein. Eight wounds (n=8) from the backs of four animals were excised for every experimental time point and used for protein isolation. Ctrl skin refers to nonwounded skin. p68 protein is indicated by an arrow.

3.4.2 p68 protein is restrictively localized in nuclei of keratinocytes *in vivo*

As a next step, we determined the localization of p68 protein at the wound site. We did so, as an absent immunopositive signal for p68 protein in Western blot analysis does not necessarily mean the total absence of the protein at the wound site. Thus, we analyzed 5 day wounds of C57BLKS control mice by immunohistochemistry. It is important to note that we indeed detected immunopositive signals for p68 protein at the wound site. Interestingly, p68 expression was clearly restricted to keratinocyte nuclei of non-wounded skin (**Figure 3.16*a***) and of the developing epithelium (**Figure 3.16b**).

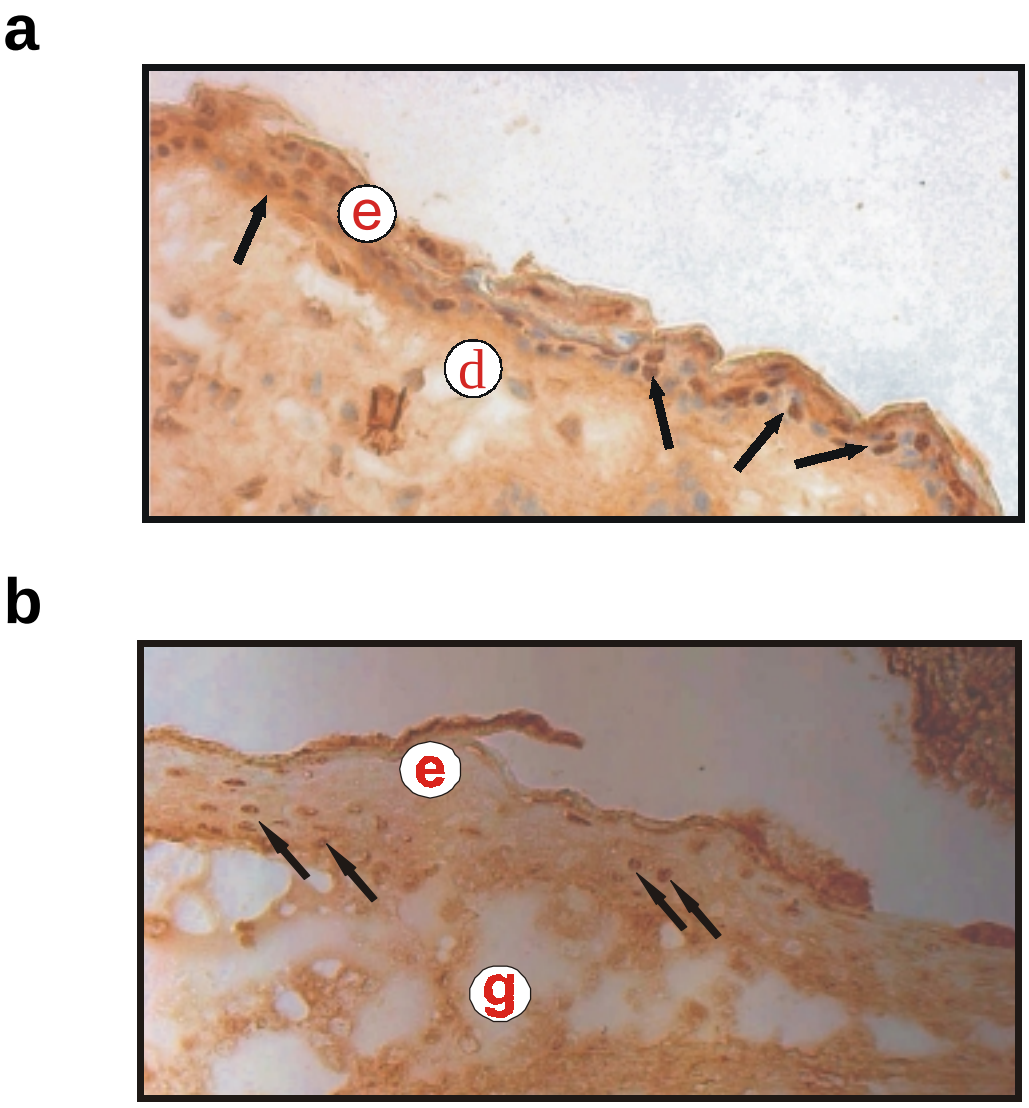

Figure 3.16 p68 is localized in keratinocytes *in vivo*. frozen sections (6µm) from nonwounded mouse skin (*a*) and mouse wounds at day 5 post-wounding (*b*) were incubated with the polyclonal antiserum directed against p68. All sections were stained with the avidin-biotin-peroxidase complex system using 3,3-diaminobenzidine-tetrahydrochloride as a chromogenic substrate. Immunopositive signals in nuclei of the developing epithelium are indicated with *arrows*. As immunopositive signals localized in nuclei, we did not counterstain nuclei with hematoxylin. *d*, dermis; *e*, epithelium; *g*, granulation tissue. *c*, lysates of non-wounded and wounded back skin (day 5 and 7 after injury as indicated) isolated from C57BLKS mice were separated into cytosolic and nuclear fractions by differential centrifugation. Cytosolic and nuclear fractions were subsequently analyzed by immunoblot for the presence of p68 protein as indicated. Eight wounds (n=8) from the backs of four animals were excised for every experimental time point and used for protein isolation. p68 protein is indicated by an *arrow*.

Moreover, our p68 antibody recognizes only about one third of the epithelial nuclei, suggesting that the nuclear presence of p68 might be associated with a distinct phase of the cell cycle (**Figure 3.16*a***, *arrows*). Additionally, it is important to note that the particularly weak p68-specific staining of the nuclei could only be detected when nuclei were not counterstained with hematoxylin (**Figure 3.16*a***). Evidently, the weak immunopositive signals in wound sections confirmed the low levels of p68 protein observed by immunoblotting, as the protein indeed was present, but clearly detectable, only in small amounts at the wound site. However, histological data suggested that we might succeed to detect p68 protein at early states of healing by immunoblot, when we enrich the wound lysates for nuclei. As shown in **Figure 3.16*b***, we now detected clearly visible amounts of p68 protein in the nuclear fractions of 5 and 7 day wound tissue, strongly confirming our immunohistological findings.
Interestingly, p68 mRNA was present in epidermal keratinocytes (wound margin) and mesenchymal cells of the dermis (inner wound) (**Figure 3.17a**). However, only keratinocytes expressed p68 protein (**Figure 3.17b**).

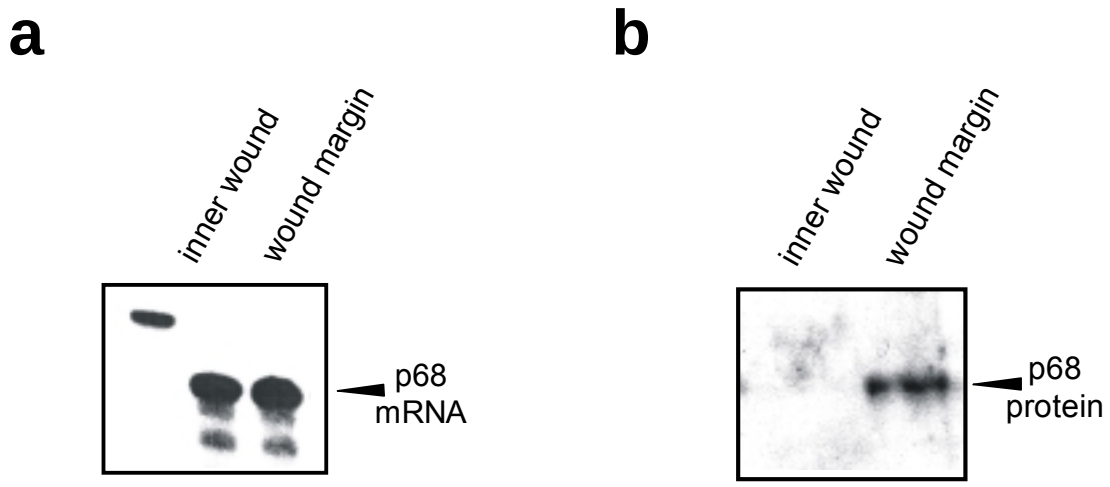

Figure 3.17 Distribution of p68 expression in 1 d wounds. *a*, RNase protection assay demonstrating distribution of p68 mRNA from C57BLKS (wt) at the wound margin and inner region of wound. 1000 counts of the hybridization probe was used as a size marker. *b*, total protein (100 µg) from lysates of the wound margin and inner region of wound isolated from C57BLKS (wt). p68 protein is indicated by an arrow.

3.5 Silencing p68 RNA helicase protein expression by short interfering RNA (siRNA)

To gain more information about p68 protein function, we specifically down-regulate p68 gene expression by short interfering RNA (siRNA). The siRNA technique uses molecules that bind the target messenger RNA in a sequence-specific manner and subsequently catalyze the endonucleolytic cleavage of this mRNA (Fire *et al*., 1998; Elbashir et al., 2001). In order to investigate p68 protein function HaCat keratinocytes were transfected with p68-specific siRNA. **Figure 3.18** shows the down-regulation of endogenous, FCS induced p68 using p68-specific siRNA molecules.

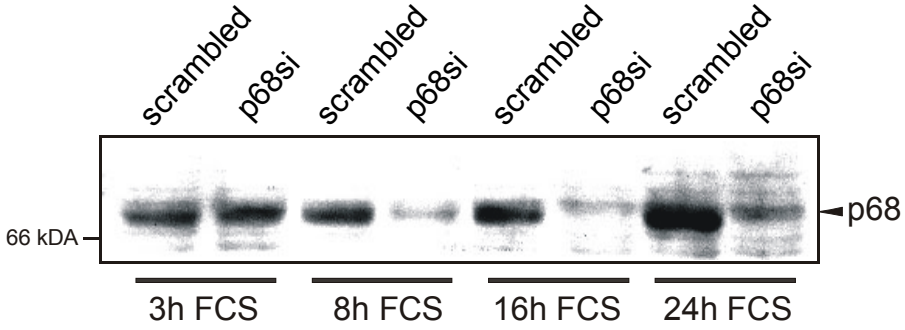

Figure 3.18 Silencing p68 gene expression by siRNA. HaCaT keratinocytes were transfected with p68-specific siRNA (p68si) or scrambled oligos and grown in the presence of 10% FCS for the indicated time periods. Lysates (50 µl) were analyzed by immunoblot.

3.6 p68 expression is functionally connected to keratinocyte proliferation and VEGF gene expression

Finally, we determined whether p68 expression was implicated in the control of those important keratinocyte functions that also participate in skin repair. Thus, we investigated the role of p68 protein for keratinocyte proliferation and VEGF gene expression. First, we established HaCaT keratinocyte cell lines which stably overexpressed p68 protein (**Figure 3.4d**). As shown in **Figure 3.19a** (*left panel*), a constitutive and stable overexpression of p68 led to a strong increase in keratinocyte proliferation rates (+38 ± 6.1% within 24 h) as determined by incorporation of [^{3}H]-thymidine into the cells. It is important to note that induction of endogenous p68 by serum (**Figure 3.8c**) in control cell lines attenuated the difference in cell proliferation (+20 ± 3.5%) between control and p68-overexpressing cell lines (**Figure 3.19a**, *right*

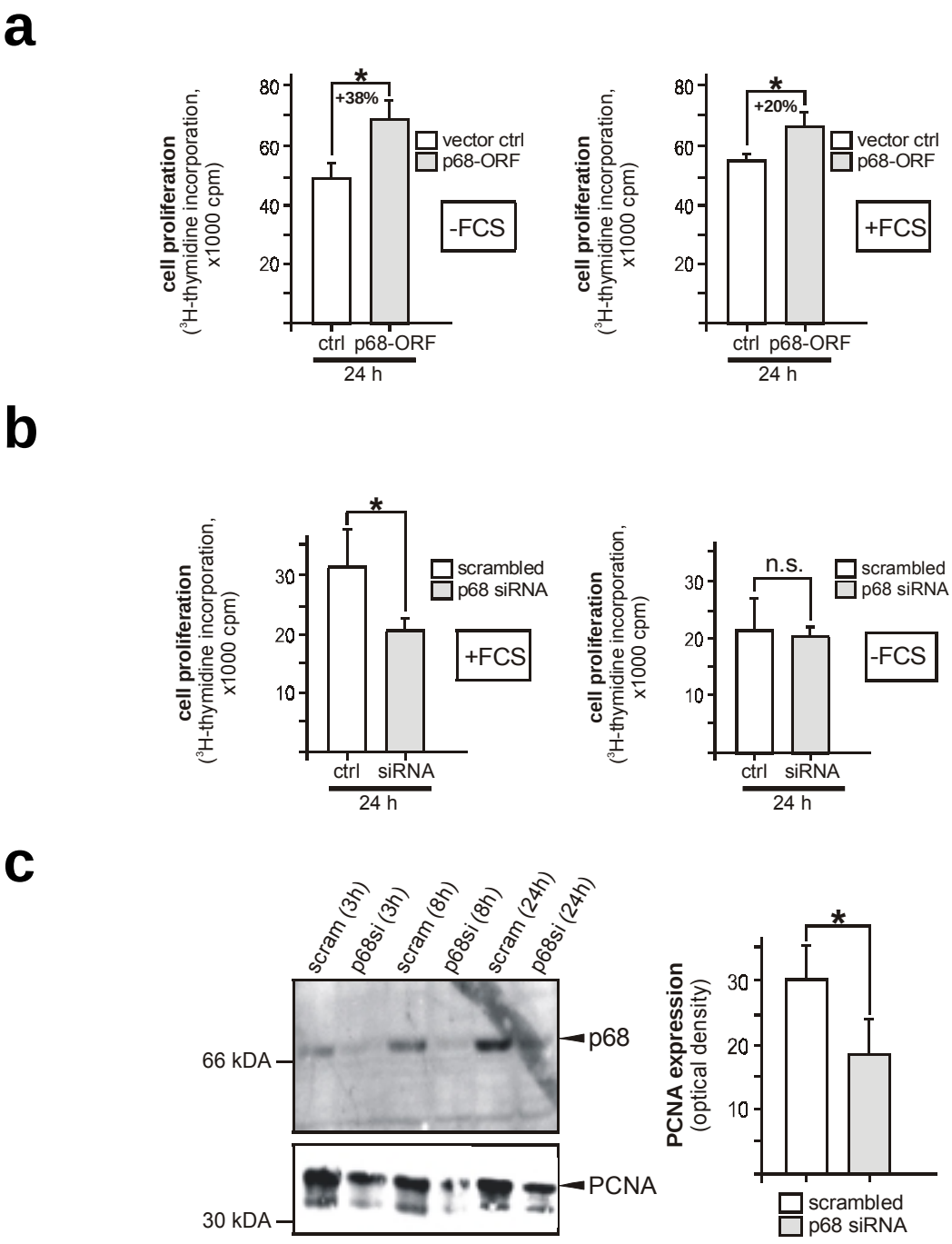

Figure 3.19 p68 functionally contributes to keratinocyte proliferation. *a*, stably transfected vector control (*vector ctrl*) and p68-overexpressing (*p68-ORF*) HaCaT cell lines were grown in the absence (*left panel*) or presence (*right panel*) of 5% FCS as indicated. After 24 h, cell proliferation was determined by [^{3}H]-thymidine-incorporation into the cells. *, $P < 0.05$ (Student's *t* test) as indicated by the brackets. Bars indicate the mean ±SD obtained from three (n=3) independent cell culture experiments. *b*, A quantification of [^{3}H]-thymidine-incorporation 24 h after transfection of the siRNA oligonucleotides (*p68 siRNA*) is shown for serum treated (*left panel*) and non-treated (*right panel*) cells. *, $P < 0.05$; n.s., not significant (Student's *t* test) as indicated by the bracket. Bars indicate the mean ±SD obtained from three (n=3) independent cell culture experiments. *c*, immunoblots showing the down-regulation of endogenous, FCS-induced p68 by p68-specific siRNA (*left panel*) and the subsequent down-regulation of PCNA. PCNA amounts were quantified by optical density (*right panel*).

panel). In line with these findings, a down-regulation of endogenous p68 by siRNA techniques in unprocessed HaCaT keratinocytes markedly reduced cellular proliferation rates. [^{3}H]-thymidine-based proliferation assays of non-stimulated and serum-induced HaCaT cells clearly demonstrated the pivotal role of p68 in keratinocyte proliferation. In serum-free conditions, when p68 is not induced in the cells, a transfection of p68-specific siRNA did not significantly alter the slow keratinocyte proliferation behavior (**Figure 3.19b**, *right panel*). By contrast, transfection of p68-specific siRNA potently shut off serum-induced p68 protein synthesis in the cells (**Figure 3.18**). The observed and potent down-regulation of p68 protein in serum-stimulated cells nearly completely abolished the mitogenic effect which was mediated by serum in the cells (**Figure 3.19b**, *left panel*). In line, immunoblot analysis determined a marked reduction of proliferating cell nuclear antigen (PCNA) as a marker of cell proliferation in siRNA-treated keratinocytes (**Figure 3.19c**).

As DEAD box proteins participate in the regulation of RNA/protein interactions (Tanner and Linder, 2001), we investigated the possibility that p68 is also functionally implicated in the control of gene expression in keratinocytes. VEGF has been shown to be expressed in wound margin keratinocytes, and its expression undergoes a complex regulation by growth factors, cytokines and NO in these cells (Brown *et al*., 1992; Frank *et al*., 1995, 1999). For this reason we finally investigated the role p68 in serum- and NO-induced VEGF expression in HaCaT keratinocytes (**Figure 3.20**). Keratinocyte cell lines, which stably overexpressed p68 protein (*p68-ORF #1* and *2*), were treated with serum for 5 h. Serum is known to represent an inducer of VEGF expression in keratinocytes (Frank *et al*., 1995, 1999). Upon serum treatment, the p68 overexpressing cells were characterized by a marked increase in VEGF mRNA levels (**Figure 3.20a**). VEGF has been described as a NO-induced gene in keratinocytes (Frank *et al*., 1999), sharing this property with p68 (this study). Thus, it was tempting to speculate that NO-induced p68 might functionally participate in NO-induced VEGF expression. To evidence this hypothesis, we induced treated HaCaT keratinocytes with GSNO in the presence or absence of p68-specific siRNA for 24 h and subsequently analyzed the cell culture supernatants by ELISA. As shown in **Figure 3.20b**, down-regulation of endogenous p68 by siRNA transfection significantly reduced the amount of NO-induced VEGF protein (1120 ± 133 pg/ml vs. 752 ± 47

pg/ml; p < 0.05) compared to cells which received the scrambled siRNA oligonucleotides as a control.

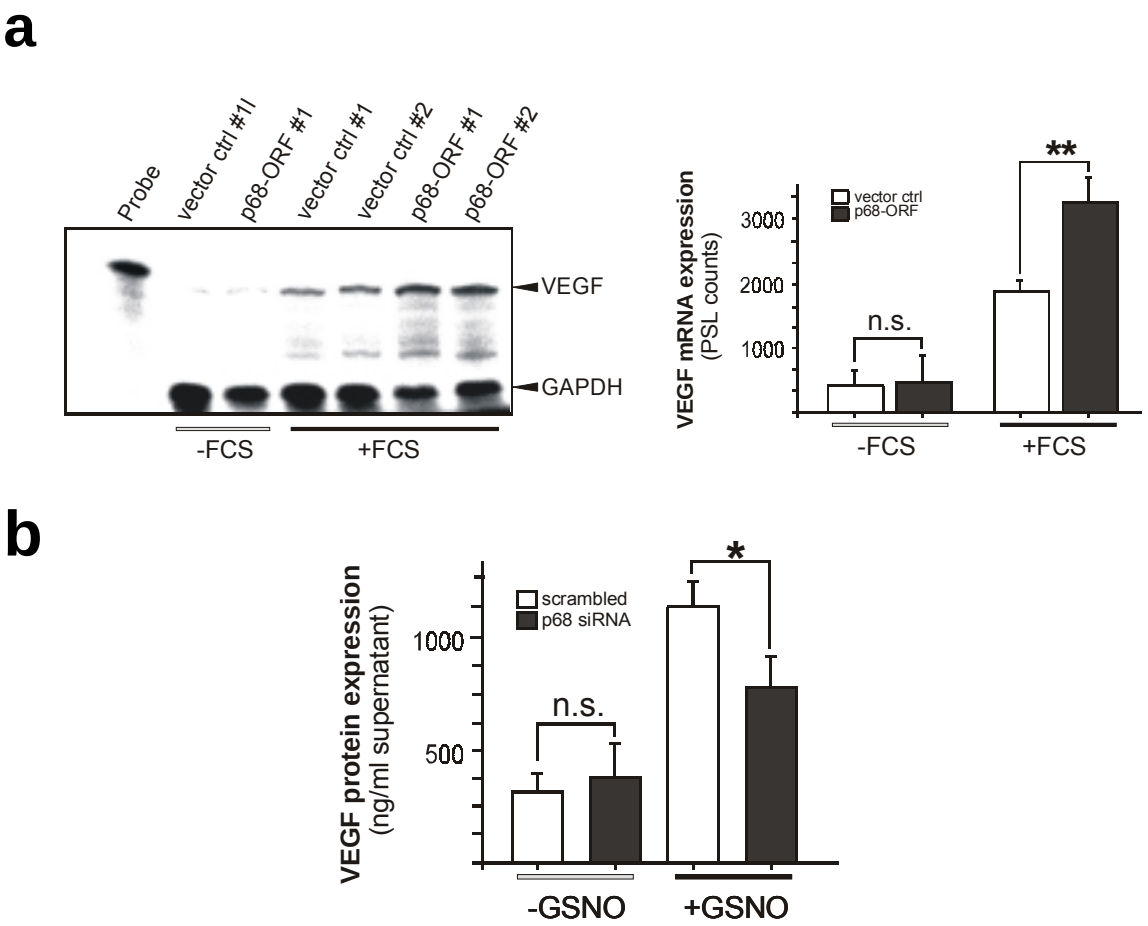

Figure 3.20 p68 functionally participates in keratinocyte VEGF expression. *a*, quiescent stably transfected keratinocyte control (*vector ctrl*) and p68-overexpressing (*p68-ORF*) cell lines s were cultured in the absence (*-FCS*) or presence (*+FCS*) of 10% FCS for 5 h as indicated. Induction of VEGF mRNA expression in the cells was assessed by RNase protection assay (*upper panel*). 1000 counts of the hybridization probe was used as a size marker. A quantification of VEGF mRNA in control (*vector ctrl*) and p68-overexpessing (*p68-ORF*) cell lines is shown in the *lower panel*. **, $P < 0.01$; n.s., not significant (Student's *t* test) as indicated by the brackets. Bars indicate the mean ±SD obtained from three (n=3) independent cell culture experiments. *b*, quantification of VEGF protein in cell culture supernatants from non-treated (*-GSNO*) and GSNO-treated (*+GSNO*) HaCaT keratinocytes after transfection of scrambled (*scrambled*) or p68-specific siRNA (*p68 siRNA*) oligonucleotides.*, $P < 0.05$; n.s., not significant (Student's *t* test) as indicated by the bracket. Bars indicate the mean ±SD obtained from three (n=3) independent cell culture experiments.

4

Discussion

4.1 Nitric oxide and skin

Nitric oxide (NO) is now well established as an important messenger molecule in normal skin biology and also diseased skin (Bruch-Gerharz *et al*., 1998; Weller, 1999). Studies on skin tissue have also demonstrated a key function of NO in the process of cutaneous wound healing (Frank *et al*., 2002). iNOS-deficient mice suffered from a delay in wound repair (Yamasaki *et al*., 1998). In line, an early induction of iNOS upon wounding has been well documented (Frank *et al*., 1998a), and inhibition of iNOS enzymatic activity during healing resulted in a markedly reduced reepithelialization (Stallmeyer *et al*., 1999). These findings strongly suggested NO to function as a potent mitogenic mediator for skin keratinocytes *in vivo*. Accordingly, it has been convincingly demonstrated that proliferation of cultured human keratinocytes could be mediated by low concentrations of NO (Krischel *et al*., 1998; Frank *et al*., 2000a). However, it is particularly not much known about how NO exerts its unique actions on keratinocytes. To gain further insight into these mechanisms, we established and screened a subtractive keratinocyte cDNA library for NO-regulated genes to characterize new players in NO actions from the cells.

4.2 Nitric oxide and p68 RNA helicase

4.2.1 p68 is a novel NO-induced gene

In this study the p68 DEAD box RNA helicase was identified as a novel NO-induced gene in keratinocytes. Besides not yet characterized transcripts which have been additionally isolated using this approach, we focused on p68, as previous work strongly suggested a role of this protein in dynamic cellular movements such as proliferation, transcription, translation, RNA splicing and stability, or ribosome assembly (Tanner and Linder, 2001). We hypothesized that p68 might at least partially contribute to or, moreover, mediate some of the well-established actions of

NO in keratinocyte biology. NO has been shown to control mRNA levels of a series of wound-related genes in keratinocytes such as VEGF or different chemokines (Frank *et al*., 1999, 2000c; Wetzler *et al*., 2000). Additionally, Cu/Zn superoxide dismutase (Cu/Zn SOD) has been identified to be exclusively induced by NO in keratinocytes. Furthermore, it was shown that the enzymatic actions of the Cu/Zn SOD are functionally connected to keratinocyte proliferation. Nevertheless, overexpression of the SOD enzyme did not alter gene expression in the cells (Frank *et al*., 2000a). Thus, NO actions on keratinocyte gene expression and proliferation appeared to be clearly dissected in molecular terms, as we had not yet identified a regulatory player in NO-controlled gene expression that also participated in the control of keratinocyte proliferation. Regarding published data, it was now reasonable to suggest that p68 might serve a control of both keratinocyte gene expression as well as proliferation.

4.2.2 How does nitric oxide exert its action on p68?

We could convincingly demonstrate the potency of exogenous NO to induce p68 expression in keratinocytes. Furthermore, we could demonstrate that NO acts by transcriptional activation of the p68 gene in keratinocytes and is independent from *de novo* protein synthesis. However, the situation for p68 actions appeared to be complex with respect to NO. Although lower amounts of NO (250 µM) were also capable to increase cellular p68 levels, a potent induction of p68 was only achieved with NO concentrations which have been shown to be cytostatic for cultured keratinocytes and characterized by a subsequent differentiation of the cells (Krischel *et al*., 1998). Furthermore, we could not detect an influence of endogenous NO on p68 expression. This is most probably due to the delayed appearance of iNOS in the cells after 12 h (Frank *et al*., 1998b, 2000a) and/or to the strong p68 induction by pro-inflammatory cytokines which preceded the parallel NO-induced p68 expression. However, the in *vivo* situation during the process of wound healing differs from the *in vitro* situation. Despite proliferating keratinocytes of the wound margin, PMN and Mϕ potently express iNOS and subsequently produce NO (Frank *et al*., 1998a). Thus, keratinocyte p68 expression *in vivo* most likely depends on the total amount of NO present at the wound site. Experiments which were performed in order to elucidate the signaling pathway by which NO exerts its action on p68 mRNA expression showed that neither the activation of the soluble guanylate cyclase nor the activation of MAPK cascades are involved in the modulation of p68 expression. This suggests

NO-induced p68 gene expression to be regulated by a direct modulation of transcription factors such as nitrosylation, nitration, and oxidation (Pfeilschifter *et al*., 2001; Grisham *et al*., 1999). Until now, an ultimate "NO-responsive promoter element" has not been identified. NO is a molecule with both, anti-oxidant and pro-oxidant properties, depending on the availability and concentration of potential reaction partners such as superoxide and hydrogen peroxide or other reactive oxygen species (ROS) (Pfeilschifter *et al.,* 2001). It turned out that NO preferentially alters transcription factors that are sensitive to changes in the cellular redox status (Beck *et al*., 1999; Kröncke and Carlberg, 2000; Marshal *et al*., 2000; Pfeilschifter *et al.,* 2001) such as NF-κB, activator protein 1 (AP-1) and Sp-1. Notably, Rössler *et al.* (2000) could demonstrate that the p68 promoter contains a high affinity binding site for Sp1.

4.3 p68 expression is triggered by wound-related keratinocyte mitogens and inflammatory stimuli

The process of keratinocyte proliferation and differentiation represents one central process during tissue regeneration after cutaneous injury. Reepithelialization of the wounded area is driven by highly proliferative keratinocytes, which start to proliferate from the cut edges of the injured tissue, and subsequently migrate into the wound bed. This highly dynamic process finally leads to the formation of a massive bulk of proliferative keratinocytes, the hyperproliferative epithelium, which serves as a cellular source to drive the epithelial tongue to cover the wound area (Clark, 1996; Martin, 1997). Obviously, reepithelialization, essentially occurring in a close spatial and functional connection to the underlying granulation tissue, is central to wound closure. Therefore, formation of new epithelial structures has to be tightly controlled. Key players driving these processes are cytokines, growth factors, mitogens and NO (Moulin, 1995; Martin, 1997; Frank *et al*., 2002). We observed that pro-inflammatory cytokines were able to potently induce p68 gene and protein expression. Moreover, we could demonstrate that typical wound-related keratinocyte mitogens, such as EGF, TGF-α, KGF, and serum appeared to potently trigger an increase in p68 in the cells *in vitro*. This observation was in line with a previous report that demonstrated the induction of p68 in serum-induced proliferating 3T3 fibroblasts (Stevenson *et al*., 1998). Moreover, p68 has been associated to hyperproliferative states of epithelial

cells, as p68 was described to be overexpressed in nuclei from colorectal adenocarcinomas (Causevic *et al.,* 2001). Accordingly, in our excisional wound healing model we found p68 protein to be exclusively expressed in epidermal keratinocytes. Interestingly, p68 mRNA was present in the epidermis and in the dermis of mouse skin. However, only keratinocytes and not fibroblasts were able to translate the p68 mRNA into protein. This is in contrast to the situation for 3T3 cells observed by Stevenson *et al* (1998) mentioned above. The discrepancy might be due to the different expression patterns already observed for p68 expression in vivo and in immortalized cell lines in vitro (Stevenson *et al*., 1998).

4.4 p68 and proliferation

p68 is developmentally and growth regulated and correlates with organ differentiation and maturation in the fetus (Stevenson *et al*., 1998). Another example arguing for p68 to be associated with cellular growth is a study by Iggo *et al.* (1991). The authors demonstrated that Dbp2p, the *S. cerevisiae* p68 homologue, plays a prominent role in the rRNA processing pathway. Interestingly, another publication convincingly showed that an accumulation of 35S pre-mRNA in a dbp2Δ yeast strain and the resulting growth defect could be reversed by human p68 (Bond *et al*., 2001).

In terms of wound healing, the reepithelialization process is crucial to wound closure and characterized by keratinocyte proliferation and differentiation. We hypothesized that p68 might promote reepithelialization as our results clearly supported the direct contribution of p68 in the process of keratinocyte proliferation. We could show that p68 overexpression stimulated and p68 down-regulation attenuated the proliferative behavior of keratinocytes. It is important to note that p68 action on cell proliferation was restricted to mitogen-induced conditions. Thus, we could not find a marked attenuation of keratinocyte proliferation after down-regulation of endogenous p68 under basal, non-stimulated conditions. Evidently, the augmentation of p68 expression seems to represent a pivotal prerequisite to drive serum-induced proliferation in the cells. Therefore, it is reasonable to speculate that serum and, most likely, EGF and KGF as p68-inducing keratinocyte mitogens *in vitro*, might exert parts of their mitogenic potencies on wound keratinocytes by induction of p68. During the highly dynamic process of reepithelialization the proliferating and migrating wound keratinocytes induce the transcription of several genes such as VEGF, different

chemokines, integrins and different matrix metalloproteases (Clark, 1990; Saarialho *et al.,* 1994; Salo *et al*., 1994; Clark *et al.,* 1996; Pilcher *et al*., 1997; Frank *et al*., 1999, 2000c; Wetzler *et al*., 2000). These changes in gene and protein expression require an active transcriptional and translational machinery. Accordingly, p68 is known to be involved in gene transcription, splicing and rRNA processing (Iggo *et al*., 1991; Endoh *et al*., 1999; Watanabe *et al.,* 2001; Bond *et al.*, 2001; Liu, 2002; Fujita *et al*., 2003; Guil *et al*., 2003).

4.5 Nuclear p68 localizes in nucleoli of keratinocytes

An increasing number of nuclear proteins is described to interact with p68. Thus, it has been demonstrated that p68 is associated with the cAMP-dependent protein kinase-anchoring protein AKAP95 in the nuclear matrix of mammalian cells (Akileswaran *et al*., 2001). Furthermore, p68 was found to co-localize with the nucleolar protein fibrillarin in nascent nucleoli during late telophase (Nicol *et al*., 2000). These findings are consistent with our observation of an overall nuclear localization of p68 in keratinocytes, especially in nucleolar structures as assessed by our co-localization experiments using nucleolin as a prototypical nucleolar marker protein. Interestingly, p68 has an additional RNA-binding site in its C-terminus (aa 477-504) (Hirling *et al*., 1989) which is commonly found in RNA-binding proteins (Mattaj *et al*., 1993; Burd *et al*., 1994), such as nucleolin (Ghisolfi *et al*., 1992) or heterogeneous nuclear ribonucleoprotein particle (hnRNP) A1 (Liu and Dreyfuss, 1995). In the 1960s, it was demonstrated that nucleoli are the site of ribosome biogenesis (Scherl *et al*., 2002). However, the molecular mechanisms governing the assembly of ribosome biogenesis are still poorly defined. Recently, Scherl *et al.* (2002) confirmed the proposed plurifunctional nature of the nucleolus (Bond and Wold, 1993; Pederson, 1998; Buonomo *et al*., 1999; Olson *et al*., 2000) by a functional proteomic analysis of the human nucleolus. The authors showed that, in addition to the expected ribosomal proteins and proteins involved in ribosome biogenesis, regulators and components of the translation machinery (ribosomes, tRNAs, signal recognition particle, mRNAs), chaperones and proteins involved in mRNA processing are also present within the nucleoli. Accordingly, Scherl *et al.* (2002) speculate about transcription and translation being coupled in nucleoli.

Notably, p68 is a member of the DEAD-box family which is discussed to be involved in transcriptional and also in translational events (Tanner and Linder, 2001).

4.6 Is p68 a transcriptional co-activator of VEGF gene expression?

Evidently, p68 RNA helicase might function also as a transcriptional co-activator. Endoh *et al.* (1999) showed that p68 acts as a specific co-activator of the human estrogen receptor α AF-1 (hERαAF-1), thus pointing out a role for p68 in hormonal-driven transcription. Moreover, p68 has been shown to directly interact with the transcriptional coactivators p300 and CREB-binding protein (CBP) to promote gene transcription in complex with RNA polymerase II (Rossow and Janknecht, 2003). p300 and CBP are essential during embryogenesis and can modulate gene expression programs involved in cell growth, differentiation, homeostasis and viral pathogenesis (Goodman and Smolik, 2000; Janknecht *et al*., 2002). Noteably, p68 has been found to associate with nuclear cAMP-dependent protein kinase-anchoring protein 95 (AKAP95) (Akileswaran *et al*., 2001) which contains a DNA and a protein kinase A (PKA) binding domain and is thought to link the nuclear matrix to specific cell-signaling events (Coghlan *et al*., 1994). Since p68 also interacts with p300, the interaction between p68 and AKAP95 may serve as a mechanism to drive cAMP regulated gene expression. Interestingly, CBP/p300 proteins have been demonstrated to essentially contribute in hypoxia-induced transcriptional activation of the VEGF gene *in vitro* and in a model of tumor growth *in vivo* (Kung *et al*., 2000). In this study we could show that p68 expression is functionally connected to keratinocyte VEGF gene expression. Furthermore, we could demonstrate that NO-induced p68 is able to alter NO-induced VEGF protein expression, as down-regulation of endogenous p68 by siRNA transfection experiments significantly reduced the amount of NO-increased VEGF protein. p68 overexpression alone was not able to induce VEGF gene expression. Thus, it is reasonable to speculate that p68 acts as transcriptional co-activator. However, we could not rule out that p68 might also control VEGF expression at different post-transcriptional levels, as RNA helicases are known to essentially participate in the formation and function of the spliceosome (Will and Lührmann, 1997; Staley and Guthrie, 1998), in ribosome biogenesis (Tanner and Linder, 2001) and the initiation of translation (Pause and Sonenberg, 1993; Svitkin *et al*., 2001).

4.7 p68 and wound healing

Wound healing is a well-ordered and highly coordinated process involving inflammation, cell proliferation, matrix deposition, and tissue remodeling. After injury, new tissue formation comprises reepithelialization and granulation tissue formation. The latter process encompasses macrophage accumulation, fibroblast ingrowth, matrix formation, and angiogenesis (Clark, 1996). Inflammation, reepithelialization, and granulation tissue formation are driven in part by a complex mixture of growth factors and cytokines, which are released coordinately into the area of injury. We have observed p68 to be induced by NO, wound-related keratinocyte mitogens, and pro-inflammatory cytokines and, moreover, we could demonstrate that p68 promotes keratinocyte proliferation and VEGF gene expression *in vitro*. Thus, it was interesting to investigate p68 mRNA and protein expression during wound healing. Our wound healing studies supported the suggestion that keratinocyte mitogens might overcome the potency of NO to control p68 expression. We found a constitutive expression of p68 in non-wounded skin, which was restricted to the nucleoli of epidermal keratinocytes. In line, a previous study indicated the ubiquitous expression of p68 in newborn and adult mice and rats, respectively. However, although skin tissue was not included, this study suggested that the presence of p68 did not necessarily reflect the extent of cell proliferation in the adult (Stevenson *et al*., 1998). It was completely unexpected for us to recognize elevated levels of p68 mRNA and protein in iNOS-deficient animals compared to wild-type mice. We found lowest amounts of p68 in the inflammatory phase of wounding, which is characterized by a dramatic increase in proliferation of keratinocytes located at the margins of the wound. However, it is important to note that p68 had not diminished, but could be clearly localized in keratinocyte nuclei of the developing neo-epithelium. Moreover, p68 mRNA was present at the wound margins (hyperproliferative epithelia) and in the inner region of the wound (granulation tissue) whereas p68 protein was predominantly expressed at the wound margins. These results clearly suggest keratinocytes as predominant producers of p68 protein. Interestingly, only a defined number (about 20% to 30%) of wound keratinocytes expressed p68. Thus, it is tempting to speculate that the presence of p68 in keratinocyte nuclei might be associated to a distinct phase of the cell cycle. Consistently, p68 has been described to localize in the nuclei of interphase cells *in vitro* (Lamm *et al*., 1996; Nicol *et al*., 2000), an observation that supports the presence of high numbers of p68 negative cells in normal wound tissue, as the neo-

epithelium is largely characterized by mitogenic cells (Stallmeyer *et al*., 1999). Evidently, the localization of p68 in interphase cells might provide the explanation for elevated p68 levels observed in NO-deficient healing. iNOS-deficient mice were characterized by a marked delay in wound closure (Yamasaki *et al*., 1998) and inhibition of iNOS during repair resulted in a nearly complete loss of wound keratinocyte proliferation (Stallmeyer *et al*., 1999). Thus, the increased levels of p68 in the absence of the keratinocyte mitogen NO strongly argues for high numbers of interphase cells and might reflect the non-proliferative status of keratinocytes in NO-deficient wounds. However, this argumentation must remain unsolved with respect to cell culture conditions, as, by contrast, we had to recognize that serum-induced keratinocyte proliferation was dependent on the co-induction of p68 *in vitro*. Thus, the early re-increase and over-representation of p68 in impaired repair in NO-deficient animals might be interpreted as an adaptive mechanism to overcome the disturbed responsiveness of keratinocytes to mitotic stimuli in conditions of delayed healing.

4.8 Clinical relevance

The biological functions of RNA helicases are diverse and include gene transcription, RNA processing, mRNA translation, ribosome assembly, cell differentiation, cell development and division (Tanner and Linder, 2001). Therefore, these proteins are considered to be promising candidates for anticancer drugs (Tanner and Linder, 2001). Indeed, there are examples of DEAD box proteins which are implicated not only in growth and division but also in tumor development. For example, the DEAD-box family member Rck/p54 has been shown to be overexpressed in neuroblastoma, glioblastoma, rhabdomyosarcoma and lung cancer cells as well as in colorectal tumors (Akao *et el*., 1995; Nakagawa *et al*., 1999). Furthermore, the DDX1 RNA helicase gene is often co-amplified with N-myc in retino- and neuroblastomas (Godbout and Squire, 1993; Squire *et al*., 1995; George *et al.*, 1996). p68 itself has a binding site for Myc, is overexpressed in colorectal tumors when compared to normal tissue samples (Causevic *et al.,* 2001), and involved in splicing regulation of c-H-*ras* proto-oncogene (Guil *et al*., 2003). Moreover, mutated p68 was identified to be the immunodominant antigen responsible for tumor rejection in mice (Dubey *et al.*, 1997). The authors showed that the antigen, which was generated by a somatic point mutation in the p68 gene, was recognized by $CD8^+$ T cells and thus led to the

rejection of the previous transplanted tumor cell line. In line with these data, our observations demonstrated, that p68 promoted proliferation and most likely functions as transcriptional co-activator in VEGF gene transcription. VEGF is known to be an angiogenic growth factor and a potent stimulant for vascularization of solid tumors (Brekken *et al*., 1998). Thus, p68 might promote tumor growth by enhancing VEGF transcription. It is known that CBP/p300 proteins contribute in hypoxia-induced transcriptional activation of the VEGF gene *in vitro* and in a model of tumor growth *in vivo* (Kung *et al*., 2000). As p68 has been found to interact with the multiprotein complex containing Pol II and CBP/p300 (Rossow and Janknecht, 2003), one might speculate that p68 promotes VEGF gene transcription as part of the CBP/p300/Pol II complex. The modulation of VEGF gene expression is also of interest in terms of wound healing. VEGF has been shown to stimulate wound angiogenesis and its reduced expression or its accelerated degradation were found to be associated with wound healing defects (Frank *et al*., 1995; Swift *et al*., 1999; Lauer *et al*., 2000; Kämpfer *et al.,* 2001).

In addition, it seems reasonable to speculate that p68 is implicated in the inflammatory skin disease psoriasis. Histological examination of psoriatic plaques reveals three major pathogenic factors: abnormal keratinocyte differentiation, hyperproliferation of keratinocytes and infiltration of inflammatory cells into the skin (Ortonne, 1996). Moreover, several studies demonstrated the involvement of different inflammatory cytokines, chemokines and their receptors in psoriasis (Castells-Rodellas *et al*., 1992; Kapp, 1993; Schlaak *et al.,* 1994; Michel *et al*., 1997; Debets *et al.,* 1997; Kulke *et al.,* 1998;). As we found p68 to be potently induced by pro-inflammatory cytokines and to participate in proliferation, this helicase is a likely candidate to be implicated in psoriasis.

5

Summary

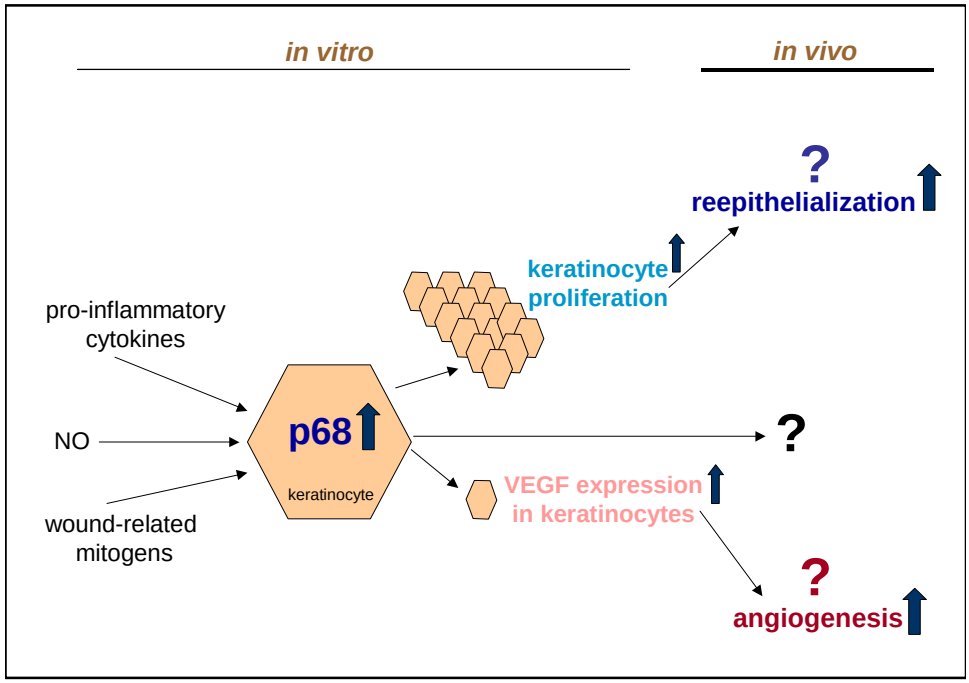

Figure 4.1 Schematic view of the hypothesized functional roles of p68 in keratinocyte biology and during wound healing

Nitric oxide (NO) represents a short-lived mediator that pivotally drives keratinocyte movements during cutaneous wound healing. In this study, we have identified p68 DEAD box RNA helicase (p68) from a NO-induced differential keratinocyte cDNA library. Subsequently, we have analyzed regulation of p68 by wound-associated mediators in the human keratinocyte cell line HaCaT. NO, serum, growth factors and pro-inflammatory cytokines were potent inducers of p68 expression in the cells. p68 was constitutively expressed in murine skin, but rapidly down-regulated upon injury. The down-regulation appeared to be transient, as p68 protein expression increased again after the inflammatory phase of repair. However, p68 protein expression did not completely disappear during wound inflammation, as immunohistochemistry and cell fractionation analysis revealed a restricted localization of p68 in keratinocyte nuclei of the developing epithelium. In line, cultured human (HaCaT) and murine

(PAM 212) keratinocyte cell lines showed a nuclear localization of the helicase. Moreover, confocal microscopy revealed a strong localization of p68 protein within the nucleoli of the keratinocytes. Functional analyses demonstrated that p68 strongly participates in keratinocyte proliferation and gene expression. Keratinocytes that constitutively overexpressed p68 protein were characterized by a marked increase in serum-induced proliferation and vascular endothelial growth factor (VEGF) expression, whereas down-regulation of endogenous p68 using small interfering RNA (siRNA) markedly attenuated serum-induced proliferation and VEGF expression. Altogether, our results suggest a tightly controlled expression and nucleolar localization of p68 in keratinocytes *in vitro* and during skin repair *in vivo* that functionally contributes to keratinocyte proliferation and gene expression.

6

References

Abraham JA, Klagsbrun M: Modulation of wound repair by members of the fibroblast growth factor family. In: Clark RAF (ed.). *The Molecular and Cellular Biologie of Wound Repair*. New York: Plenum Press, 1996, pp 195-248

Ahlen K, Rubin K: Platelet-derived growth factor-BB stimulates synthesis of the integrin α2-subunit in human diploid fibroblasts. *Exp Cell Res* 215:347-353, 1994

Akao Y, Marukawa O, Morikawa H, Nakao K, Kamei M, Hachiya T, Tsujimoto Y: The rck/p54 candidate proto-oncogene product is a 54-kilodalton D-E-A-D box protein differentially expressed in human and mouse tissues. *Cancer Res* 55:3444-3449, 1995

Akileswaran L, Taraska JW, Sayer JA, Gettemy JM, Coghlan VM: A-kinase-anchoring protein AKAP95 is targeted to the nuclear matrix and associates with p68 RNA helicase. *J Biol Chem* 276:17448-17454, 2001

Baek KJ, Thiel BA, Lucas S, Stuehr DJ: Macrophage nitric oxide synthase subunits. Purification, characterization, and a role of prosthetic groups and substrate in regulating their association into a dimeric enzyme. *J Biol Chem* 268:21120-21129, 1993

Baggiolini M: Chemokines and leukocyte traffic. *Nature* 392:565-568, 1998

Barbul A, Regan MC: The regulatory role of T lymphocyte in wound healing. *J Trauma* 30:97-100, 1990

Barrandon Y, Green H: Cell migration is essential for sustained growth of keratinocytes colonies: The roles of transforming growth factor-α and epidermal growth factor. *Cell* 50:1131-1137, 1987

Battegay EF, Rupp J, Iruela-Arispe L, Sage EH, Pech M: PDGF-BB modulates endothelial proliferation and angiogenesis *in vitro* via PDGF ß-receptors. *J Cell Biol* 125:917-928, 1994

Baudouin JE, Tachon P: Constitutive nitric oxide synthase is present in normal human keratinocytes. *J Invest Dermatol* 106: 428-431, 1996

Beck KF, Eberhardt W, Frank S, Huwiler A, Messmer UK, Mühl H, Pfeilschifter J: Inducible NO-synthase: role in cellular signalling. *J Exp Biol* 202: 645-653, 1999

Bickenbach JR, Mackenzie IC: Identification and localization of label-retaining cells in hamster epithelia. *J Invest Dermatol* 82:618–622,1984

Bickenbach JR: Identification of label-retaining cells in oral mucosa and skin. *J Dent Res* 60:1611–1620, 1981

Birnboim HC, Doly J: A rapid alkaline extraction procedure for screening recombinant plasmid DNA. *Nucleic Acids Res* 7: 1513-1523, 1979

Blotnick SL, Peoples GE, Freeman MR, Eberlein Tj, Klagsburg M: T lymphocytes synthesize and export heparin-binding epidermal growth factor-like growth factor and basic fibroblast growth factor, mitogens for vascular cells and fibroblasts: differential production and release by $CD4^+$ and $CD8^+$ T-cells. *Proc Natl Acad Sci USA* 91:2890-2894, 1994

Boismenu R, Havran WL: Modulation of epithelial cell growth by intraepithelial γδT-cells. *Science* 266:1253-1255; 1994

Boissel JP, Ohly D, Bros M, Gödtel-Armbrust U, Förstermann U, Frank S: The neuronal nitric oxide synthase is upregulated in mouse skin repair and in response to epidermal growth factor in human HaCaT keratinocytes. *J Invest Dermatol* 2004 (in press)

Bond AT, Mangus DA, He F, Jacobson A: Absence of Dbp2p alters both nonsense-mediated mRNA decay and rRNA processing. *Mol Cell Biol* 21:7366-7379, 2001

Bond VC, Wold B: Nucleolar localization of myc transcripts. *Mol Cell Biol* 13:3221-3230, 1993

Boukamp B, Petrussevska RT, Breitkreuz D, Hornung J, Markham A, Fusenig NE: Normal keratinization in a spontaneously immortalized aneuploid human keratinocyte cell line. *J Cell Biol* 106:761-771, 1988

Brekken RA, Huang X, King SW, Thorpe PE: Vascular endothelial growth factor as a marker of tumor endothelium. *Cancer Res* 58:1952-1959, 1998

Brooks PC, Clark RAF, Cheresh DA: Requirement of vascular integrin ωß3 for angiogenesis. *Science* 264:569-571, 1994

Brown GL, Curtsinger L 3rd, Brightwell JR, Ackerman DM, Tobin GR, Polk HCJr, George-Nascimento C, Valenzuela P, Schultz GS: Enhancement of epidermal regeneration by biosynthetic epidermal growth factor. *J Exp Med* 163:1319-1324, 1986

Brown LF, Yeo KT, Berse B, Yeo TK, Senger DR, Dvorak HF, van de Water L: Expression of vascular permeability factor (vascular endothelial growth factor) by epidermal keratinocytes during wound healing. *J Exp Med* 176:1375-1379, 1992

Bruch-Gerharz D, Fehsel K, Suschek C, Michel G, Ruzicka T, Kolb-Bachofen V: A proinflammatory activity of interleukin 8 in human skin: expression of the inducible nitric oxide synthase in psoriatic lesions and cultured keratinocytes. *J Exp Med* 184:2007-2012, 1996

Bruch-Gerharz D, Ruzicka T, Kolb-Bachofen V: Nitric oxide and its implications in skin homeostasis and disease. *Arch Dermatol Res* 290:643-651, 1998

Buelt MK, Glidden BJ, Storm DR: Regulation of p68 RNA helicase by calmodulin and protein kinase *C. J Biol Chem* 269:29367-29370, 1994

Bugler B, Caizergues-Ferrer M, Bouche G, Bourbon H, Amalric F: Detection and localization of a class of proteins immunologically related to a 100-kDa nucleolar protein.*Eur J Biochem* 128:475-480, 1982

Buonomo SB, Michienzi A, De Angelis FG, Bozzoni I: The Rev protein is able to transport to the cytoplasm small nucleolar RNAs containing a Rev binding element. *RNA* 5:993-1002, 1999

Burd CG, Dreyfuss G: Conserved structures and diversity of functions of RNA-binding proteins. *Science* 265:615-621, 1994

Callsen D, Pfeilschifter J, Brüne B: Rapid and delayed p42/p44 MAPK activation by nitric oxide: the role of cGMP and tyrosine phosphatase inhibition. *J Immunol* 161:4852-4858, 1998

Carmeliet P, Moons L, Luttun A, Vincenti V, Compernolle V, De Mol M, Wu Y, Bono F, Devy L, Beck H, Scholz D, Acker T, DiPalma T, Dewerchin M, Noel A, Stalmans I, Barra A, Blacher S, Vandendriessche T, Ponten A, Eriksson U, Plate KH, Foidart JM, Schaper W, Charnock-Jones S, Hicklin DJ, Herbert JM, Collen D, Persico MG: Synergism between vascular endothelial growth factor and placental growth factor contributes to angiogenesis and plasma extravasation in pathological conditions. *Nature Med* 7:575-583, 2001

Caruthers JM, Johnson ER, McKay DB: Crystal structure of yeast initiation factor 4A, a DEAD-box RNA helicase. *Proc Natl Acad Sci USA* 97:3080-3085, 2000

Castells-Rodellas A, Castell JV, Ramirez-Bosca A, Nicolas JF, Valcuende-Cavero F, Thivolet J: Interleukin-6 in normal skin and psoriasis. *Acta Derm Venereol* 72:165-168, 1992

Causevic M, Hislop RG, Kernohan NM, Carey FA, Kay RA, Steele RJC, Fuller-Pace FV: Overexpression and polyubiquitylation of the DEAD-box RNA helicase p68 in colorectal tumours. *Oncogene* 29:7734-7743, 2001

Cha D, O'Brien P, O'Toole EA, Woodley DT, Hudson LG: Enhanced modulation of keratinocyte motility by transforming growth factor-alpha (TGF-alpha) relative to epidermal growth factor (EGF). *J Invest Dermatol* 106:590-597, 1996

Chen P, Xie H, Sekar MC, Gupta K, Wells A: Epidermal growth factor receptor-mediated cell motility: phospholipase C activity is required, but mitogen-activated protein kinase activity is not sufficient for induced cell movement. *J Cell Biol* 127:847-857, 1994

Chromczynski P, Sacchi N: Single-step method of RNA isolation by acid guanidinium thiocyanate-phenol-chloroform extraction. *Anal Biochem* 162:156-159, 1987

Clark RAF, Ashcroft GS, Spencer MJ, Larjava H, Ferguson MWJ: Reepithelialization of normal human excisional wounds is associated with a switch from$\alpha v\beta 5$ to $\alpha v\beta 6$ integrins. *Br J Dermatol* 135:46-51, 1996

Clark RAF, Folkvord JM, Hart CE, Murray MJ, McPherson JM: Platelet isoforms of platelet-derived growth factor stimulate fibroblasts to contract collagen matrices*. J Clin Invest* 84:1036-1040, 1989

Clark RAF: Fibronectin matrix deposition and fibronectin receptor expression in healing and normal skin. *J Invest Dermatol* 94:128-134, 1990

Clark RAF: Wound repair: overview and general considerations. In: Clark RAF (ed.). *The Molecular and Cellular Biologie of Wound Repair*. New York: Plenum Press, 1996, pp 3-50

Coffey RJ Jr, Bascom CC, Sipes NJ, Graves-Deal R, Weissman BE, Moses HL: Selective inhibition of growth-related gene expression in murine keratinocytes by transforming growth factor ß. *Mol Cell Biol* 8:3088-3093, 1988

Coghlan VM, Langeberg LK, Fernandez A, Lamb NJ, Scott JD: Cloning and characterization of AKAP 95, a nuclear protein that associates with the regulatory subunit of type II cAMP-dependent protein kinase. *J Biol Chem* 269:7658-7665, 1994

Dale BA: Filaggrins. In Goldman RW, Steinert PM, eds. *Cellular and Molecular Biologie of Intermediate Filaments.* New York: Plenum 393, 1990

Danilenko DM, Ring BD, Tarpley JE, Morris B, Van GY, Morawiecki A, Callahan W, Goldenberg M, Hershenson S, Pierce GF: Growth factors in porcine full and partial thickness burn repair. Differing targets and effects of keratinocyte growth factor, platelet-derived growth factor-BB, epidermal growth factor, and neu differentiation factor. *Am J Pathol* 147:1261-1277, 1995

de la Cruz D, Kressler P, Linder P: Unwinding RNA in *Saccharomyces cerevisiae*: DEAD-box proteins and related families. *Trends Biochem Sci 24:*192-198, 1999

Debets R, Hegmans JP, Croughs P, Troost RJ, Prins JB, Benner R, Prens EP: The IL-1 system in psoriatic skin: IL-1 antagonist sphere of influence in lesional psoriatic epidermis. *J Immunol* 158:2955-2963, 1997

Derynck R: Transforming growth factor-α, *Cell* 54:593-595, 1988

Desmouliere A, Gabbiani G: The role of the myofibroblast in wound healing and fibrocontractive diseases. In: Clark RAF (ed.). *The Molecular and Cellular Biologie of Wound Repair*. New York: Plenum Press, 1996, pp 391-423

Desmouliere A, Redard M, Darby I, Gabbiani G: Apoptosis mediates the decrease in cellularity during the transition between granulation tissue and scar. *Am J Pathol* 146:56-66, 1995

Detmar M, Yeo KT, Nagy JA, Van de Water L, Brown LF, Berse B, Elicker BM, Ledbetter S, Dvorak HF: Keratinocyte-derived vascular permeability factor (vascular endothelial growth factor) is a potent mitogen for dermal microvascularendothelial cells. *J Invest Dermatol* 105:44-50, 1995

DiPietro LA, Burdick M, Low QE, Kunkel SL, Strieter RM: MIP-1α as a critical macrophage chemoattractant in murine wound repair. *J Clin Invest* 101:1693-1698, 1998

DiPietro LA, Polverini PJ, Rahbe SM, Kovacs EJ: Modulation of JE/MCP-1 expression in dermal wound repair. *Am J Pathol* 146:868-875, 1995

Dovi JV, He LK, DiPietro LA: Accelerated wound closure in neutrophil-depleted mice. *J Leukoc Biol* 73:448-455, 2003

Dubey P,Hendrickson RC, Meredith SC, Siegel CT, Shabanowitz J, Skipper JCA, Engelhard VH, Hunt DF, Schreiber H: The immunodominant antigen of an ultraviolet-induced regressor tumor is generated by a somatic point mutation in the DEAD box helicase p68*. J Exp Med* 185:695-706, 1997

Elbashir SM, Lendeckel W, Tuschl T: RNA interference is mediated by 21- and 22-nucleitide RNAs. *Genes Dev* 15:188-200, 2001

Elsbach P, Weiss J: Oxygen-independent antimicrobial systems of phagocytosis. In: Gallin JI, Goldstein IM, Snyderman R (eds.). *Inflammation: Basic Pronciples and Clinical Correlates.* New York: Raven Press, 1992, pp 603-636

Endoh H, Maruyama K, Masuhiro Y, Kobayashi Y, Goto M, Tai H, Yanagisawa J, Metzger D, Hashimoto S, Kato S: Purification and identification of p68 RNA helicase acting as a transcriptional coactivator specific for the activation function 1 of human estrogen receptor alpha. *Mol Cell Biol* 19:5363-5372, 1999

Ferguson MWJ, Whitby DJ, Shah M, Armstrong J, Siebert JW, Longaker MT: Scar formation: the spectral nature of fetal and adult wound repair. *Plast Reconstr Surg* 97:845-860, 1996

Fire A, Xu S, Montgomery MK, Kostas SA, Driver SE, Mello CC: Potent and specific genetic interference by double-stranded RNA in *Caenorhabditis elegans*. Nature 391:806-811, 1998

Fishel RS, Barbul A, Beschorner WE; Wasserkrug HL, Efron G: Lymphocyte participation in wound healing: morphologic assessment using monoclonal antibodies. *Ann Surg* 206:25-29, 1987

Folkman J, Shing T: Angiogenesis. *J Biol Chem* 267:10931-10934, 1992

Folkman J: Angiogenesis and angiogenesis inhibition. *EXS* 79:1-8, 1997

Ford MJ, Anton IA, Lane DP: Nuclear protein with sequence homology to translation initiation factor eIF-4A. *Nature* 332:736-738, 1988

Förstermann U, Boissel J-P, Kleinert H: Expressional control of the `constitutive` isoforms of nitric oxide synthase (NOS I and NOS III). *FASEB J* 12:773-790, 1998

Frank S, Hübner G, Breier G, Longaker MT, Greenhalgh DG, Werner S: Regulation of vascular endothelial growth factor expression in cultured keratinocytes. Implications for normal and impaired wound healing. *J Biol Chem* 270:12607-12613, 1995

Frank S, Madlener M, Werner S: Transforming growth factors-ß1, -ß2, and –ß3 and their receptors are differentially regulated during normal and impaired wound healing. *J Biol Chem* 271:10188-10193, 1996

Frank S, Madlener M, Pfeilschifter J, Werner S: Induction of inducible nitric oxide synthase and its tetrahydrobiopterin-cofactor-synthesizing enzyme GTP-cyclohydrolase I during cutaneous wound repair. *J Invest Dermatol* 111:1058-1064, 1998a

Frank S, Kolb N, Werner ER, Pfeilschifter J: Coordinated induction of inducible nitric oxide synthase and GTP-cyclohydrolase I is dependent on inflammatory cytokines and interferon-χ in HaCaT keratinocytes: implications for the model of cutaneous wound repair. *J Invest Dermatol* 111:1065-1071, 1998b

Frank S, Stallmeyer B, Kämpfer H, Kolb N, Pfeilschifter J: Nitric oxide triggers enhanced induction of vascular endothelial growth factor expression in cultured keratinocytes (HaCaT) and during cutaneous wound repair. *FASEB J* 13:2002-2014, 1999

Frank S, Kämpfer H, Podda M, Kaufmann R, and Pfeilschifter J: Identification of Copper/Zinc Superoxide Dismutase as a Nitric Oxide-regulated Gene in human Keratinocytes (HaCaT): Implications for Keratinocyte Proliferation. *Biochem J* 346:719-728, 2000a

Frank S, Stallmeyer B, Kämpfer H, Kolb N, and Pfeilschifter J: Leptin enhances wound reepithelialization: Implication for a direct function of leptin in skin repair. *J Clin Invest* 106:501-509, 2000b

Frank S, Kämpfer H, Wetzler C, Stallmeyer B, and Pfeilschifter J: Large induction of the chemotactic cytokine RANTES during wound repair: a regulatory role for nitric oxide in keratinocyte-derived RANTES expression. *Biochem J* 347:265-273, 2000c

Frank S, Kämpfer H, Wetzler C, and Pfeilschifter J: Nitric oxide drives skin repair: novel functions of an established mediator. *Kidney Int* 61:882-888, 2002

Freinkel RK, Woodley DT: *The biology of the skin*. London: The Parthenon Publishing Group, 2001

Fujita T, Kobayashi Y, Wada O, Tateishi Y, Kitada L, Yamamoto Y, Takashima H, Murayama A, Yano T, Baba T, Kato S, Kawabe Y, Yanagisawa J: Full activation of estrogen receptor alpha activation function-1 induces proliferation of breast cancer cells. *J Biol Chem* 278:26704-26714, 2003

Fukuyama K, Kakimi S, Epstein WL: Detection of a fibrous cmponent in keratohyalin granules of newborn rat epidermis. *J Invest Dermatol* 74:174-180, 1980

Gabbiani G, Chapponnier C, Huttner I: Cytoplasmic filaments and gap junctions in epithelial cells and myofibroblasts during wound healing. *J Cell Biol* 76:561-568, 1978

Gailit J, Xu J, Bueller H, Clark RA: Platelet-derived growth factor and inflammatory cytokines have differential effects on the expression of integrins α1ß1 and α5ß1 by human dermal fibroblasts in vitro. *J Cell Physiol* 169:281-289, 1996

Gambardella L, Barrandon Y: The multifaceted adult epidermal stem cell. *Curr Opin Cell Biol* 15:771-777, 2003

Garthwaite J, Charles SL, Chess-Williams R: Endothelium-derived relaxing factor release on activation of NMDA receptors suggests a role as intercellular messenger in brain. *Nature* 336:385-388, 1988

Gath I, Closs EI, Gödtel-Armbrust U, Schmitt S, Nakane M, Wessler I, Förstermann U: Inducible NO synthase II and neuronal NO synthase I are constitutively expressed in different structures of guinea pig skeletal muscle: implications for contractile function. *FASEB J* 10:1614-1620, 1996

George RE, Kenyon RM, McGuckin AG, Malcom AJ, Pearson AD, Lunec J: Investigation of coamplification of the candidate genes ornithine decarboxylase, ribonucleotide reductase, syndecan-1 and a DEAD box gene, DDX1, with N-myc in neuroblastoma. United Kingdom Children's Cancer Study Group. *Oncogene* 12:1583-1587, 1996

Ghisolfi L, Kharrat A, Joseph G, Amalric F, Erard M: Concerted activities of the RNA recognition and the glycine-rich C-terminal domains of nucleolin are required for efficient complex formation with pre-ribosomal RNA. *Eur J Biochem* 209:541-548, 1992

Gille J, Khalik M, Konig V, Kaufmann R: Hepatocyte growth factor/scatter factor (HGF/SF) induces vascular permeability factor (VPF/VEGF) expression by cultured keratinocytes. *J Invest Dermatol* 111:1160-1165, 1998

Godbout R, Squire J: Amplification of a DEAD box protein gene in retinoblastoma cell lines. *Proc Natl Acad Sci U S A* 90:7578-7582, 1993

Goodman RH, Smolik S: CBP/p300 in cell growth, transformation, and development. *Genes Dev* 14:1553-1577, 2000

Gray AJ, Bishop JE, Reeves JT, Laurent GJ: Aa and Bß chains of fibrinogen stimulate proliferation of human fibroblasts. *J Cell Sci* 104: 409-413, 1993

Grisham MB, Jourd`heuil D, Wink DA: Nitric Oxide. I. Physiological chemistry of nitric oxide and its metabolites: implications in inflammation. *Am J Physiol* 276:315-321, 1999

Grondahl-Hansen J, Lund RL, Ralfkiaer E, Ottevanger V, Dano K: Urokinase- and tissue-type plasminogen activators in keratinocytes during wound reepithelialization *in vivo. J Invest Dermatol* 90:790-795, 1988

Guil S, Gattoni R, Carrascal M, Abian J, Stevenin J, Bach-Elias M: Roles of hnRNP A1, SR proteins, and p68 helicase in c-H-ras alternative splicing regulation. *Mol Cell Biol* 23:2927-2941, 2003

Guo N, Krutzsch HC, Inman JK, Roberts DD: Thrombospondin 1 and type I repeat peptides of thrombospondin 1 specifically induce apoptosis of endothelial cells. *Cancer Res* 57:1735-1742, 1997

Haake A, Glynis AS, Holbrooke KA: Structure and function of the skin:overview of the epidermis and dermis. In Freinkel RK, Woodley DT (ed*). The biology of the skin*. London: The Parthenon Publishing Group, 2001, pp 19-46

Heino J, Ignotz RA, Hemler ME,Crouse C, Massague J: Regulation of cell adhesion receptors by transforming growth factor-ß. Concomitant regulation of integrins that share a common ß1 subunit. *J Biol Chem* 264:380-388, 1989

Hirling H, Scheffner M, Restle T, Stahl H: RNA helicase activity associated with the human p68 protein. *Nature* 339:562-564, 1989

Hloch P, Schieder G, Stahl H: Complete cDNA sequence of the human p68 protein. *Nucleic Acids Res* 18:3045, 1990

Holash J, Wiegand SJ, Yancopoulos GD: New model of tumor angiogenesis: dynamic balance between vessel regression and growth mediated by angiopoietins and VEGF. *Oncogene* 18:5356-5362, 1999

Hsieh P, Chen LB: Behaviour of cells seeded on isolated fibronectin matrices. *J Cell Biol* 96:1208-1217, 1983

Huang Y, Liu ZR: The ATPase, RNA unwinding, and RNA binding activities of recombinant p68 RNA helicase. *J Biol Chem* 277:12810-12815, 2002

Hübner G, Brauchle M, Smola H, Madlener M, Fässler R, Werner S: Differential regulation of proinflammatory cytokines during wound healing in normal and glucocorticoid-treated mice. *Cytokine* 8:548-556, 1996

Hunt TK (ed): *Wound healing and wound infection: theory and surgical practice.* New York: Appleton-Century-Crofts, 1980

Hynes RO: Integrins: versatility, modulation, and signaling in cell adhesion. *Cell* 69:11-25, 1992

Igarashi A, Okochi H, Bradham DM, Grotendorst GR: Regulation of connective tissue growth factor gene expression in human skin fibroblasts and during wound repair. *Mol Cell Biol* 4:637-645, 1993

Iggo RD, Jamieson DJ, MacNeill SA, Southgate J, McPheat J, Lane DP: p68 RNA helicase: identification of a nucleolar form and cloning of related genes containing a conserved intron in yeasts. *Mol Cell Biol* 11:1326-1333, 1991

Iggo RD, Lane DP: Nuclear protein p68 is an RNA-dependent ATPase. *EMBO J* 8:1827-1831, 1989

Ignotz RA, Massague J: Transforming growth factor-ß stimulates the expression of fibronectin and collagen and their incorporation into extracellular matrix. *J Biol Chem* 261:4337-4340, 1986

Iruela-Arispe ML, Dvorak HF: Angiogenesis: a dynamic balance of stimulators and inhibitors. *Thromb Haemost* 78:672-677, 1997

Janknecht R: The versatile functions of the transcriptional coactivators p300 and CBP and their roles in disease. *Histol Histopathol* 17:657-668, 2002

Jankowsky E, Gross CH, Shumann S, Pyle AM: Active disruption of an RNA-protein interaction by a DexH/D RNA helicase.*Science* 291**:**121-125, 2001

Kadare G, Haenni AL: Virus-encoded RNA helicases. *J Virol* 71:2583-2590, 1997

Kämpfer H, Pfeilschifter J, Frank S: Expressional regulation of angiopoietin-1 and -2 and Tie-1 and -2 receptor tyrosine kinase during cutaneous wound healing: a comparative study of normal and impaired repair. *Lab Invest* 81:361-373, 2001

Kapp A: The role of cytokines in the psoriatic inflammation. *J Dermatol Sci* 5:133-142, 1993

Keck PJ, Hauser SD, Krivi G, Sanzo K, Warren T, Feder J, Connolly DT: Vascular permeability factor, an endothelial cell mitogen related to PDGF. *Science* 246:1309-1313, 1989

Kim JL, Morgenstern KA, Griffith JP, Dwyer MD, Thomson JA, Murcko MA, Lin C, Caron PR: Hepatitis C virus NS3 RNA helicase domain with a bound oligonucleotide: the crystal structure provides insights into the mode of unwinding. *Structure* 6:89-100, 1998

Klatt P, Schmidt K, Uray G, Mayer B: Multiple catalytic functions of brain nitric oxide synthase. Biochemical characterization, co-factor requirement, and the role of N-omega-hydroxy-L-arginine as an intermediate*. J Biol Chem* 268:14781-14787, 1993

Klebanoff SJ: Oxygen metabolites from phagocytes. In: Gallin JI, Goldstein IM, Snyderman R (eds.). *Inflammation: Basic Pronciples and Clinical Correlates.* New York: Raven Press, 1992, pp 541-601

Koch AE, Polverini PJ, Kunkel SL, Harlow LA, DiPietro LA, Elner VM, Elner SG, Strieter RM: Interleukin-8 as a macrophage-derived mediator of angiogenesis. *Science* 258: 1798-1801, 1992

Krischel V, Bruch-Gerharz D, Suschek C, Kröncke KD, Ruzicka T, Kolb-Bachofen V: Biphasik effect of exogenous nitric oxide on proliferation and differentiation in skin derived keratinocytes but not fibroblasts. *J Invest Dermatol* 111:286-291, 1998

Kröncke KD, Carlberg C: Inactivation of zinc finger transcription factors provides a mechanism for a gene regulatory role of nitric oxide. *FASEB J* 13:1666-1673, 2000

Kuhn A, Fehsel K, Lehmann P, Krutmann J, Ruzicka T, Kolb-Bachofen V: Aberrant timing in epidermalexpression of inducible nitric oxide synthase after UV irradiation in cutaneous lupus erythematosus. *J Invest Dermatol* 111:149-153, 1998

Kulke R, Bornscheuer E, Schluter C, Bartels J, Rowert J, Sticherling M, Christophers E: The CXC receptor 2 is overexpressed in psoriatic epidermis. *J Invest Dermatol* 110:90-94, 1998

Kung AL, Wang S, Klco JM, Kaelin WG, Livingston DM: Suppression of tumor growth through disruption of hypoxia-inducible transcription. *Nat Med* 6:1335-1340, 2000

Kurkinem M, Vaheri A, Roberts PJ, Stenman S: Sequential appearance of fibronectin and collagen in experimental granulation tissue. *Lab Invest* 43:47-51, 1980

Laemmli UK: Cleavage of structural proteins during the assembly of the head of bacteriophage T4. *Nature* 227:680-685, 1970

Lajtha LG: Stem cell concepts. *Differentiation* 14:23–34,1979

Lamm GM, Nicol SM, Fuller-Pace F, Lamond AI: p72: A human nuclear DEAD box protein highly related to p68. *Nucl Acid Res* 24:3739-3747, 1996

Lander HM, Jacovina AT, Davis RJ, Tauras JM: Differential activation of mitogen-activated protein kinases by nitric-oxide-related species. *J Biol Chem* 271:19705-19709, 1996

Lane DP, Hoeffler WK: SV40 large T shares an antigenic determinant with a cellular protein of molecular weight 68,000. *Nature* 288:167-170, 1980

Lane TF, Iruela-Arispe ML, Johnson RS, Sage EH: SPARC is a source of copper-binding peptides that stimulate angiogenesis. *J Cell Biol* 125:929-943, 1994

Lauer G, Sollberg S, Cole M, Flamme I, Sturzebecher J, Mann K, Krieg T, Eming SA: Expression and proteolysis of vascular endothelial growth factor is increased in chronic wounds. *J Invest Dermatol* 115:12-18, 2000

Lavker RM, Sun T-T: Heterogeneity in epidermal basal keratinocytes: morphological and functional correlations. *Science* 215:1239–1241, 1982

Lee PC, Salyapongse N, Bragdon GA, ShearsII LL, Watkins SC, Edington HDJ, Billiar TR: Impaired wound healing and angiogenesis in eNOS-deficient mice. *Am J Physiol* 277:1600-1608, 1999

Leibovich SJ, Ross R: The role of the macrophage in wound repair: A study with hydrocortisone and antimacrophage serum. *Am J Pathol* 78:71-100, 1975

Lemaire L, Heinlein UA: High-level expression in male germ cells of murine p68 RNA helicase mRNA. *Life Sci* 52:917-926, 1993

Levenson SM, Geever EF, Crowley LV, Oates JF III, Berard CW, Rosen H: The healing of rat skin wounds. *Ann Surg* 161:293-308, 1965

Lin C, Kim JL: Structure-based mutagenesis study of hepatitis C virus NS3 helicase. *J Virol* 73:8798-8807, 1999

Linder P, Lasko PF, Ashburner M, Leroy P, Nielsen PJ, Nishi K, Schnier J, Slonimski PP: Birth of the D-E-A-D box. *Nature* 337:121-122, 1989

Linder P, Tanner NK, Banroques J: From RNA helicases to RNPases. *Trends Biochem Sci* 26:339-341, 2001

Liu Q, Dreyfuss G: *In vivo* and *in vitro* arginine methylation of RNA-binding proteins. *Mol Cell Biol* 15:2800-2808, 1995

Liu ZR: p68 RNA helicase is an essential human splicing factor that acts at the U1 snRNA-5`splice site duplex. *Mol Cell Biol* 22:5443-5450, 2002

Lüking A, Stahl U, Schmidt U: The protein family of RNA helicases. *Crit Rev Biochem Mol Biol* 33:259-296, 1998

Luster AD: Chemokines-chemotactic cytokines that mediate inflammation. *N Engl J Med* 338:436-445, 1998

MacMicking J, Xie QW, Nathan C: Nitric oxide and macrophage function. *Annu Rev Immunol* 15: 323-50, 1997

Madri JA, Bell L, Marx M, Merwin JR, Basson CT, Prinz C: The effects of soluble factors and extracellular matrix components on vascular behavior *in vitro* and *in vivo*: Models of deendothelialization and repair. *J Cell Biochem* 45:1-8, 1991

Madri JA, Bell L, Merwin JR: Modulation of vascular cell behavior by transforming growth factors eta. *Mol Reprod Dev* 32:121-126, 1992a

Madri JA, Merwin JR, Bell L, Basson CT, Kocher O, Perlmutter R, Prinz C: Interactions of matrix components and soluble factors in vascular cell responses to injury: Modulation of cell phenotype. In: Simionescu N, Simionescu M (ed.). *Endothelial Cell Dysfunction*. New York: Plenum Press, 1992, pp 11-30

Mansbridge JN, Knapp AM: Changes in keratinocyte maturation during wound healing. *J Invest Dermatol* 89:253-263, 1987

Marchese C, Chedid M, Dirsch OR, Csaky KG, Santanelli F, Latini C, LaRochelle WJ, Torrisi MR, Aaronson SA: Modulation of keratinocyte growth factor and its receptor in re-epithelialising human skin. *J Exp Med* 182:1369-1376, 1995

Marshall HE, Merchant K, Stamler JS: Nitrosation and oxidation in the regulation of gene expression. *FASEB J* 14:1889-1900, 2000

Martin P: Mechanism of wound healing in the embryo and fetus. *Curr Top Dev Biol* 32:175-203, 1996

Martin P: Wound healing-Aiming for perfect skin regeneration*. **Science*** 276:75-81, 1997

Mattaj IW: RNA recognition: a family matter? *Cell* 73:837-840, 1993

Melton DA, Krieg PA, Rebagliati MR, Maniatis T, Zinn K, Green MR: Efficient *in vitro* synthesis of biologically active RNA and RNA hybridization probes from plasmids containing a bacteriophage SP6 promoter. *Nucleic Acids Res* 12:7035-7056, 1984

Michel G, Mirmohammadsadegh A, Olasz E, Jarzebska-Deussen B, Muschen A, Kemeny L, Abts HF, Ruzicka T: Demonstration and functional analysis of IL-10 receptors in human epidermal cells: decreased expression in psoriatic skin, down-modulation by IL-8, and up-regulation by an antipsoriatic glucocorticosteroid in normal cultured keratinocytes. *J Immunol* 159:6291-6297, 1997

Mignatti P, Rifkin DB, Welgus HG, Parks WC: Proteinases and tissue remodeling. In: Clark RAF (ed.). *The Molecular and Cellular Biologie of Wound Repair*. New York: Plenum Press, 1996, pp 427-474

Moncada S, Palmer RM, Higgs EA: Nitric oxide: physiology, pathophysiology and pharmacology. *Pharmacol Rev* 43:109-142, 1991

Monte D, Coutte L, Baert JL, Angeli I, Stehelin D, de Launoit Y: Molecular characterization of the ets-related human transcription factor ER81. *Oncogene* 11:771-779, 1995

Montesano R, Orci L: Transforming growth factor-ß stimulates collagen-matrix contraction by fibroblasts: implications for wound healing. *Proc Natl Acad Sci USA* 85:4894-4897, 1988

Moulin V: Growth factors in skin wound healing*. Eur J Cell Biol* 68:1-7, 1995

Mullis K, Faloona F: Specific synthesis of DNA *in vitro* via a polymerase catalysed chain reaction. *Meth Enzymol* 55:335-350, 1987

Nakagawa Y, Morikawa H, Hirata I, Shiozaki M, Matsumoto A, Maemura K, Nishikawa T, Niki M, Tanigawa N, Ikegami M, Katsu K, Akao Y: Overexpression of rck/p54, a DEAD box protein, in human colorectal tumours. *Br J Cancer* 80:914-917, 1999

Nakane M, Schmidt HH, Pollock JS, Förstermann U, Murad F: Cloned human brain nitric oxide synthase is highly expressed in skeletal muscle. *FEBS Lett* 316:175-180, 1993

Nanney LB, Stoscheck CM, King LE Jr, Underwood RA, Holbrook KA: Immunolocalization of epidermal growth factor receptors in normal developing human skin. *J Invest Dermatol* 94:742-748, 1990

Nanney LB, King LE: Epidermal growth factor and transforming growth factor–α. In: Clark RAF (ed.). *The Molecular and Cellular Biologie of Wound Repair*. New York: Plenum Press, 1996, pp171-194

Nathan C, Sporn M: Cytokines in context. *J Cell Biol* 113:981-986, 1991

Nathan C, Xie Q: Regulation of biosynthesis of nitric oxide. *J Biol Chem* 269:13725-13728, 1994

Newman SL, Henson JE, Henson PM: Phagocytosis of senescent neutrophils by human monocyte derived macrophages and rabbit inflammatory macrophages. *J Exp Med* 156:430-442, 1982

Nicol SM, Causevic M, Prescott AR, Fuller-Pace FV: The nuclear DEAD box RNA helicase p68 interacts with the nucleolar protein fibrillarin and colocalizes specifically in nascent nucleoli during telophase. *Exp Cell Res* 257:272-280, 2000

Odland G, Ross R: Human wound repair. I. Epidermal regeneration. *J Cell Biol* 39:135-157, 1968

Olson MO, Dundr M, Szebeni A: The nucleolus: an old factory with unexpected capabilities. *Trends Cell Biol* 10:189-196, 2000

Ornitz DM, Xu J, Colvin JS, McEwen DG, MacArthur CA, Coulier F, Gao G, Goldfarb M: Receptor specificity of the fibroblast growth factor family. *J Biol Chem* 271:15292-15297, 1996

Ortonne JP: Aetiology and pathogenesis of psoriasis. *Br J Dermatol* 135:1-5, 1996

Pause A, Methot N, Sonenberg N: The HRIGRXXR region of the DEAD box RNA helicase eukaryotic translation initiation factor 4A is required for RNA binding and ATP hydrolysis. *Mol Cell Biol* 13:6789-6798, 1993

Pause A, Sonenberg N: Helicases and RNA unwinding in translation. *Curr Opin Struct Biol* 3:953-959, 1993

Pause A, Sonenberg N: Mutational analysis of DEAD box RNA helicase: the mammalian translation initiation factor eIF-4A. *EMBO J* 11:2643-2654, 1992

Pederson T: The plurifunctional nucleolus. *Nucleic Acids Res* 26:3871-3876, 1998

Perez-Ruiz M, Ros J, Morales-Ruiz M, Navasa M, Colmenero J, Ruiz-Del-Arbol L, Cejudo P, Claria J, Rivera F, Arroyo V, Rodes J, Jimenez W: Vascular endothelial growth factor production in peritoneal macrophages of cirrhotic patients: regulation by cytokines and bacterial lipopolysaccharide. *Hepatology* 29:1057-1063, 1999

Pfeilschifter J, Eberhardt W, Beck KF: Regulation of gene expression by nitric oxide. *Pflügers Arch: Eur J Physiol* 442:479-486; 2001

Pfeilschifter J, Huwiler A: Nitric oxide stimulates stress-activated protein kinases in glomerular endothelial and mesanglial cells. *FEBS Lett* 396:67-70, 1996

Pilcher BK, Dumin JA, Sudbeck BD, Krane SM, Welgus HG, Parks WC: The activity of collagenase-1 is required for keratinocyte migration on a type I collagen matrix. *J Cell Biol* 137:1445-1457, 1997

Pintucci G, Bikfalvi A, Klein S, Rifkin DB: Angiogenesis and the fibrinolytic system. *Semin Thromb Hemost* 22:517-524, 1996

Potten CS: *Stem Cells*. London: Academic Press, 1997

Qureshi AA, Hosoi J, Xu S, Takashima A, Granstein RD, Lerner EA: Langerhans cells express inducible nitric oxide synthase and produce nitric oxide. *J Invest Dermatol* 107:815-821, 1996

Rappolee DA, Mark D, Banda MJ., Werb Z: Wound macrophages express TGF-α and other growth factors *in vivo*: Analysis by mRNA phenotyping, *Science* 241:708-712, 1988

Reichner JS, Meszaros AJ, Louis CA, Henry WL, Mastrofrancesco B, Martin BA, Albina JE: Molecular and metabolic evidence for the restricted expression of inducible nitric oxide synthase in healing wounds. *Am J Pathol* 154:1097-1104, 1999

Riches DWH: Macrophages involvement in wound repair, remodeling, and fibrosis. –α. In: Clark RAF (ed.). *The Molecular and Cellular Biologie of Wound Repair*. New York: Plenum Press, 1996, pp 95-141

Roberts AB, Sporn MB, Assoian RK, Smith JM, Roche NS, Wakefield LM, Heine UI, Liotta LA, Falanga V, Kehrl JH *et al*.: Transforming growth factor-ß: rapid induction of fibrosis and angiogenesis *in vivo* and stimulation of collagen formation. *Proc Natl Acad Sci USA* 83:4167-4171, 1986

Romer J, Lund LR, Eriksen J, Pyke C, Kristensen P, Dano K: The receptor for urokinase-type plasminogen activator is expressed by keratinocytes at the leading edge during re-epithelialization of mouse skin wounds. *J Invest Dermatol* 102:519-522, 1994

Romer J, Lund LR, Eriksen J, Ralfkiaer E, Zeheb R, Gelehrter TD, Dano K, Kristensen P: Differential expression of urokinase-type plasminogen activator and ist type-I inhibitor during healing of mouse skin wounds. *J Invest Dermatol* 97:803-811, 1991

Romero-Graillet C, Aberdam E, Biagoli N, Massabni W, Ortonne JP, Ballotti R: Ultraviolet B radiation acts through the nitric oxide and cGMP signal transduction pathway to stimulate melanogenesis in human melanocytes. *J Biol Chem* 271:28052-28056, 1996

Ross RR, Raines EW: Platelet-derived growth factor and cell proliferation. In: Sara VR (ed.). *Growth Factors: From Genes to Clinical Application*. New York: Raven Press, 1990, pp 193-199

Rössler OG, Hloch P, Schütz N, Weitzenegger T, Stahl H: Structure and expression of the human p68 RNA helicase gene. *Nucleic Acids Res* 28:932-939, 2000

Rossow KL, Janknecht R: Synergism between p68 RNA helicase and the transcriptional coactivators CBP and p300. *Oncogene* 22:151-156, 2003

Rowe A, Farell AM, Bunker CB: Constitutive endothelial and inducible nitric oxide synthase in inflammatory dermatoses. *Br J Dermatol* 136:18-23, 1997

Ruggeri ZM: Von Willebrand factor and fibrinogen. *Curr. Opin. Cell Biol*. 5**:**898-906, 1993

Ruoslahti E: Integrins. *J Clin Invest* 87:1-5, 1991

Saarialho-Kere UK, Pentland AP, Birkedal-Hansen H, Parks WC, Welgus: Distinct populations of basal keratinocytes express stromelysin-1 and stromelysin-2 in chronic wounds. *J Clin Invest* 94:79-88, 1994

Sabath DE, Broome HE, Prystowsky MB: Glyceraldehyde-3-phosphate dehydrogenase mRNA is a major interleukin-2-induced transcript in a cloned T-helper lymphocyte. *Gene* 91:189-191, 1990

Sakai LY, Keene DR, Engvall E: Fibrillin, a new 350-kDa glycoprotein, is a component of extracellular microfibrils. *J Cell Biol* 103:2499-2509, 1986

Salo T, Makela M, Kylmaniem M, Autio-Harmainen H, Larjava H: Expression of matrix metalloproteinase-2 and –9 during early human wound healing. Lab Invest 70:176-182, 1994

Sambrook J, Fritsch EF, Maniatis T: Molecular Cloning: A Laboratory Manual. New York: Cold Spring Harbor Laboratory Press, 1989

Sanger F, Nicklen S, Coulsen AR: DNA sequencing with chain terminating inhibitors. *Proc Natl Acad Sci USA* 74:5463-5467, 1977

Sarret Y, Woodley DT, Grigsby K, Wynn K, O'Keefe EJ: Human keratinocyte locomotion: the effect of selected cytokines. *J Invest Dermatol* 98:12-16, 1992

Schaffer MR, Tantry U, Gross SS, Wasserburg HL, Barbul A: Nitric oxide regulates wound healing. *J Surg Res* 63:237-240, 1996

Scherl A, Coute Y, Deon C, Calle A, Kindbeiter K, Sanchez J-C, Greco A, Hochstrasser D, Diaz J-J: Functional proteomic analysis of human nucleolus. *Mol Biol Cell* 13:4100-4109, 2002

Schiro JA, Chan BM, Roswit WT, Kassner PD, Pentland AP, Hemler ME, Eisen AZ, Kupper TS*:* Integrin α2ß1 (VLA-2) mediates reorganization and contraction of collagen matrices by human cells. *Cell* 67:403-410, 1991

Schlaak JF, Buslau M, Jochum W, Hermann E, Girndt M, Gallati H, Meyer zum Buschenfelde KH, Fleischer B: T cells involved in psoriasis vulgaris belong to the Th1 subset. *J Invest Dermatol* 102:145-149, 1994

Schmitt HHHW, Walter U: NO at work. *Cell* 78:919-925, 1994

Schultz GS, White M, Mitchell R, Brown G, Lynch J, Twardzik DR, Todaro GJ: Epithelial wound healing enhanced by transforming growth factor alpha and vaccinia growth factor. *Science* 235:350-352, 1987

Schwer B: A new twist on RNA helicases: DexH/D box proteins as RNPases. *Nat Struct Biol* 8:113-116, 2001

Sellheyer K, Bickenbach JR, Rothnagel JA, Bundman D, Longley MA, Krieg T, Roche NS, Roberts AB, Roop DR: Inhibition of skin development by overexpression of transforming growth factor ß1 in the epidermis of transgenic mice. *Proc Natl Acad Sci USA* 90:5237-5241, 1993

Shaw PJ, Jordan EG: The nucleolus. *Annu Rev Cell Dev Biol* 11:93-121, 1995

Shimizu Y, Sakai M, Umemura Y, Ueda H: Immunohistochemical localization of nitric oxide synthase in normal human skin: expression of endothelial-type and inducible-type nitric oxide synthase in keratinocytes. *J Dermatol* 24:80-87, 1997

Simpson CJ, Fothergill-Gilmore LA: Isolation and sequence of a cDNA encoding human platelet phosphofructokinase. *Biochem Biophys Res Commun* 180:197-203, 1991

Singer AJ, Clark RAF: Mechanisms of Disease. *N Engl J Med* 341:738-746, 1999

Sirsjo A, Karlsson M, Gidlof A, Rollman O, Torma H: Increased expression of inducible nitric oxide synthase in psoriatic skin and cytokine-stimulated cultured keratinocytes. *Br J Dermatol* 134:643-648, 1996

Sporn MB, Roberts AB: Transforming growth factor-ß: recent progress and new challenges. *J Cell Biol* 119:1017-1021, 1992

Squire JA, Thorner PS, Weitzman S, Maggi JD, Dirks P, Doyle J, Hale M, Godbout R: Co-amplification of MYCN and a DEAD box gene (DDX1) in primary neuroblastoma. *Oncogene* 10:1417-1422, 1995

Srivastava M, Pollard HB: Molecular dissection of nucleolin's role in growth and cell proliferation: new insights.*FASEB J* 13:1911-1922, 1999

Staley JP, Guthrie C: Mechanical devices of the spliceosome: motors, clocks, springs, and things. *Cell* 92:315-326, 1998

Stallmeyer B, Kämpfer H, Kolb N, Pfeilschifter J, Frank S: The function of nitric oxide in wound repair: Inhibition of inducible nitric oxide-synthase severly impairs wound reepithelialization. *J Invest Dermatol* 113:1090-1098, 1999

Stallmeyer B, Kämpfer H, Podda M, Kaufmann R, Pfeilschifter J, Frank S: A novel keratinocyte mitogen:regulation of leptin and its functional receptor in skin repair. *J Invest Dermatol* 117:98-105, 2001

Stallmeyer B, Anhold M, Wetzler C, Kahlina K, Pfeilschifter J, Frank S: Regulation of eNOS in normal and diabetes-impaired skin repair: implications for tissue regeneration. *Nitric oxide: Biology and Chemistry* 6:168-177, 2002

Stevenson RJ, Hamilton SJ, MacCallum DE, Hall PA, Fuller-Pace FV: Expression of the `dead box`RNA helicase p68 is developmentally and growth regulated and correlates with organ differentiation/maturation in the fetus. *J Pathol* 184:351-359, 1998

Svitkin YV, Pause A, Haghighat A, Pyronnet S, Witherell G, Belsham GJ, Sonenberg N: The requirement for eukaryotic initiation factor 4A (eIF4A) in translation is in direct proportion to the degree of mRNA 5` secondary structure. *RNA* 7:382-394, 2001

Swift ME, Kleinman HK, DiPietro LA: Impaired wound repair and delayed angiogenesis in aged mice. *Lab Invest* 79:1479-1487, 1999

Tanner NK, Linder P: DexD/H box RNA helicases: from generic motors to specific dissociation functions. *Mol Cell* 8:251-262, 2001

Thews G, Mutschler E, Vaupel P: *Anatomie, Physiologie, Pathophysiologie des Menschen.* Stuttgart: Wissenschaftliche Verlagsgesellschaft, 1999

Thornton FJ, Schaffer MR, Witte MB, Moldawer LL, MacKay SL, Abouhamze A, Tannahill CL, Barbul A: Enhanced collagen accumulation following direct transfection of the inducible nitric oxide synthase gene in cutaneous wounds. *Biochem Biophys Res Commun* 246:654-659, 1998

Tokunaga K, Nakamura Y, Sakata K, Fujimori K, Ohkubo M, Sawada K, Sakiyama S: Enhanced expression of glyceraldehyde-3-phosphate dehydrogenase gene in human lung cancer. *Cancer Res* 47:5616-5619, 1987

Tonnesen MG, Worthen GS, Johnston RBJ: Neutrophil emigration, activation, and tissue damage. In: Clark RAF, Henson PM (eds.). *The Molecular and Cellular Biologie of Wound Repair*. New York: Plenum Press, 1988, pp 149-183

Uitto J, Pulkkinem L, Chu ML: Collagen. In Freedberg I, ed. *Fitzpatrick`s Dermatology in General Medicine*, 5th edn. New York: McGraw Hill, 1999

Vaalamo M, Mattila L, Johansson N, Kariniemi AL, Karjalainen-Lindsberg ML, Kahari VM, Saarialho-Kere U: Distinct populations of stroma cells express collagenase-3 (MMP-13) and collagenase-1 (MMP-1) in chronic ulcers but not in normally healing wounds. *J Invest Dermatol* 109:96-101, 1997

Wang R, Ghahary A, Shen YJ, Scott PG, Tredget EE: Human dermal fibroblasts produce nitric oxide and express both constitutive and inducible nitric oxide synthase isoforms. *J Invest Dermatol* 106:419-427, 1996

Wasserman DA, Steitz JA: Alive with DEAD proteins. *Nature* 349:463-464, 1991

Watanabe M, Yanagisawa J, Kitagawa H, Takeyama K, Ogawa S, Arao Y, Suzawa M, Kobayashi Y, Yano T, Yoshikawa H, Masuhiro Y, Kato S: A subfamily of RNA-binding DEAD-box proteins acts as an estrogen receptor alpha coactivator through the N-terminal activation domain (AF-1) with an RNA coactivator, SRA. *EMBO J* 20:1341-1352, 2001

Weindel K, Marme D, Weich HA: AIDS-associated Kaposi`s sarcoma cells in culture express vascular endothelial growth factor. *Biochem Biophys Res Commun* 183:1167-1174, 1992

Welch MP, Odland GF, Clark RAF: Temporal relationships of F-actin bundle formation, collagen and fibronectin matrix assembly, and fibronectin receptor expression to wound contraction. *J Cell Biol* 110:133-145, 1990

Weller R: Nitric oxide, skin growth and differentiation: more question than answers? *Clin Exp Dermatol* 24:388-391, 1999

Werner S, Peters KG, Longaker MT, Fuller-Pace F, Banda M, Williams LT: Large induction of keratinocyte growth factor expression in the dermis during wound healing. *Proc Natl Acad Sci USA* 89:6896-6900, 1992

Werner S, Smola H, Liao X, Longaker MT, Krieg T, Hofschneider PH, Williams LT: The function of KGF in morphogenesis of epithelium and reepithelialization of wounds. *Science* 266:819-822, 1994

Werner S: Keratinocyte growth factor: a unique player in epithelial repair processes. *Cytokine Growth Factor Rev 2*:153-165, 1998

Werner S, Grose R: Regulation of wound healing by growth factors and cytokines. *Physiol Rev* 83:835-870, 2003

West SC: Processing of recombinant intermediates by the RuvABC proteins. *Annu Rev Genet* 31:213-244, 1997

Wetzler C, Kämpfer H, Pfeilschifter J, Frank S: Keratinocyte-derived chemotactic cytokine: Expressional modulation by nitric oxide *in vitro* and during cutaneous wound repair *in vivo. Biochem Biophys Res Commun* 274:689-696, 2000

Will CL, Lührmann R.: Protein functions in pre-mRNA splicing. *Curr Opin Cell Biol* 9: 32ß-8

Woodley DT, Yamauchi M, Wynn KC, Mechanic G, Briggaman RA: Collagen telopeptides (cross-linking sites) play a role in collagen gel lattice contraction. *J Invest Dermatol* 97:580-585, 1991

Xu J, Clark RAF: Extracellular matrix alters PDGF regulation of fibroblast integrins. *J Cell Biol* 132:239-249, 1996

Yamasaki K, Edington HDJ, McClosky C, Tzeng E, Lizonova A, Kovesdi I, Steed DL, Billiar TR: Reversal of impaired wound repair in iNOS-deficient mice by topical adenoviral-mediated iNOS gene transfer. *J Clin Invest* 101:967-971, 1998

Yanagishita M: A brief history of proteoglycans. *EXS* 70:3-7, 1994

7

Appendix

7.1 Abbreviations

aa	amino acid
AKAP95	cAMP-dependent protein kinase-anchoring protein 95
Ang	angiopoietin
AP-1	activator protein 1
ATP	adenosine triphosphate
bFGF	basic fibroblast growth factor
BSA	bovine serum albumin
CBP	CREB binding protein
cDNA	copy of complementary DNA
cGMP	cyclic guanosine monophosphate
CHX	cycloheximide
CO	carbon monoxide
cpm	counts per minute
CREB	cAMP response element binding protein
ctrl	control
cyt	cytokine
d	day
DEPC	diethyl pyrocarbonate
dest	distilled
DETA-NO	(Z)-1-[2-(2-aminoethyl)-N-(2-ammonioethyl)amino]diazen-1-ium-1,2-diolate
DG	diacylglycerol
DMEM	Dulbecco`s Modified Eagles Media
DMF	dimethylformamide
DMSO	dimethylsulfoxide
DNA	deoxyribonucleic acid
DNase	deoxyribonuclease
DTT	dithiothreitol
E. coli	*Escherichia coli*

ECL	enhanced chemiluminescence
EDTA	ethylenediaminetetraacetic acid
EGF	epidermal growth factor
eIF-4a	eucaryotic initiation factor-4A
ELISA	enzyme-linked immunosorbent assay
eNOS	endothelial nitric oxide synthase
ERK	extracellular signal regulated kinase
et al.	*et alter*
FCS	fetal calf serum
fig	figure
g	gravitation (9.81m/s^2)
GAPDH	glyceraldehyde 3-phosphate dehydrogenase
GFP	green fluorescent protein
GSNO	S-nitroso-glutathione
h	hour(s)
HEK	human embryonal kidney cells
HEPES	N-(2-hydroxyethyl)piperazine-N`-(2-ethanesulfonic acid)
hERαAF-1	human estrogen receptor α AF-1
hnRNP	heterogeneous nuclear ribonucleoprotein particle
IFN	interferon
IGF	insulin-like growth factor
IL	interleukin
iNOS	inducible nitric oxide synthase
IPTG	isopropylthiogalactoside
IκB	inhibitor of κB
JNK	c-Jun-N-terminal kinase
kDa	kilo Dalton
KGF	keratinocyte growth factor
LB	Lauria-Bertani
L-NIL	L-N^6-(1-iminoethyl)lysine
L-NMMA	N^G-monomethyl-L-arginine
LPS	lipopolysaccharide
MAPK	mitogen activated protein kinase
MCP	monocyte chemoattractant protein
min	minute(s)

MIP	macrophage inflammatory protein
MMP	matrix metalloproteinase
mRNA	messenger RNA
NF	nuclear factor
nNOS	neuronal nitric oxide synthase
NO	nitric oxide
NS 2028	[4*H*-8-Bromo-1,2,4-oxadiazolo(3,4-d)benz(b)(1,4)oxazin-1-one]
nt	nucleotides
OD	optical density
ODQ	[1*H*-[1,2,4]Oxadiazole[4,3-a]quinoxalin-1-one]
p68	p68 DEAD box RNA helicase
PAGE	polyacrylamid gel elektrophoresis
PBS	phosphate buffer saline
PDGF	platelet-derived growth factor
pH	potentia hydrogenii
PIPES	piperazine-N,N`-bis(2-ethanesulfonic acid)
PKA	protein kinase A
PKC	protein kinase C
poly-(A)	polyadenyclic acid
PVDF	polyvinylidene fluoride
RNA	ribonucleic acid
RNase	ribonuclease
ROS	reactive oxygen species
rpm	rounds per minute
RPMI	Roswell Park Memorial Institute
RT	reverse transcription
SAP	stress activated protein kinase
SDS	sodium dodecyl sulfate
sGC	soluble guanylyl cyclase
siRNA	small interfering RNA
SNP	sodium nitroprusside
SpNO	spermine-NONOate
SV40	simian virus 40
TCA	trichloroacetic acid
TEMED	N,N,N`,N`-tetramethylethylenediamine

TGF	transforming growth factor
Th	T helper cell
TNF	tumor necrosis factor
TNFα	tumor necrosis factor α
TPA	12-O-tetradecanoylphorbol-13-acetate
Tris	tris(hydroxymethyl)aminomethane
tRNA	transfer RNA
U	unit(s)
UTP	uridine 5`-triphosphate
v/v	volume per volume
VEGF	vascular endothelial growth factor
w/v	weight per volume
wt	wild type
X-gal	5-bromo-4-chloro-3-indolyl-ß-D-galactoside
YC-1	[3-(5`-Hydroxymethyl-2`-furyl)-1-benzylindazole]

7.2 Publications

7.2.1 Journal publications

Münchow S, Ferring D, **Kahlina K**, Jansen RP:
Characterization of *Candida albicans ASH1* in *Saccharomyces cerevisiae*
Curr Genet 41:73-81, 2002

Stallmeyer B, Anhold M, Wetzler C, **Kahlina K**, Pfeilschifter J, Frank S:
Regulation of eNOS in normal and diabetes-impaired skin repair: implications for tissue regeneration.
Nitric oxide: Biology and Chemistry 6:168-177, 2002

Kahlina K, Goren I, Pfeilschifter J, Frank S:
P68 DEAD box RNA helicase expression in keratinocytes: regulation, nucleolar localization, and functional connection to proliferation and VEGF gene expression
J Biol Chem 279: 44872-44882, 2004

7.2.2 Talks

Kahlina K, Pfeilschifter J, Frank S
Identification of p68 RNA helicase as a novel mediator of no function on keratinocyte gene expression and proliferation
45. Spring meeting of DGPT, Mainz, 2004, N-S Arch Pharmacol 369: 158 Suppl.

7.2.3 Poster presentations

Kahlina K, Wetzler C, Pfeilschifter J, Frank S:
Inflammation at the wound site: leptin differentially regulates chemokine expression and subsequent leukocyte infiltration into peripheral skin wounds.
53. Mosbacher Kolloquium, 2002, abstract booklet

7.3 Acknowledgment

I am very grateful to Prof. Dr. Josef Pfeilschifter for giving me the opportunity to work in his laboratory and his scientific support.

Many thanks go to my direct supervisor PD Dr. Stefan Frank, who gave me the chance to work on the very intersting topic of wound healing. I appreciate his critical and encouraging advice and ,especially, the scientific freedom he gave me and thereby let me “grow up” as a scientist.

I thank Prof. Dr. Bernd Ludwig for his readiness to give his expert opinion on my work and to be the official supervisor of this thesis.

Very special thanks to all members of our group: Dr. Itamar Goren, the Dr. Kämpfer-Kolbs (Nicole and Heiko) and Dr. Christian Wetzler. They were always ready to help and to give valuable hints, particularly my *Haver* Itamar who was never tired to discuss recent results and new ideas.

I want to thank my lab-mates Sonja Höfler, Dr. Jens Paulukat, Dr. Markus Hellmuth, Marcel Nold and their group leader PD Dr. Heiko Mühl as well as my office-mates Carmen Pereda, Claudia Petry and Dr. Markus Manderscheid. I really enjoyed to work with them.

Moreover, I like to acknowledge all my colleagues at the institute for the scientific help and a pleasant working atmosphere.

A special *hvala* to my parents for supporting me throughout the years.

Finally, I would like to thank my beloved Rochus for the strength he gave me and for his enormous patience. He was always by my side, supporting me in- and outside the lab.

7.4 Deutsche Zusammenfassung

7.4.1 Haut und Wundheilung

Die Haut grenzt als größtes Organ den Körper von seiner Umwelt ab. Sie schützt den Organismus vor schädigenden Einwirkungen sowie vor eindringenden Mikroorganismen. Neben diesen protektiven Aufgaben vermittelt die Haut als Sinnesorgan durch zahlreiche Sensoren Berührungs-, Druck-, Temperatur- und Schmerzreize. Zusätzlich ist sie an der Regulation der Körpertemperatur und des Wasserhaushaltes beteiligt (Thews *et al*., 1999; Freinkel und Woodley, 2001). Eine Verletzung der Haut zieht daher schwerwiegende Folgen nach sich, weshalb eine schnelle funktionelle Wiederherstellung dieses Organs unabdingbar ist. Der Prozess der Wundheilung gliedert sich in verschiedene Phasen, die sowohl zeitlich als auch räumlich überlappen (Moulin, 1995, Singer und Clark, 1999).

Bei einer Verletzung werden Blutgefäße beschädigt. Es kommt zu Blutung, Aggregation und Degranulation von Blutplättchen, Koagulation des Blutes und schlussendlich zur Bildung des Wundschorfes. Aktivierte, degranulierende Blutplättchen setzen hierbei eine Reihe wichtiger chemotaktischer Moleküle und Wachstumsfaktoren frei. Der Wundschorf, der sich hauptsächlich aus einem Netz von Fibrinfibrillen, Fibronektin, Vitronektin und Thrombospondin zusammensetzt, dient als provisorische Matrix, durch die und über die Zellen während des Heilungsprozesses wandern können (Clark, 1996; Martin, 1997).

Der Beginn der Entzündungsphase ist gekennzeichnet durch einen massiven Einstrom neutrophiler Phagozyten (PMN), welche bereits wenige Minuten nach Verletzung in das verwundete Gewebe einwandern (Martin, 1997). Neutrophile werden hierbei hauptsächlich von chemotaktischen Zytokinen der CXC-Familie an den Wundort rekrutiert (Luster, 1998; Baggiolini, 1998). Einströmende Neutrophile haben die Aufgabe, eingedrungene Mikroorganismen zu phagozytieren und dienen als Quelle wichtiger Zytokine wie IL-1ß und TNF-α (Hübner *et al*., 1996). Etwa 24h nach Verletzung lösen Makrophagen (Mϕ) die PMN als vorherrschende Immunzellen ab. Verantwortlich für die Einwanderung der Mϕ sind überwiegend chemotaktische Zytokine der CC-Familie (DiPietro *et al*., 1995, 1998). Mϕ schütten eine Vielzahl von Zytokinen und Wachstumsfaktoren aus und spielen so eine wichtige Rolle im Wundheilungsprozess (DiPietro *et al*., 1995, Moulin, 1995).

Die Reepithelialisierung setzt wenige Stunden nach Verletzung ein. Charakteristisch für diese Phase des Wundheilungsprozesses sind eine gesteigerte Keratinozytenproliferation sowie die Migration der Keratinozyten über das Wundbett. Hierbei bilden Keratinozyten an den Wundrändern große hyperproliferierende Epithelien aus, welche fortwährend neu gebildete Zellen ins Wundinnere abgeben und so zu einem epithelialen Wundschluss beitragen. Verantwortlich für den Anstieg der Zellteilung sind hauptsächlich die Keratinozyten-Mitogene EGF, TGF-α, KGF und Stickstoffmonoxid (Stallmeyer *et al*., 1999; Werner und Grose, 2003). Die Migration erfolgt mittels Substratadhäsion, wobei Integrine an Komponenten der extrazellulären Wundmatrix (Fibronektin, Vitronektin, Kollagen) binden (Clark, 1990; Clark *et al*., 1996), sowie durch die Sekretion verschiedener Proteasen, u.a. Matrix-Metalloproteasen, die die Matrixproteine des Wundschorfes verdauen (Salo *et al*., 1994; Pilcher *et al*., 1997; Saarialho *et al*., 1994).

Die Bildung von Granulationsgewebe beginnt etwa vier Tage nach Verletzung. Der Aufbau der Matrix wird hauptsächlich durch das Zusammenspiel von Fibroblasten, Mϕ und Endothelzellen verrichtet und steht unter besonderer regulatorischer Kontrolle von TGF-ß1 (Clark *et al*., 1995). Eine ausreichende Versorgung des neu gebildeten Gewebes mit Sauerstoff und Nährstoffen wird durch die Blutgefäßneubildung (Angiogenese) erzielt. Die daran beteiligten mikrovaskulären Zellen (Madri *et al*., 1991, 1992a,b) werden durch eine große Zahl von Faktoren zur Migration und Proliferation angeregt. VEGF repräsentiert hier einen der wichtigsten Faktoren (Keck *et al*., 1989), der nach Verletzung vor allem von Keratinozyten des hyperproliferativen Epithels sekretiert wird (Brown *et al*., 1992; Frank *et al*., 1995).

Die Remodellierungsphase repräsentiert das Ende der Gewebsregeneration und ist gekennzeichnet durch einen kontrollierten Kollagenumbau, der von Matrix Metalloproteasen gesteuert wird (Mignatti, 1996). Eine perfekte Rekonstruktion des beschädigten adulten Gewebes ist selbst unter optimalen Bedingungen nicht zu erreichen.

7.4.2 Sickstoffmonoxid und Wundheilung

Wie man heute weiß, ist das Gas Stickstoffmonoxid (NO) in eine Vielzahl verschiedener physiologischer und pathophysiologischer Prozesse involviert (Beck *et al*., 1999; Moncada *et al*., 1991). NO wird von drei verschiedenen Isoenzymen, den

NO-Synthasen (NOS) gebildet, welche die Umwandlung der Aminosäure L-Arginin in die Produkte Zitrullin und NO katalysieren (Nathan und Xie, 1994). Die endotheliale NOS (eNOS) sowie die neuronale NOS (nNOS) werden Ca^{2+}/Calmodulin-abhängig reguliert, während die induzierbare NOS (iNOS) in ein einer Vielzahl verschiedener Zelltypen erst nach Stimulation mit pro-entzündlichen Zytokine und Endotoxin exprimiert wird (Moncada *et al*., 1991; Nathan und Xie, 1994).

Alle drei NO-Synthasen werden in der Haut exprimiert. Das entstehende NO ist hier an der Regulation der Vasodilatation, der Melanogenese und der Abwehr von pathogenen Mikroorganismen beteiligt (Bruch.Gerharz *et al*., 1998). Darüber hinaus spielt dieses Gas eine wichtige Rolle während der kutanen Wundheilung. Eine verzögerte Gewebsregeneration ist charakteristisch für iNOS-defiziente Mäuse. Dieser Wundheilungsdefekt konnte jedoch durch die Applikation eines adenoviralen iNOS-cDNA-Konstruktes nahezu vollständig aufgehoben werden (Yamasaki *et al.,* 1998). Grundsätzlich kommt es nach Verletzung zu einer Induktion der iNOS. Die iNOS wird dabei überwiegend von PMN, Mϕ und Keratinozyten des hyperproliferierenden Gewebes exprimiert (Frank *et al*., 1998a; Reichner *et al*., 1999). Weiterhin ist bekannt, dass die Hemmung der iNOS durch den selektiven iNOS-Hemmstoff L-NIL zu einer verminderten Zellteilung in den Keratinozyten des Wundrandes führt (Stallmeyer *et al*., 1999). Neben dieser Funktion als Keratinozyten-Mitogen reguliert NO die Expression verschiedener wundassoziierter Gene (VEGF, Cu/Zn SOD, Chemokine) in Keratinozyten (Frank *et al*., 1999, 2000a, c; Wetzler *et al*., 2000).

7.5.3 p68 RNA Helikase und Wundheilung

Die p68 RNA Helikase ist ein Mitglied der DEAD-Box Familie RNA abhängiger Helikasen. Identifiziert wurde p68 im Jahre 1980 eher zufällig, da es mit dem Antikörper gegen das große T-Antigen das Affenvirus 40 (SV 40) kreuzreagierte (Lane und Hoeffler, 1980). Das Sequenzierungsergebnis der entsprechenden p68 komplementären DNA (cDNA) klassifizierte dieses Molekül als Homolog des eukaryontischen Translations-Initiationsfaktor eIF-4A (Ford *et al*., 1988). Beiden Proteinen war eine hoch konservierte Domäne gemein, die DEAD (Asp-Glu-Ala-Asp)-Domäne, die im Folgenden der Familie ihren Namen gab (Linder *et al*., 1989). DEAD Proteine katalysieren mittels Nucleosid-Triphosphat (NTP) Hydrolyse das

Aufwinden doppelsträngiger RNA Moleküle (Tanner and Linder, 2001). Diese hoch-konservierten Proteine sind damit an Prozessen des RNA-Metabolismus beteiligt. Hierzu zählen Transkription, prä-mRNA Splicing, RNA-Export, Translation und RNA-Degradation (de la Cruz *et al*., 1999; Kadare and Haenni, 1997). Die Aminosäuresequenz der p68 Helikase ist ebenfalls stark konserviert So sind das humane und murine Protein zu 98% identisch (Lemaire and Heinlein, 1993) und selbst das Homolog der Hefe *Saccharomyces cerevisiae*, Dbp2, stimmt zu 55% mit dem humanen p68 überein (Iggo *et al*., 1991). Auch die Funktion der p68 Helikase hat sich im Laufe der Evolution kaum verändert. Einen Beweis hierfür liefert die Arbeit von Bond *et al.* (2001), in welcher die Autoren den Wachstumsdefekt dbp2-defizienten Hefezellen durch die Transformation des humanen Homologs aufheben können.

Die Expression der p68 ist assoziiert mit der Zellteilung und korreliert mit der Reifung und Differenzierung fötaler Organe (Stevenson *et al*., 1998). Dieser Zusammenhang zwischen Proliferationsstatus der Zelle und p68-Induktion besteht jedoch nicht immer. So beobachteten Stevenson *et al.* (1998), dass Organe mit hoher Zellteilungsrate nicht zwangsläufig einen hohen p68-Spiegel aufweisen, während eine p68 Überexpression im Tumorgewebe bei Mast- und Dickdarmkrebs gefunden wurde (Causevic *et al*., 2001). Weiterhin ist die p68 Helikase ein essentieller Spleiß-Faktor (Liu, 2002), sowie ein Transkriptions-Kofaktor (Endoh *et al*., 1999; Watanabe *et al*., 2001:, Rossow und Janknecht, 2003).

Zusammenfassend lässt sich demnach sagen, dass es sich bei p68 um ein Protein handelt, welches an verschiedenen Prozessen des Zellmetabolismus beteiligt ist und dessen Expression mit der Zellteilung assoziiert ist. Diese Eigenschaften deuten auf eine Rolle der p68 während der kutanen Wundheilung hin, welche einen dynamischen Prozess darstellt, der durch Proliferation und Migration verschiedener Zelltypen gekennzeichnet ist (Clark, 1996; Martin, 1997).

7.5.4 NO und weitere Keratinozyten-Mitogene induzieren die Expression der p68 RNA Helikase *in vitro*

In dieser Arbeit wurde die p68 RNA Helikase als neues NO-reguliertes Gen in Keratinozyten identifiziert. Die Stimulation von HaCaT Keratinozyten mit verschiedenen NO-Donatoren (GSNO, Sp-NO) führte jeweils zu einer gesteigerten p68-Expression sowohl auf mRNA als auch auf Proteinebene. Darüber hinaus

konnte gezeigt werden, dass typische wundassoziierte Keratinozytenmitogene wie TGF-α, EGF und KGF die Expression der p68 in Keratinozyten induzieren. Ein pro-entzündliches Zytokingemisch (TNFα, IFNγ, Il-1ß) bewirkte ebenfalls eine Expressionssteigerung.

7.5.5 p68 lokalisiert in Keratinozyten Nucleoli

In der Literatur finden sich Beispiele, die eine Interaktion von p68 mit Kernproteinen belegen. Akileswaran *et al*. (2001) konnten zeigen, dass p68 an das cAMP-abhängige Proteinkinase Anker Protein AKAP95 assoziiert. Eine Kolokalisation mit Fibrillarin in Nucleoli während der späten Telophase wurde ebenfalls anschaulich dokumentiert (Nicol *et al*., 2000). Diese Beobachtungen sind in Übereinstimmung mit unseren Ergebnisse: p68 ist sowohl *in vitro* (HaCaT und PAM Keratinozyten) als auch *in vivo* (Wunden) im Kern von Keratinozyten lokalisiert. Mit Hilfe eines p68-GFP Fusionsproteins konnten wir die p68 Lokalisation näher charakterisieren. Neben der erwarteten Kernlokalisation, zeigte p68 eine Akkumulation in den Keratinozyten-Nuleoli. Als spezifisches Nucleoli-Marker Protein wurde Nucleolin verwendet (Bugler *et al*., 1982; Shaw and Jordan, 1995). Nucleoli sind Organellen, in denen ribosomale RNA transkribiert und die Ribosomen-Untereinheiten zusammengesetzt werden. In jüngster Zeit werden sie als Zellbestandteile mit plurifunktionellem Charakter diskutiert, in denen sowohl transkriptionelle als auch translationelle Vorgänge vonstatten gehen (Scherl *et al*., 2002).

7.5.6 p68 beeinflußt die Zellteilung in Keratinozyten

Die Reepithelialisierungsphase während des Prozesses der Wundheilung ist unter anderem gekennzeichnet durch einen Anstieg der Zellteilungsrate von Keratinozyten. Da die p68 Expression mit der Zellteilung assoziiert ist (Stevenson *et al*., 1998), liegt ein Zusammenhang zwischen dem zellulären p68-Spiegel und dem Proliferationsstatus in Keratinozyten nahe. Zur Klärung dieser Hypothese wurden p68-überexprimierende Zelllinien untersucht. Parallel wurde die p68 Protein Expression mittels spezifischer siRNA Moleküle gehemmt. Es zeigte sich, dass eine p68 Überexpression einen Anstieg der Keratinozytenproliferation zur Folge hatte, während die Hemmung des p68 Proteins die Zellteilungsrate sinken ließ. Folglich ist

p68 ein Regulator der Proliferation von Keratinozyten *in vitro* und damit auch ein potentieller Modulator der Keratinozytenproliferation während der Reepithelialisierung.

7.5.7 p68 ist beteiligt an der Regulation der VEGF-Expression

Eine effiziente Angiogenese stellt die Nähr- und Sauerstoffversorgung im regenerierenden Gewebe sicher. VEGF gilt hierbei als ein wichtiger angiogenetischer Faktor (Keck *et al*., 1989), der vor allem von Keratinozyten des Wundrandes gebildet wird. Die VEGF-Expression unterliegt einer komplexen Regulation verschiedener Wachstumsfaktoren, Zytokine und NO (Brown *et al*., 1992; Frank *et al*., 1995, 1999). Die Transkriptionskofaktoren CBP und p300 sind zusammen mit der RNA-Polymerase II maßgeblich an der Hypoxie-induzierten VEGF-Expression beteiligt (Kung *et al*., 2000). Endoh *et al.* (1999) konnten demonstrieren, dass p68 gemeinsam mit CBP/p300/RNA-Pol II an der Genexpression beteiligt ist. Wir vermuteten daher einen Zusammenhang zwischen p68-Induktion und VEGF-Expression. p68-überexprimierende Keratinozyten-Zelllinien zeigten unter mitogenen Bedingungen einen Anstieg der VEGF-Produktion, während die Hemmung des p68 Proteins mit Hilfe spezifischer siRNA Moleküle die VEGF-Expression in NO-induzierten HaCaT Keratinozyten senkte. Daraus ergibt sich, dass p68 an der Mitogen-induzierten VEGF-Expression funktionell beteiligt ist. Eine Funktion als Transkriptionskofaktor zusammen mit CBP/p300/RNA-Pol II erscheint daher möglich.

7.5.8 p68 Expression während der kutanen Wundheilung *in vivo*

Mit Hilfe eines exzisionalen Wundheilungsmodells der Maus wurde die Expression der p68 RNA Helikase während der Wundheilung untersucht. Es zeigte sich, dass in unverletzter Haut p68 konstitutiv exprimiert wird. Nach Verletzung und während des gesamten Wundheilungsverlaufs bleibt der p68 mRNA-Spiegel nahezu konstant, während die p68-Proteinspiegel erst drei Tage nach Verwundung wieder detektierbar sind. Eine Trennung von Epidermis und Dermis zeigte, dass beide Gewebe in der Lage sind p68 mRNA zu transkribieren. Das entsprechende p68 Protein wird allerdings nur von Keratinozyten der Epidermis und nicht von mesenchymalen Zellen der Dermis translatiert. Bestätigend zeigten immunohistochemische

Untersuchungen, dass sich die p68 Expression auf epidermale Keratinozyten beschränkt.

Überraschend ist in iNOS-defizienten Mäusen der p68-Spiegel vergleichsweise höher. Dieser unerwartete Umstand ist vielleicht durch einen kompensatorischen Anpassungsmechanismus in iNOS-defizienten Tiere zurückzuführen, die eine verminderte Keratinozytenproliferation aufweisen (Yamasaki *et al.,* 1998; Stallmeyer *et al*., 1999).

7.5 Curriculum vitae

Persönliche Daten

Name:	Kornelija Kahlina
Geburtsdatum:	26.03.1975
Geburtsort:	Gross-Umstadt
Staatsbürgerschaft:	kroatisch
Anschrift:	Hauptstrasse 68 59889 Eslohe

Schulausbildung

1981-1985	Grundschule im Kirchgarten in Babenhausen
1985-1991	Joachim-Schumann-Gesamtschule in Babenhausen
1991-1994	Bachgau-Oberstufengymnasium in Babenhausen

Studium und Dissertation

10/1994-03/1997	Biologiestudium an der TU-Darmstadt,
04/1997-07/2000	Biologiestudium an der Ruprecht-Karls-Universität Heidelberg
04/1999	mündliche Diplomprüfungen im Hauptfach Zellbiologie (Prof. Dr. B. Dobberstein und Prof. Dr. W. Dröge) und in den Nebenfächern Mikrobiologie (Prof. Dr. H. U. Schairer) und Ökologie (Prof. Dr. Dr. V. Storch)
10/1999-07/2000	Diplomarbeit am ZMBH der Universität Heidelberg unter der Betreuung von Dr. R.P. Jansen zum Thema „Isolierung und funktionelle Charakterisierung des *ASH1* Gens aus *Candida albicans*“
03/2001-02/2004	Doktorarbeit am Institut für Allgemeine Pharmakologie und Toxikologie (Direktor: Prof. Dr. J. Pfeilschifter) des Klinikums der Johann Wolfgang Goethe-Universität Frankfurt unter der Betreuung von PD Dr. S. Frank. Titel der Dissertationsschrift: „p68 RNA helicase: a novel mediator of nitric oxide and mitogen functions in keratinocytes“